ELUCIDATING THE MECHANISMS THROUGH WHICH TISSUE NON-SPECIFIC ALKALINE PHOSPHATASE MEDIATES INTRACELLULAR LIPID ACCUMULATION

Eleanor Margaret Cave

A Thesis submitted to the Faculty of Health Sciences, University of the Witwatersrand, in fulfilment of the requirements for the degree of Doctor of Philosophy

Johannesburg, 2017

Declaration

I, Eleanor Margaret Cave declare that this thesis is my own work. It is being submitted for the degree of Doctor of Philosophy in the University of the Witwatersrand, Johannesburg. It has not been submitted for any other examination at this or any other University.

_____

_____1_____Day of _November_ 2017

Dedication

This work is dedicated to my parents Roger and Muriel Cave for all of their love and support throughout my studies and my life as a whole.

Publications and presentations arising from this thesis

Conference Proceedings

1. **Cave, E** and Crowther N. (April 2016). Tissue non-specific alkaline phosphatase is a positive regulator of cholesterol ester droplet accumulation in the Y1 adrenocortico cell line. Society for Endocrinology, Metabolism and Diabetes of South Africa Congress, Cape Town, South Africa
2. **Cave E** and Crowther N. (September 2015). "Inhibition of the pyrophosphate transporter (ANK) enhances intra-cellular lipid accumulation in murine 3T3-L1 preadipocytes." United Kingdom Congress on Obesity 2015, Glasgow, Scotland
3. **Cave, E** and Crowther N. (August 2015). TNF receptor associated factor 2 mRNA is down regulated during intracellular lipid accumulation in the 3T3-L1 mouse preadipocyte cell line. PathRed Congress, Johannesburg, South Africa.
4. **Cave, E** and Crowther N. (April 2014). Tissue non-specific alkaline phosphatase functions to generate inorganic phosphate which mediates lipid accumulation in 3T3-L1 preadipocytes. Society for Endocrinology, Metabolism and Diabetes of South Africa Congress, Durban, South Africa.
5. **Cave, E** and Crowther N. (March 2014). Tissue non-specific alkaline phosphatase functions to generate inorganic phosphate which mediates lipid accumulation in 3T3-L1 preadipocytes. Keystone Symposium: Lipid Pathways in Biology and Disease, Dublin, Ireland.

Publications

1. **Cave, E** and Crowther N. (Under Review). Tissue non-specific alkaline phosphatase is a positive regulator of cholesterol ester droplet accumulation in the Y1 adrenocortical cell line. Annals of Anatomy

Abstract

Background: Tissue non-specific alkaline phosphatase (TNAP) is an enzyme which functions within the body to catalyze the hydrolysis of pyrophosphate to phosphate, and is a well-known mediator of bone mineralization. It has also been identified as a positive mediator of intracellular lipid accumulation (ICLA) in both murine and human preadipocytes as well as in the hepatocellular cell line HepG2. However, the mechanism through which TNAP functions to control ICLA is not known. Both osteoblasts and adipocytes are both of mesenchymal origin and thus may share conserved mechanisms through which TNAP functions. Within bone, TNAP converts pyrophosphate (which inhibits mineralization) to phosphate. This phosphate is essential to the mineralization process through binding to hydroxyapatite crystals, and it also activates the transcription of genes whose products function in osteoblast differentiation, including NRF2. This thesis therefore aimed to determine the role of both pyrophosphate and TNAP-generated phosphate in ICLA. In addition, it is possible that TNAP may interact with other proteins, as it is known that TNAP is able to dephosphorylate proteins such as tau. This thesis therefore aimed to determine whether TNAP binds to other proteins in the context of ICLA.

Lipids are not only stored within hepatocytes and adipocytes, but are also found in cells of the adrenal cortex, and TNAP is known to be expressed within such cells. Therefore, this thesis also aimed to determine whether TNAP is involved in the accumulation of cholesterol esters within lipid droplets in the adrenal cortex.

Methods: To determine the effect of high intracellular pyrophosphate levels on ICLA, 3T3-L1 cells (a preadipocyte cell line) were cultured in the presence and absence of probenecid, an inhibitor of the pyrophosphate transporter ANK, and induced to

accumulate lipids. Lipid accumulation was monitored through Oil red O staining. The effect of probenecid treatment on TNAP activity and intracellular pyrophosphate levels was also analysed. To determine whether TNAP functions in ICLA by producing phosphate for gene induction, 3T3-L1 cells were stimulated to undergo ICLA in the presence and absence of the TNAP inhibitor levamisole, which in turn blocks ICLA. Levamisole treated cells were also incubated with phosphate to see if this would overcome the inhibitory effect of levamisole on ICLA. The ability of phosphate to induce gene expression of NRF2 was determined through real-time PCR. In addition, an NRF2 expressing plasmid was transfected into cells treated with the TNAP inhibitor levamisole to determine if this would also overcome the block on ICLA caused by TNAP inhibition.

In silico analysis identified TRAF2 as a potential binder of TNAP. The expression of TRAF2 during ICLA was determined through real time PCR, and the effect of overexpression of TRAF2 on intracellular lipid accumulation was determined through the transfection of a TRAF2 expressing plasmid in cells induced to undergo ICLA.

To determine whether TNAP modulates lipid accumulation in cells of the adrenal cortex, the Y1 murine adrenocortical cell line was cultured in the presence and absence of TNAP inhibitor levamisole, and ICLA measured by Oil Red O staining. The location of TNAP within Y1 cells was identified by histochemical staining.

Results: Cells treated with probenecid showed increased pyrophosphate levels (expressed as a % of levels observed at baseline) when compared to untreated controls (155.5 ± 15.1 % vs 51.1 ± 18.9 %; p=0.001) after 24 hours of culture. Increased pyrophosphate levels resulted in ICLA within 3T3-L1 cells surpassing levels seen in untreated controls (507.4 ± 30.4 % vs 337.6 ± 16.17 %; p=0.004). This

increase in pyrophosphate was coupled to an increase in TNAP activity within the initial 24 hours (291.5 ± 72.8 % vs baseline of 100%; p=0.038) compared to that seen in control experiments (103.43 ± 24.3 % vs baseline of 100%; p=0.848). Cells treated with levamisole showed minimal ICLA and when exogenous phosphate was added, lipid levels were reconstituted to levels similar to that seen in cells induced to accumulate lipids in the absence of levamisole (284.01 ± 62.52% vs 275.86 ± 35.52%; p= 0.83). In the presence of levamisole plus exogenous phosphate, NRF2 expression was upregulated within 1 hour of treatment to levels greater than that seen in the absence of phosphate but presence of levamisole (216.64 ± 19.24% vs 98.28 ± 3.79%; p=0.004). Expression of NRF2 (through transfection with an NRF2 expression plasmid) in cells deficient in TNAP activity (via levamisole treatment), and induced to accumulate lipids, was not able to completely reconstitute ICLA when compared to cells not treated with levamisole (193.72 ± 16.51 vs 326.46 ± 47.64; p = 0.019), but ICLA was still greater than that observed at baseline.

In silico analysis predicted that TNAP would bind to TRAF2, yet neither band shift assays nor immune co-precipitation showed evidence of this. However, TRAF2 mRNA was down regulated within 3T3-L1 cells during adipogenesis, reaching levels of 15.27 ± 10.27% (p= 0.014) of baseline (levels prior to induction of intracellular lipid accumulation) by day 4 of lipid accumulation. Overexpression of TRAF2 during adipogenesis markedly reduced intracellular lipid accumulation (147.88 ± 11.28% vs 326.46 ± 47.64%; p=0.028 (after 8 days of culture)).

In Y1 cells TNAP activity is upregulated during ICLA, reaching 233 ± 37.56% (p=0.019 vs. baseline) of baseline levels within the initial 24 hours. Inhibition of TNAP activity through levamisole treatment resulted in a decrease in ICLA when compared to cells

not treated with levamisole. Histochemical analysis showed that TNAP activity was localised to the lipid droplet.

Discussion and Conclusions: Within 3T3-L1 cells TNAP mediates intracellular lipid accumulation through the generation of phosphate. The phosphate is able to increase the expression of NRF2, however it is likely that NRF2 is not the only gene whose expression is regulated by TNAP-generated phosphate. It was found that TNAP and TRAF2 do not bind to each other in the context of ICLA; however TRAF2 is a negative mediator of ICLA through a TNAP-independent mechanism. Functional TNAP is necessary for the accumulation of cholesterol esters within the Y1 cell line, suggesting that TNAP is essential for lipid accumulation in cell types that store lipids in intracellular membrane-bound droplets in the form of triglycerides or cholesterol esters.

Acknowledgements

I would like to acknowledge my supervisor Prof. Nigel Crowther for all of his help and guidance.

I would further like to acknowledge Ms. Tracy Snyman for running the TNAP activity assays on the ADVIA 1800.

This work has been funded by the National Research Foundation Thuthuka program, the National Health Laboratory Services Research Development Trust and the University of the Witwatersrand Faculty Research Committee.

Table of Contents

List of figures

List of Tables

List of abbreviations

ALPL	Gene from which TNAP is transcribed
ANK	progressive ankylosis –pyrophosphate transporter
ANKH	Human homologue of the progressive ankylosis gene product – pyrophosphate transporter
ARE	Anti-oxidant response elements
ATCC	American Type Culture Collection
ARDP	Adipose differentiation related protein
ATP	Adenosine triphosphate
bZIP	Basic leucine zipper transcription factor
CBFa1	Core binding factor alpha 1
C/EBPα	CCAAT enhancer binding protein alpha
ECACC	European Collection of Cell Cultures
EGFR	Epidermal growth factor receptor
ENPP-1	Ectonucleotide pyrophosphate/phosphodiesterase 1
GPI	Glycosylphosphatidylinositol
HEPG2	Human hepatoma cell line
ICLA	Intracellular lipid accumulation
MAF	Musculoaponeurotic fibrosarcoma protien
MAPK	Osteoblast precursor cell line
MC3T3-E1	Mitogen activated protein kinase
NF-κβ	Nuclear factor kappa light chain enhancer of activated B cells
NRF2	Nuclear factor E2-related factor – also known as Nfe2l2
ob/ob mice	Obese murine model with deficient leptin genes
Pi	Inorganic phosphate
PiT	Phosphate transporter

pNPP	p-nitrophenyl phosphate
PPARγ	Peroxisome proliferator-activated receptor gamma
PPi	Inorganic pyrophosphate
RUNx	Runt-related transcription factor
TNFR	Tumour necrosis factor receptors
TRAF 2	TNF receptor associated factor 2
Y1	Murine adreno-cortical cell line
ZnTN	Zinc transporters
3T3-L1	Murine preadipoyte cell line

1 Literature Survey

1.1 Alkaline phosphatases

Alkaline phosphatases are well known enzymes which act to dephosphorylate a variety of substrates (Pike et al., 2013). Within humans there are four different isoforms of alkaline phosphatase. Three of which are tissue specific, namely intestinal (found in the brush borders of the intestinal mucosa), placental (seen in the placenta after the 12th week of gestation) and placental-like alkaline phosphatases (found in the testes and the thymus) (Harris, 1990). The fourth isoform, tissue non-specific alkaline phosphatase (TNAP) is located throughout the tissues of the body (Harris, 1990, McComb, 1979), and is also known as liver/bone/kidney alkaline phosphatase. Across the four variants, TNAP is the most divergent, showing 57% DNA-sequence similarity to the tissue specific variants (Weiss et al., 1988) (Figure 1.1). Interestingly, molecular modelling show that apart from a two residue deletion found in one α-helix within TNAP, all secondary structures are conserved throughout all of the TNAP variants (Le Du and Millan, 2002). In addition, TNAP differs from the other alkaline phosphatases in the region associated with the formation of dimers, which is highly conserved in the tissue-specific variants. In TNAP, there are 4 substitutions (namely E7K, R117E, N13R and P68R) which create repulsive amino acid interactions, preventing the formation of heterodimers with the tissue-specific alkaline phosphatases (Le Du and Millan, 2002).

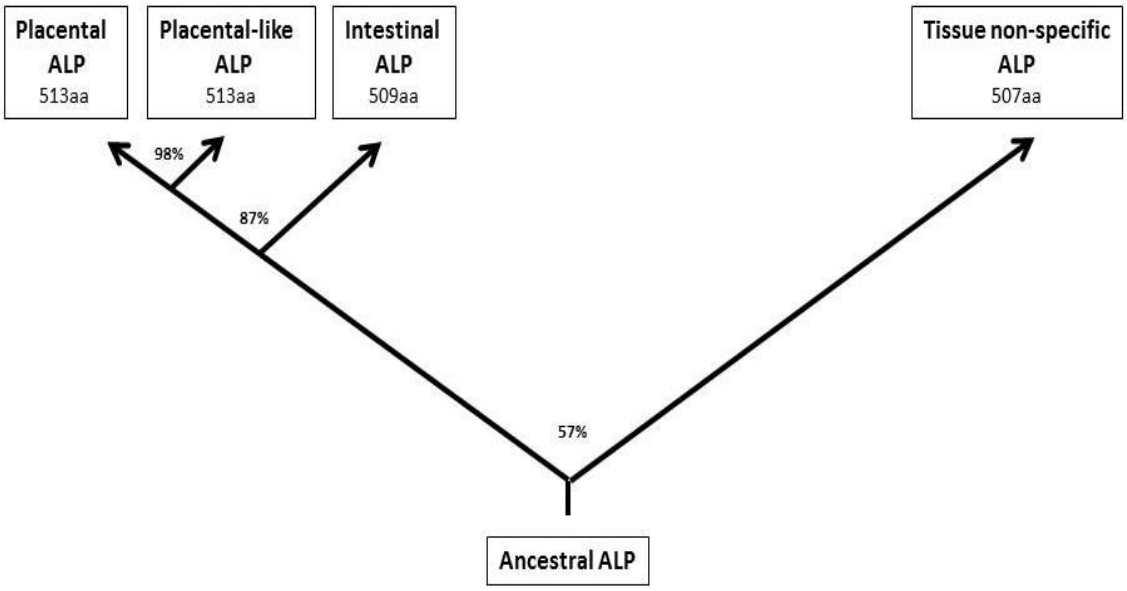

Figure 1.1: Figure showing the genetic divergence of TNAP from the tissue specific alkaline phosphatases. TNAP is 507 amino acids in length and only shares a 57% sequence homology with its tissue specific counterparts. Intestinal ALP shares 87% homology with the other tissue specific ALPs and placental and placental-like ALP share 98% sequence homology. Figure adapted from (Harris, 1990).

1.2 Tissue non-specific alkaline phosphatase

Tissue non-specific alkaline phosphatase is a glycosylated metalloenzyme which acts to catalyze the hydrolysis of pyrophosphate to inorganic phosphate at an alkaline pH (Harris, 1990, Balcerzak et al., 2003). It exhibits its physiological functions within the body as an 80 KDa homodimer (Fukunaka et al., 2011). The enzyme is found in two forms, one form is bound to the lipid membrane and the second is soluble (Bolean et

al., 2011). The membrane-bound form of TNAP is attached to lipid bilayers by a glycosylphosphatidylinositol (GPI) anchor, which allows it some lateral mobility (Bolean et al., 2011).

The membrane-bound form is known to be located on the cell plasma membrane, nuclear membrane, and the endoplasmic reticulum (Leung et al., 1989). Tissue non-specific alkaline phosphatase has been shown to be located on the surface of osteoclast and chondrocyte derived matrix vesicles (extracellular membrane bound vesicle located at the site of mineralization), and interestingly the location of TNAP on these vesicle membranes plays a role in determining which substrate TNAP will hydrolyze (Bolean et al., 2011). It is also found on the lipid monolayer surrounding adipose and hepatocellular lipid droplets (Ali et al., 2005, Chirambo et al., 2017).

1.2.1 Activation of TNAP within the cell

The catalytic site of TNAP contains three metal ion binding sites at its core, two zinc (M1 and M2) and one magnesium (M3), and requires the binding of zinc ions to M1 and M2 to function and the binding of magnesium to M3 for allosteric activation (Hoylaerts et al., 2015). The full activation of TNAP requires the presence of all three ions and relies on the zinc transporters ZnT1, ZnT4 and metallothionein (MT) (Fujimoto et al., 2013). A fourth binding site for calcium (M4) has been located on the periphery of the binding site which appears to be able to substitute for magnesium binding albeit at a 40% loss of TNAP function (Hoylaerts et al., 2015). It has recently

been shown that although the presence of calcium can cause the activation of TNAP at high concentrations, calcium is able to reduce TNAP activity by outcompeting zinc for the M1 and M2 binding sites (Hoylaerts et al., 2015).

1.2.2 The ALPL gene

The ALPL gene codes for TNAP and is located on chromosome 1 and contains 12 exons with the active site of the enzyme located on 5 of the 12 exons (exons 3, 5, 6, 9 and 10), (Figure 1.2) (Weiss et al., 1988).

The enzyme is widely expressed throughout the body (Harris, 1990, Balcerzak et al., 2003). Transcription of TNAP is under the control of a promotor which is GC rich, contains numerous CpG methylation sites and four Sp1 sites (Kiledjian and Kadesch, 1990, Weiss et al., 1988). Expression of the TNAP gene is known to be under epigenetic control, with different promotor methylation levels seen in different tissues (Delgado-Calle et al., 2011). A study comparing the levels of ALPL promotor methylation with relative gene transcription between primary human osteoblasts, a mammary cell line (MCF-7) and the MG-63 osteoblastic cell line demonstrated that the level of promoter methylation is inversely correlated to the level of mRNA expression. The ability of hypermethylation to decrease transcription was further demonstrated by the ability of the DNA demethylating agent AzadC to induce ALPL transcription only in the hypermethylated MCF-7 cell line and not in the hypomethylated primary human osteoblasts (Delgado-Calle et al., 2011).

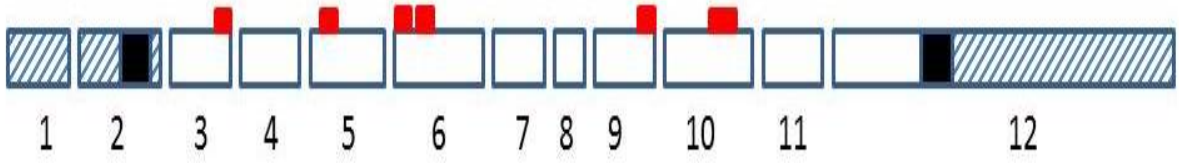

Figure 1.2: Schematic representation of the ALPL gene. The gene contains 12 exons (represented by rectangles) which are flanked by untranslated regions (striped regions). Regions representing the active pocket of TNAP are highlighted in red and the signal peptide (amino terminus) and the hydrophobic amino acids at the carboxyl terminal are represented by solid black boxes. Adapted from Weiss and colleagues (Weiss et al., 1988)

1.2.3 TNAP glycosylation

The TNAP enzyme is differentially glycosylated according to the tissue in which it is expressed (Weiss et al., 1988). The presence of O-linked glycosylation is found within bone and kidney TNAP but not in the liver variant (Nosjean et al., 1997). The removal of the O-linked residues resulted in decreased levels of enzyme activity for kidney and bone TNAP, but did not affect the liver variant (Nosjean et al., 1997).

Bone, liver and kidney TNAP variants all have five potential N-linked glycosylation sites (N140, N230, N271, N303 and N430) (Komaru et al., 2016). The presence of N-linked sugar residues is essential for TNAP function (Nosjean et al., 1997). A recent study by Komaru and colleagues demonstrated that the N-linked glycans at position N140 and N271 have no effect on enzyme localization or stability, however the

removal of all 5 N-linked glycans seems to result in protein destabilization with glycans N230, N271 and N303 being the minimal requirements for stable TNAP expression (Komaru et al., 2016).

1.3 TNAP function

The hydrolysis of monoesters is catalyzed by TNAP, resulting in the release of inorganic phosphate (P_i). Although TNAP is expressed ubiquitously throughout the body, the function is only known within a few tissues. It appears to be of particular importance in cells of mesenchymal origin including osteoblasts, adipocytes and chondrocytes (Johnson et al., 2000, Ali et al., 2005, Kim et al., 2010a, Balcerzak et al., 2003). The following section of this thesis will therefore describe the roles of TNAP within both osteoblasts and adipocytes and describe the molecular mechanisms by which TNAP may function, particularly via its effects on intracellular phosphate levels.

1.3.1 TNAP and Dephosphorylation

Tissue non-specific alkaline phosphatase is able to use its phosphatase activity to dephosphorylate phosphoproteins (Wang et al., 2014). In neuronal cells, TNAP is known to dephosphosphorylate the Tau protein, resulting in neural toxicity (Kellett and Hooper, 2015). The TNAP-mediated dephosphorylation of the Tau protein, allows it to act as an agonist of the muscarinic receptors M1 and M3. This results in a prolonged increase in the intracellular calcium levels, which in turn results in neuronal death

(Diaz-Hernandez et al., 2015). In addition, TNAP has been shown to dephosphorylate phospholamban (an important regulator of contractility in cardiac muscles) in the rat sarcoplasmic reticulum. This was demonstrated through injecting zinc into the tail vein of the rat, resulting in significantly higher TNAP activity as well as a corresponding decrease in the phosphorylated form of phospholamban (Wang et al., 2014).

The ability of TNAP to dephosphorylate substrates has further been demonstrated by its ability to dephosphorylate the bacterial toxin lipopolysaccharide (resulting in its detoxification) within the pregnant mouse, where TNAP supplementation resulted in increased dephosphosphorylation of the lipopolysaccharide. This in turn greatly increased the chances of the mice remaining pregnant (Lei et al., 2015).

1.3.2 TNAP is important in the maintenance of the cellular phosphate/pyrophosphate balance

The ability of TNAP to hydrolyze pyrophosphate (PPi) to phosphate provides it with a central role in maintaining the appropriate physiological levels of both pyrophosphate and phosphate within the intracellular and extracellular environment (Harmey et al., 2004). However, TNAP does not function alone in the control of the phosphate/pyrophosphate balance. Numerous factors are required in addition to TNAP, namely ectonucleotide pyrophosphatase/phosphodiesterase 1 (ENPP-1), the human homologues of the p*rogressive ankylosis* gene product (ANKH) and the class III phosphate transporter (PiT -1).

1.3.2.1 Enzymes regulating the phosphate/pyrophosphate balance

1.3.2.1.1 TNAP

Tissue non-specific alkaline phosphatase (described in section 1.2) is responsible for the hydrolysis of pyrophosphate to phosphate, therefore simultaneously depleting the cell of pyrophosphate and increasing the levels of phosphate. This function of TNAP is essential in the process of bone mineralization, which is described later in this chapter, and is emphasized by the severe bone pathology observed in subjects who carry functional mutations in this enzyme (Millan and Whyte, 2016).

1.3.2.1.2 Ectonucleotide pyrophosphatase phosphodiesterase – 1

Ectonucleotide pyrophosphatase phosphodiesterase-1 (ENPP-1), formerly known as plasma cell membrane glycoprotein-1 (PC-1), is a homodimeric transmembrane glycoprotein of approximately 230kDa (Goldfine et al., 2008). It has an N-terminal transmembrane domain, a short cytoplasmic domain and a large extracellular domain (Goldfine et al., 2008). This enzyme uses its pyrophosphatase activity to catalyze the breakdown of adenosine triphosphate (ATP) to pyrophosphate through the hydrolysis of the phosphodiester I bond of the ATP molecule (Johnson et al., 2000). It is expressed in numerous cell types including osteoblasts, chondrocytes and adipocytes (Goldfine et al., 2008, Johnson et al., 2000, Liang et al., 2007). Within bone the

function of ENPP-1 is to maintain an inhibitory concentration of extracellular pyrophosphate preventing mineralization (Johnson et al., 2000)

The chromosomal area in which ENPP-1 is located (6q22-23) has been identified as a region highly associated with the obese phenotype (Korostishevsky et al., 2010). The level of ENPP-1 expression, after a brief increase in the initial 24 hours, has been shown to decrease during the course of adipogenesis, indicative of a suppressive role within differentiation (Liang et al., 2007). With an overexpression of ENPP-1, adipogenesis and cell growth is decreased; however this is not correlated with an increase in cell death (Liang et al., 2007).

In addition, the ENPP-1 enzyme has been linked to insulin resistance (Goldfine et al., 2008). Thus, ENPP-1 binds to the insulin receptor, inhibiting its tyrosine kinase signalling activity (Santoro et al., 2009). The enzyme is overexpressed in target tissues of insulin in individuals with type 2 diabetes and insulin resistance and this increase is seen prior to the development of diabetes (Maddux et al., 1995).

1.3.2.1.3 Human homologue of the progressive ankylosis gene product

The human homologue of the progressive ankylosis gene product (ANKH) is the human homologue of the murine protein progressive ankylosis (ANK), which share the same function - to transport pyrophosphate across cellular membranes. The ANKH and ANK genes share a 98% sequence homology with amino acids differing in 8

positions (Ho et al., 2000, Gurley et al., 2006). The ANKH gene is located on chromosome 5p and it encodes a multi-pass transmembrane protein which acts to transport polar pyrophosphate across the cell membrane (Ho et al., 2000, Zhao et al., 2012).

1.3.2.1.4 Class III phosphate transporter

Phosphate is unable to cross the cell membrane passively, and maintenance of the intracellular phosphate balance is mediated by transporters. Transport of phosphate across the membrane requires the sodium-coupled phosphate transporter, class III phosphate transporter (PiT) (Kim et al., 2010a, Beck, 2003). This protein crosses the membrane multiple times and is considered to be a type III integral membrane protein (Khoshniat et al., 2011).

1.3.3 The mineralization pathway

The best understood function of TNAP is to mediate bone mineralization. The mechanism through which it functions within bone is through modulating the levels of both pyrophosphate and phosphate. It functions together with ENPP-1, ANKH and PiT to control the phosphate/pyrophosphate balance within osteoblasts and the extracellular environment in which mineralization occurs (Figure 1.3).

Bone mineralisation involves the formation of hydroxyapatite crystals which are insoluble in the extracellular milieu (Balcerzak et al., 2003). Hydroxyapatite crystals are formed through the interaction of calcium ions (Ca^{2+}) and inorganic phosphate (Prosdocimo et al., 2009). Inorganic phosphate is known to stimulate bone mineralization whilst inorganic pyrophosphate inhibits this process (Johnson et al. 2000). Thus, TNAP is able to promote mineralization in osteoblasts, by counteracting the inhibitory effect of extracellular inorganic pyrophosphate as well providing the necessary phosphate for mineralisation.

Mutations within TNAP, which decrease its activity, have been reported. These mutations result in the development of a condition known as hypophosphatasia (Millan and Whyte, 2016). Loss of function of TNAP results in defective bone mineralisation (which may be fatal), the severity of which is determined by the mutation present in the TNAP gene (Millan and Whyte, 2016). The occurrence of this disease demonstrates the importance of TNAP function for the mineralisation of bone.

Mineralisation is inhibited through ENPP-1 activity. This enzyme is located on the osteoblast surface membrane where it functions to catalyse the hydrolysis of ATP to inorganic pyrophosphate (Johnson et al., 2000). Inorganic pyrophosphate accumulates both intracellularly and extracellularly, with the intracellular inorganic pyrophosphate being transported out of the cell through ANK (Ho et al., 2000). The combined actions of ANKH and ENPP-1 result in an increased extracellular pyrophosphate concentration, which is inhibitory to the formation of the hydroxyapatite crystals (Kim et al., 2010a, Kim et al., 2010b). Mutations in ANKH have been linked to skeletal abnormalities (Malkin et al., 2006)

In order for mineralisation to proceed it is necessary that the elevated extracellular pyrophosphate concentration is alleviated. The action of TNAP is essential to reduce this pyrophosphate concentration where it catalyses the hydrolysis of pyrophosphate to phosphate. With the high pyrophosphate concentration removed, phosphate is free to associate with Ca^{2+} within extracellular microvesicles (which originate from the plasma membrane) to form hydroxyapatite crystals (Balcerzak et al., 2003, Muralidharan-Chari et al., 2010). The Ca^{2+} and phosphate are taken up into the microvesicles through ion channels where the hydroxyapatite crystals are formed. Once the crystals reach a given length they are released into the extracellular milieu (Balcerzak et al., 2003), resulting in mineralisation of bone. In addition, TNAP-generated phosphate enters the cell through PiT (Ronchetti et al., 2013). The TNAP-generated phosphate enters the nucleus where it functions as a transcription factor of genes important for osteoblast differentiation (Beck, 2003) (Figure 1.3).

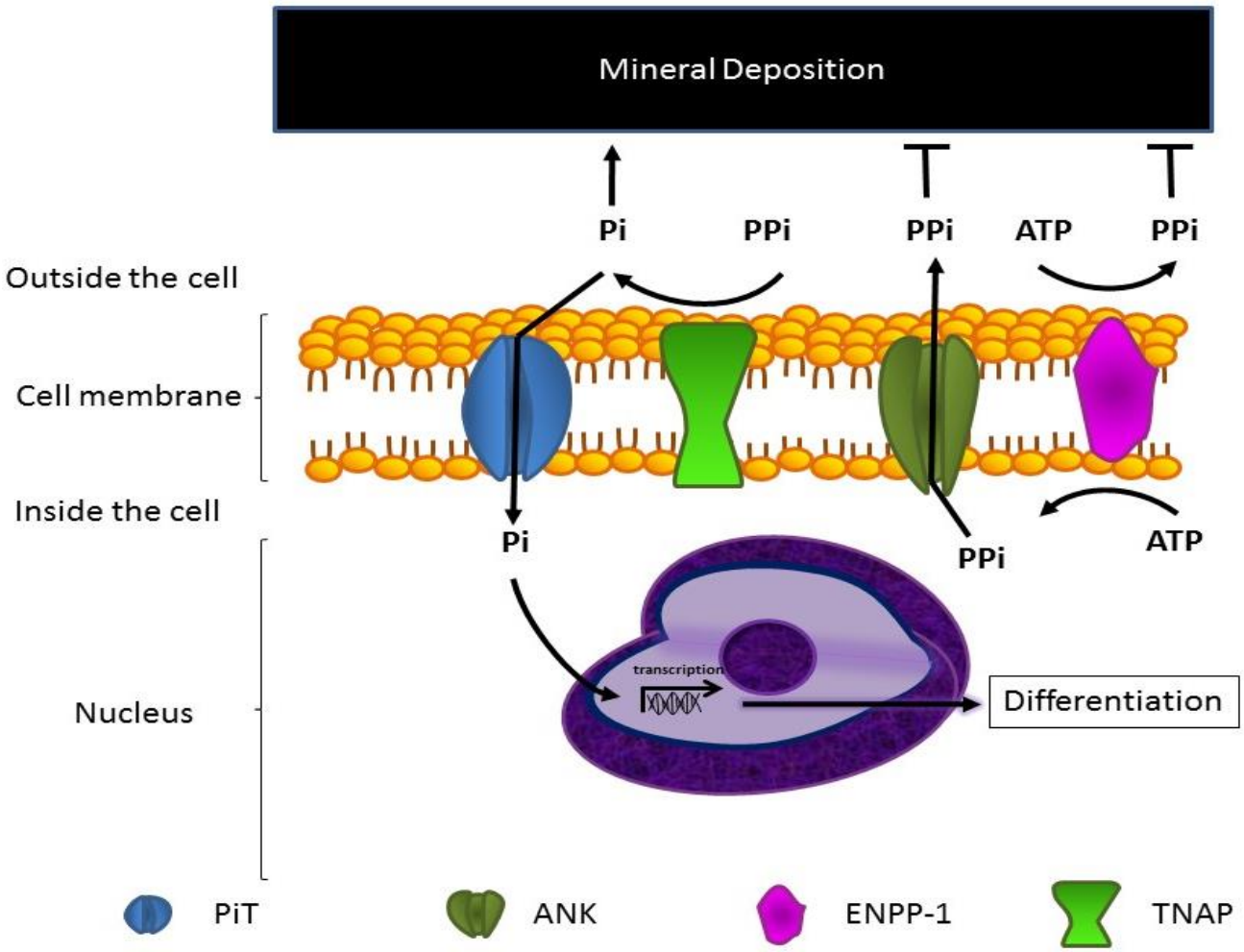

Figure 1.3: TNAP functions in bone mineralisation through the control of the pyrophosphate/phosphate balance, both intracellularly and extracellularly. Within the context of mineralisation, ENPP-1 generates pyrophosphate through the hydrolysis of ATP. Intracellular pyrophosphate is removed from the cell into the extracellular milieu through ANK generating a pyrophosphate concentration which is inhibitory to mineralisation. TNAP acts to break down the inhibitory extracellular pyrophosphate, allowing mineralisation to progress the TNAP-generated phosphate which either combines with calcium to form hydroxyapatite crystals of enter the osteoblast through PiT where it acts as a transcription factor within the nucleus inducing the expression of genes essential for osteoblast differentiation. Figure adapted from Ronchetti et al (2013)

1.3.4 TNAP-generated phosphate as a differentiation molecule

Phosphorus, the second most abundant mineral in the human body, is found mainly in the body as inorganic phosphate in the form of H_2PO_4 or HPO_4 (Khoshniat et al., 2011). Inorganic phosphate is essential for life and is found in all cells of the body. Inorganic phosphate is incorporated into sugar phosphates, phospholipids, and nucleic acids. Whilst the majority of inorganic phosphate within the body is found in bone, it is estimated that 14% is located within soft tissues (Khoshniat et al., 2011).

Levels of phosphate change throughout the human lifespan, with the highest levels being seen in the neonate. This is indicative of a role for phosphate within the differentiation of tissues (Khoshniat et al., 2011, MacGregor et al., 1995).

The role of phosphate within bone mineralization has long been understood. More recently inorganic phosphate has been demonstrated to be essential for the differentiation of numerous cell types including osteoblasts, smooth muscle cells, fibroblasts, chondrocytes and bone marrow stromal cells (Naviglio et al., 2006, Beck, 2003, Hamade et al., 2010). Inorganic phosphate is known to regulate gene expression (Naviglio et al., 2006, Hamade et al., 2010, Beck, 2003), and the role of phosphate in this process has been widely investigated over the last 20 years.

Due to the importance of phosphate in the mineralization process, many studies have indicated the importance of phosphate within the osteoblast. In 2000 George Beck

and colleagues showed that phosphate was able to specifically induce osteopontin gene expression within a murine osteoblastic cell line, MC3T3-E1 (Beck et al., 2000). Subsequent analysis of proteins upregulated within the osteoblast show that phosphate induces cell proliferation, and increases mRNA and protein expression of factors involved in oxidative phosphorylation, extracellular matrix proteins and nuclear factor E2–related factor 2 (NRF2), amongst others (Conrads, 2005, Beck et al., 2003).

Fujita *et. al*. showed that phosphate was able to bind to the promotor of type X collagen in chondrocytes and directly increase type X collagen expression (Fujita et al., 2001b). Phosphate was additionally shown to promote the export of Runt-related transcription factor-2 (RUNx2)/ core binding factor alpha 1 (CBfa1) within chondrocytes, osteoblast and osteoclasts and decrease osteocalcin expression (Fujita et al., 2001a). Furthermore, high levels of extracellular phosphate are able to inhibit the differentiation of osteoclasts through the upregulation of osteoprotegrin mRNA expression (Kanatani et al., 2003).

It is therefore clear that phosphate is able to act as a transcription regulator in numerous cell types and its utility as a transcription factor may be wide spread due to its high bioavailability within all the cells of the body.

It can therefore be seen that TNAP has an important role in the control of bone mineralization. However, TNAP is also expressed in preadipocytes and the following section will describe its role in intracellular lipid accumulation (ICLA).

1.3.5 Tissue non-specific alkaline phosphatase is a positive mediator of adipogenesis and intracellular lipid accumulation (ICLA) in the adipocyte

An important role for TNAP in the regulation of adipogenesis has been shown (Ali et al., 2006b, Ali et al., 2006a, Ali et al., 2005). Within the preadipocyte, ALPL mRNA and protein expression is increased over the duration of differentiation and ICLA (Ali et al., 2005, Ali et al., 2006b). Further, the inhibition of TNAP activity results in the cessation of adipogenesis in the 3T3-L1 mouse preadipocyte cell line and in human mammary gland preadipocytes (Ali et al., 2006b, Ali et al., 2005). In addition, TNAP knockout mice show decreased fat mass in addition to skeletal abnormalities (Narisawa et al., 1997). This data shows that functional TNAP is a prerequisite for intracellular lipid accumulation during the differentiation of preadipocytes into mature adipocytes.

1.3.5.1 Adipogenesis

Adipose tissue contains both immature (preadipocytes) and mature adipocytes. The maturation of preadipocytes contributes to hyperplasia. The process of maturation of the preadipocyte is termed adipogenesis, during which various mechanisms work together to allow the differentiation of the preadipocyte into a mature adipocyte. During adipogenesis triglycerides accumulate in the cytoplasm of the cell. Once the adipocyte is fully mature, it contains one or more large triglyceride-containing lipid droplet (Shoham and Gefen, 2012, Lowe et al., 2011).

During differentiation (Figure 1.4), genes which code for proteins that give rise to the mature cell phenotype, including the accumulation of lipid droplets in the cytoplasm of the cell, become expressed via a process that is controlled by a number of transcription factors. These factors include CCAAT enhancer binding protein alpha (C/EBPα) and peroxisome proliferator-activated receptor gamma (PPARɣ). The expression of these transcription factors occurs rapidly on stimulation of differentiation (Lowe et al., 2011, Shoham and Gefen, 2012, Tang et al., 2006).

Various factors have been identified, including hormones (Santoro et al., 2009), enzymes (Ali et al., 2005), integrins (Liu et al., 2005), microRNAs (Son et al., 2014) and transcription factors (Birsoy et al., 2008), as regulators of adipogenesis; however the full molecular pathway has yet to be elucidated.

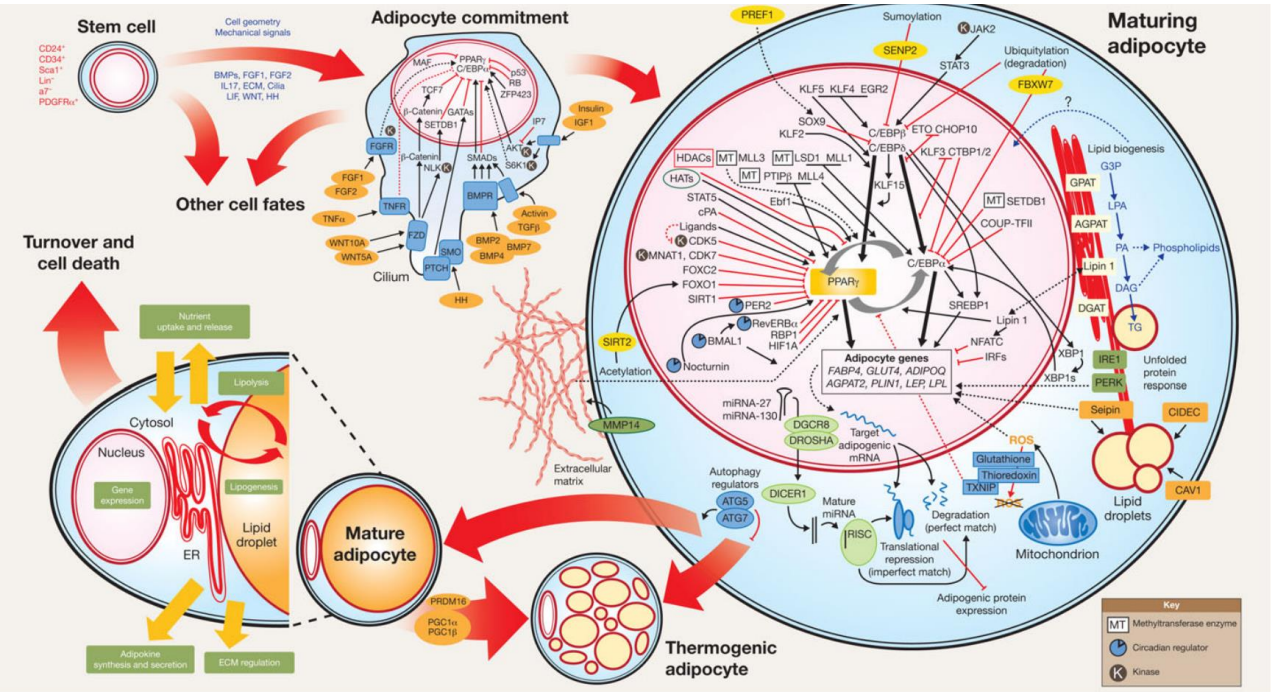

Figure 1.4: Schematic representation of the known molecular pathways involved in the differentiation of the preadipocytes into the adipocyte (Lowe et al., 2011) (Image used with permission).

Interestingly, TNAP has also been shown to play a role in *de novo* lipogenesis where levamisole mediated inhibition of TNAP resulted in a reduction in the expression of the lipogenic enzyme glycerophosphate dehydrogenase (DPDH), which acts to reduce dihydroxyacetone phosphate into glycerol 3-phosphate. This is further reduced to glycerol by DPDH (Hernandez-Mosqueira et al., 2015), which is used in the synthesis of triglycerides.

The mechanism by which TNAP may modulate cellular lipid accumulation is not known. However, its role in bone mineralization has been well characterized and the following section will describe similarities between mineralization and ICLA and suggest a possible mechanism, paralleling that seen in osteoblasts, by which TNAP may influence lipid storage.

1.4 Tissue non-specific alkaline phosphatase: a phosphate generator in both bone and adipose tissue?

Polymorphisms in genes coding for proteins involved in the mineralization pathway have been shown to be associated with obese phenotypes in humans (Meyre et al., 2005, Korostishevsky et al., 2010, Goldfine et al., 2008). Thus, polymorphisms within the ANKH gene have been associated with body mass index (weight in kg / (height in m)^2), levels of epidermal growth factor receptor (EGFR) (enhances adipogenesis) and leptin (peptide hormone which regulates body weight) as well as waist-to-hip ratio. Polymorphisms within ALPL have been associated with increased waist-to-hip ratio and EGFR levels, whereas polymorphisms within the ENPP-1 gene have been associated with BMI, and leptin levels (Korostishevsky et al., 2010). Furthermore,

mice harboring knockout mutations of the gene coding for TNAP, have very little adipose tissue (Narisawa et al., 1997). Mineralization-associated polymorphisms which are linked to aspects of obesity are summarized in Table 1.1.

In addition to gene polymorphisms, a study by Ali and colleagues looking at relative TNAP activity in the preadipocytes of different ethnic groups found that the level of TNAP was higher in the black South African population than in their white counterparts. This increased TNAP activity was associated with higher levels of obesity (Ali et al., 2015).

Table 1.1: Polymorphisms within genes involved in mineralisation and maintaining the pyrophosphate phosphate balance are associated with markers of obesity.

Gene	SNP	Obesity trait	SNP details	Citation
ALPL	rs869180 rs869179 rs1472563 rs1780314 rs10465542	Epidermal Growth Factor Receptor (EGFR)	C>T (intron variant) C>T (intron variant) C>T (intron variant) C>G (intron variant) C>G (intron variant)	(Korostishevsky et al., 2010)
ALPL	rs1780321 rs6667242 rs1780320 rs5024467	Hip-to-waist ratio	A>G A>G C>T (intron variant) C>T (intron variant)	(Korostishevsky et al., 2010)
ANKH	rs17297276 rs412056 rs826358 rs6895973 rs17297276	EGFR	C>T (intron variant) C>G (intron variant) A>G (intron variant) A>C C>T (intron variant)	(Korostishevsky et al., 2010)
ANKH	rs6895973 rs17297296	Leptin	A>C C>T	(Korostishevsky et al., 2010)

Table 1.1 continued

	rs412056		A>G (intron variant)	
ANKH	rs6895973 rs17297276 rs1353258 rs3006096 rs863118	BMI	A>C C>T (intron variant) C>T (intron variant) C>T (non-coding transcript variant) A>C>G (intron variant)	(Korostishevsky et al., 2010)
ANKH	rs6895973 rs17297276 rs412056	Hip-to-waist ratio	A>C C>T (intron variant) A>G (intron variant)	(Korostishevsky et al., 2010)
ENPP-1	Rs7754561 Rs9373000 Rs6569765	Leptin	A>G (untranslated region variant) A>G A>G	(Korostishevsky et al., 2010)
ENPP-1	Rs7754561 Rs9373000	BMI	A>G (untranslated region variant) A>G	(Korostishevsky et al., 2010, Goldfine et al., 2008, Meyre et al., 2005)

The expression of proteins within both bone and preadipocytes that are involved in the control of phosphate levels, and the observation that mutations or polymorphisms in their genes leads to bone pathology and changes in body fat mass or distribution strongly suggests that phosphate may be involved in both bone mineralization and preadipocyte lipid storage, possibly via its effects on gene transcription, as described in the following section.

1.5 Nuclear factor E2–related factor 2 (NRF2) in bone and adipocytes

In osteoblast precursor cells (MC3T3-E1), it has been shown that phosphate promotes NRF2 gene expression (Beck et al., 2003). This protein is a cap-n-collar basic leucine zipper (bZIP) transcription factor. The NRF2 heterodimerises with other transcription factors from the bZIP family including small musculoaponeurotic fibrosarcoma (MAF) proteins. The heterodimers then bind to *cis* acting elements known as antioxidant response elements (AREs) in the promoter region of genes (Hou et al., 2012) and in osteoblast precursor cells this ultimately leads to cell maturation. Interestingly, NRF2 has been shown to regulate the transcription of c/EBPβ and PPARγ, which are terminal factors responsible for adipogenesis (Chen et al., 2013). Activation of AREs by NRF2 occurs early in adipogenesis, resulting in the transcription of C/EBPβ. Deficiency of NRF2 in mouse preadipocytes and embryonic fibroblasts results in impaired adipogenesis (Pi et al., 2010). Furthermore, NRF2 knockdown mice display a decrease in fat mass, and are resistant to high fat diets (Pi et al., 2010) and *ob/ob* mice that do not express NRF2 in their adipocytes, showed reduced body weight, but also develop insulin resistance and hyperglycaemia (Xue et al., 2013).

As NRF2 has been implicated in adipogenesis, and it has been shown that in osteoblasts TNAP-generated phosphate can bind directly to the promoter region of NRF2 and induce gene expression, it is possible that the function of TNAP within adipocytes is to stimulate the expression of NRF2 (via phosphate generation) and thereby the transcription of C/EBPβ resulting in the progression of adipogenesis.

Tissue non-specific alkaline phosphatase may function to stimulate ICLA via a number of possible mechanisms. It could act to control the phosphorylation state of proteins that are integral to ICLA, function to remove PPi or generate phosphate, which then initiates the transcription of genes whose products play a role in ICLA. It is also possible that it may interact with proteins involved in the control of ICLA, and this will be described below.

1.6 Does TNAP heterodimerise in adipogenesis

It is possible that another mechanism by which TNAP may modulate ICLA is by physical interaction with other peptides that play a role in the control of cellular lipid accumulation. Le Du and colleagues demonstrated the ability of tissue specific alkaline phosphatase to heterodimerize through their monomer-monomer interface, whereas TNAP was not able to form heterodimers with the tissue specific variants (Le Du and Millan, 2002). However, there may be other sites within TNAP that allow for heterodimer formation, and this does not eliminate the possibility that TNAP binds to other proteins through its monomer-monomer interface.

A useful tool to determine what other proteins may bind to TNAP is *in silico* analysis using prediction models that are able to model possible protein-protein interactions. Thus, the STRING program consists of a database of protein-protein interactions which have previously been predicted or proven experimentally. The interactions shown by STRING may represent a direct interaction or alternatively a functional association with another protein (Szklarczyk et al., 2015). Within the STRING database a direct interaction of murine TNAP with TNF receptor-associated factor 2 (TRAF 2) is shown (http://string-db.org/). Due to TRAF 2's known function in inhibiting apoptosis (Karl et al., 2014), and it's involvement in the WNT10B pathway, which functions within adipogenesis (Katoh and Katoh, 2007), it was decided to further investigate the possible interaction of TNAP with TRAF 2 in the context of lipid accumulation.

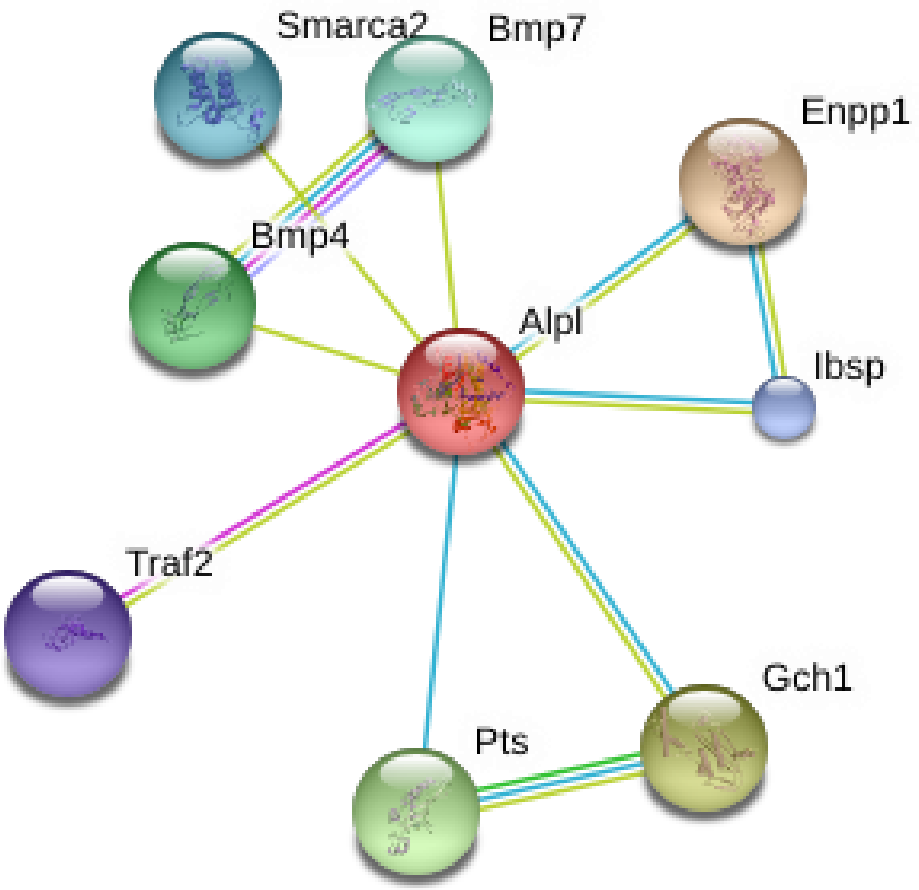

ALPL = Tissue non-specific alkaline phosphatase
SMARCA2 = SWI/SNF related, matrix associated, actin dependent regulator of chromatin, subfamily a, member 2
ENPP1 = ectonucleotide pyrophosphatase/phosphodiesterase 1
IBSP = integrin-binding sialoprotein
TRAF2 = TNF receptor-associated factor 2
GCH1 = GTP cyclohydrolase 1
BMP4 = bone morphogenetic protein 4
BMP7 = bone morphogenetic protein 7
PTS = 6-pyruvoyl-tetrahydropterin synthase

Figure 1.5: STRING protein-protein interaction graphic showing predicted and experimentally shown functional and direct interactions between TNAP (ALPL) and other proteins. The presence of the pink line is indicative of experimental data showing an interaction. Within this diagram, the pink line connecting TNAP to TRAF 2 is extrapolated from experiments showing an interaction between the human homologs of these proteins. The blue line is indicative of interactions from obtained from curated databases and the light green lines are indicative of functional partners identified through textmining. (http://string-db.org/cgi/network.pl?taskId=G7AAte5M8OVa&sessionId=gLrYVAv43EGs)

1.6.1 TRAF 2

The TRAF intracellular proteins were originally identified as signalling adaptors, which bind to the cytoplasmic region of the tumour necrosis factor receptors (TNFR) (Xie, 2013). The TRAF 2 protein contains a C-terminal TRAF domain which is involved in protein-protein interactions and therefore has an important role in linking two proteins together. This peptide is a crucial component of the TNFR superfamily signalling pathway, and is involved in the initiation of nuclear factor kappa light chain-enhancer of activated B cells (NF-κβ) and mitogen activated protein kinase (MAPK) signalling cascades (Lee and Lee, 2002).

The TRAF 2 molecule has been implicated in the differentiation pathways for numerous cells. Thus, TRAF 2 is known to mediate the development of Th17 (a distinct subset of T-cells which produces pro-inflammatory cytokines including IL-17 and IL-23) through the activation of IL-6 (Nagashima et al., 2016) and to be important in the development of the anteroventral periventricular nucleus (an oestrogen receptor dense region of the brain which mediates luteinizing hormone (LH) surges) (Petersen et al., 2012, Stockinger and Veldhoen, 2007). In addition, TRAF 2 has been shown to play a role in the WNT10B loop, which is a negative feedback loop in adipogenesis (Katoh and Katoh, 2007).

It is therefore feasible that TRAF 2, together with TNAP plays a role in the intracellular storage of lipids.

Numerous data therefore suggests that TNAP plays a role in the storage of neutral lipids i.e. triglycerides, within preadipocytes, but the exact mechanism by which it does this is not known. Furthermore, preadipocytes are not the only cell type that stores lipids, and triglycerides are not the only type of neutral lipid that can be stored within cells. The next section of this chapter will therefore discuss intracellular storage of both triglycerides and cholesterol in various cell types and the possible role of TNAP in this process.

1.7 TNAP and intracellular accumulation of all neutral lipids?

The ability of TNAP to regulate intracellular lipid accumulation is not only in seen in preadipocytes, but also in the human hepatoma cell line (HEPG2). Within HEPG2 cells inhibition of TNAP results in the cessation of the accumulation of triglycerides within these cells (Chirambo et al., 2017). This phenomenon suggests that TNAP may be involved in the intracellular lipid accumulation of neutral lipids within multiple cell types in the body. It is possible, however, that the ability of TNAP to mediate lipid accumulation, may be a function of its ability to influence the expression of lipogenic genes as described by Hernandaz-Mosqueira and colleagues (Hernandez-Mosqueira et al., 2015) early in the differentiation process.

1.8 Intracellular storage of neutral lipids

The triglycerides stored in both adipose tissue and hepatocytes are neutral lipids. Cholesterol, which is the building block of steroid hormones, is also classified as a

neutral lipid. Therefore, there are two predominant neutral lipids found within humans (Figure 1.6). Neutral lipids are essential for life. They have a net charge of 0, and they are also highly hydrophobic. Due to these properties, neutral lipids are only able to be incorporated into the cell membrane at very low levels (Athenstaedt and Daum, 2006, Pakkanen et al., 2011).

Triglycerides have several important physiological roles within the body. They represent the body's stored energy reserves, and are found mainly within the lipid droplets of the cells of adipose tissue (Schneider, 2016). Furthermore, triglycerides act as the substrate for the synthesis of phospholipids and as signaling molecules (Athenstaedt and Daum, 2006, Pakkanen et al., 2011).

Cholesterol is stored within lipid droplets in cells of the adrenal cortex, the ovaries and the testes in the form of cholesterol esters (Kraemer et al., 2013). The storage of cholesterol is essential for the production of steroid hormones within the body (Miller and Auchus, 2011).

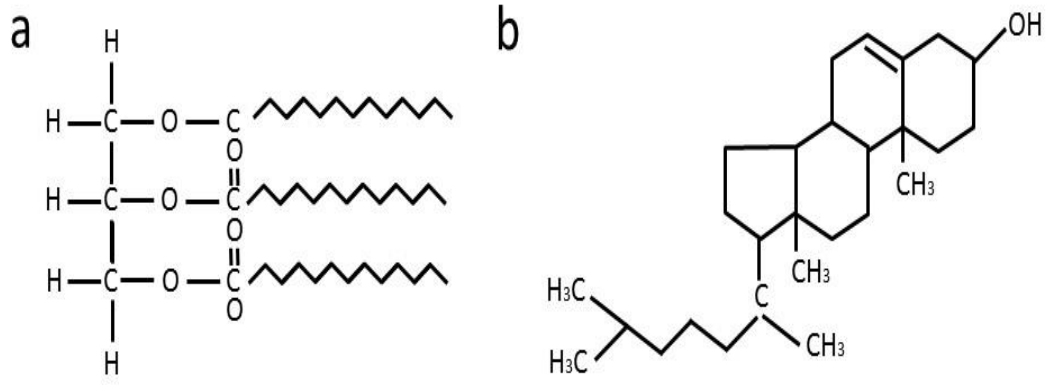

Figure 1.6: Chemical structure of (a) triglyceride, consisting of a glycerol backbone and three fatty acids and (b) cholesterol consisting of steroid rings with a hydroxyl group, a hydrogen tail and two methyl groups.

In order to utilize triglycerides and cholesterol, they need to be stored within the body as the hydrophobic core of a lipid droplet. The processes involved in the storage of neutral lipids within droplets have been well documented, in particular regarding triglyceride storage in adipose tissue and cholesterol esters in the adrenal cortex. However, the complete molecular pathways involved have yet to be fully elucidated. Due to the importance of these lipids within the body, and disorders associated with increased lipid storage such as obesity (and its associated co-morbidities) and steatohepatitis, it is important to elucidate the full mechanisms through which lipids are stored within the cells of the body.

1.9 Triglyceride and cholesterol containing lipid droplets

Lipid droplets are composed of an outer phospholipid monolayer integrated with proteins important for stabilization and lipid droplet function (Yamaguchi et al., 2015). The phospholipid monolayer encloses a core containing neutral lipid (Shen et al., 2016).

Triglycerides are stored mainly in the adipocyte (Schneider, 2016). Adipocyte lipid droplets are relatively large reaching sizes of greater than 50µm and occupy almost the entire volume of the adipocyte (Shen et al., 2016). Cholesterol ester lipid droplets within the adrenal cortex, unlike the droplets found in adipocytes are more numerous and smaller (0.5-1.5µm in diameter) (Shen et al., 2016).

The lipid droplets of steroidogenic and adipose cells are similar (Servetnick et al., 1995) with both expressing various proteins on the surface of the lipid droplets, including perilipin A, adipose differentiation related protein (ADRP) and p200 (Fong et al., 2002). A recent proteome analysis comparing the lipid droplet proteins on cholesterol ester and triglyceride containing droplets from granuloma cells identified 278 shared lipid proteins, with only 40 proteins unique to the triglyceride droplets and 68 unique to the cholesterol ester droplets (Khor et al., 2014). This huge overlap of proteins indicates that many proteins may exhibit shared functions on both the triglyceride lipid droplet and the cholesterol ester lipid droplet.

1.9.1.1 Perilipin 1

Perilipins are phosphoproteins which are located solely on the surface of lipid droplets (Servetnick et al., 1995). There are three different types of perilipins associated with lipid droplets housing neutral lipids. Perilipin A and Perilipin B are generated through differential splicing of the same mRNA transcript (Servetnick et al., 1995). Perilipin A, a 57 kDa glycosylated protein is found on lipid droplets of both adipocytes and steroidogenic cells (Servetnick et al., 1995). Perilipin B is found in smaller quantities on the lipid droplet membranes of both adrenal and adipogenic droplets. The third 42 kDa variant, perilipin C is found only on the lipid droplets containing cholesterol esters (Servetnick et al., 1995) (Figure 1.7). The amount of perilipin increases proportionally to the amount of lipid within the cell (Brasaemle et al., 1997)

1.9.1.2 Adipose differentiation related protein

Adipose differentiation related protein (ADRP), also known as perilipin 2, is a 50kDa protein whose expression is upregulated during differentiation of the preadipocytes (Fong et al., 2002). It is considered an early marker of adipocyte differentiation however its role in adipogenesis has not been established. It is thought that ADRP may function to stabilize the lipid droplet (Gao and Serrero, 1999). The presence of ADRP on lipid droplets in the liver and adrenal cortex supports this view.

1.9.1.3 p200

The phosphoprotein p200 is located on the Golgi apparatus and on lipid droplet membranes of both steroidogenic and adipogenic cells (Fong et al., 2002, Narula and Stow, 1995). It plays a role in vesicle trafficking and the budding of vesicles (Narula and Stow, 1995).

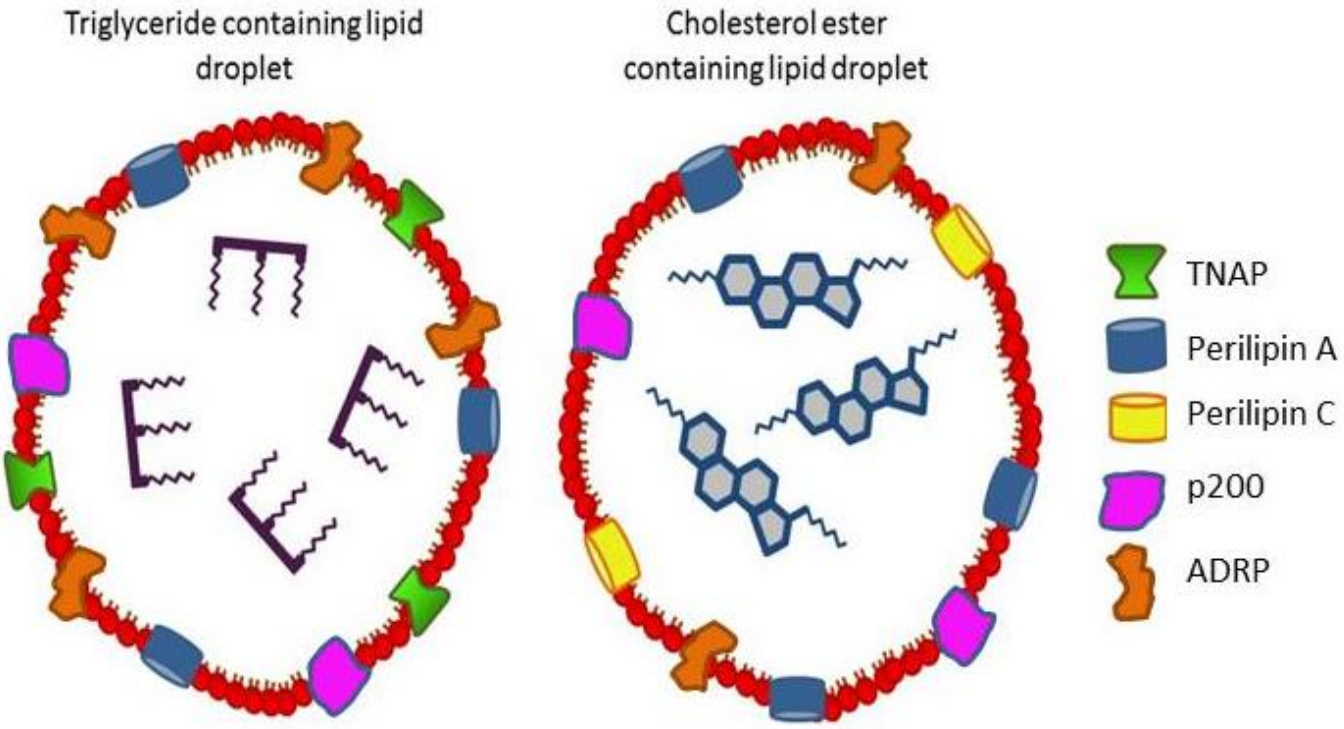

Figure 1.7: Schematic representation of steroidogenic and adipogenic lipid droplets. Perilipin A is the predominant perilipin found on both lipid droplets. Within cells containing cholesterol esters, a second perilipin, perilipin C is found on the lipid droplet surface. TNAP is located on the adipocyte lipid droplet membrane, however it is not known whether it is expressed on the lipid droplets containing cholesterol esters.

1.10 Tissue Non-specific Alkaline Phosphatase is found in the adrenal cortex

Immunocytochemical studies have identified TNAP in the cells of the adrenal cortex (McComb, 1979). Adipocytes and osteoblasts are both of mesenchymal origin, and it has been shown that it is possible to reprogram adipocytes into osteoblasts (Takahashi, 2011). In addition, the cells of the adrenal cortex are derived from the same mesenchymal origin (Yazawa et al., 2014). Thus, these three cell types may share some common molecular pathways that control cellular differentiation (including the mechanisms for storing neutral lipids) which may involve TNAP function (Figure 1.8).

The function of TNAP within the adrenal cortex is unknown. However, given the similarities between lipid droplets of steroidogenic and adipocytic cells and the presence of TNAP in both, it is possible that TNAP is involved in the control of lipid droplet formation in cells of the adrenal cortex.

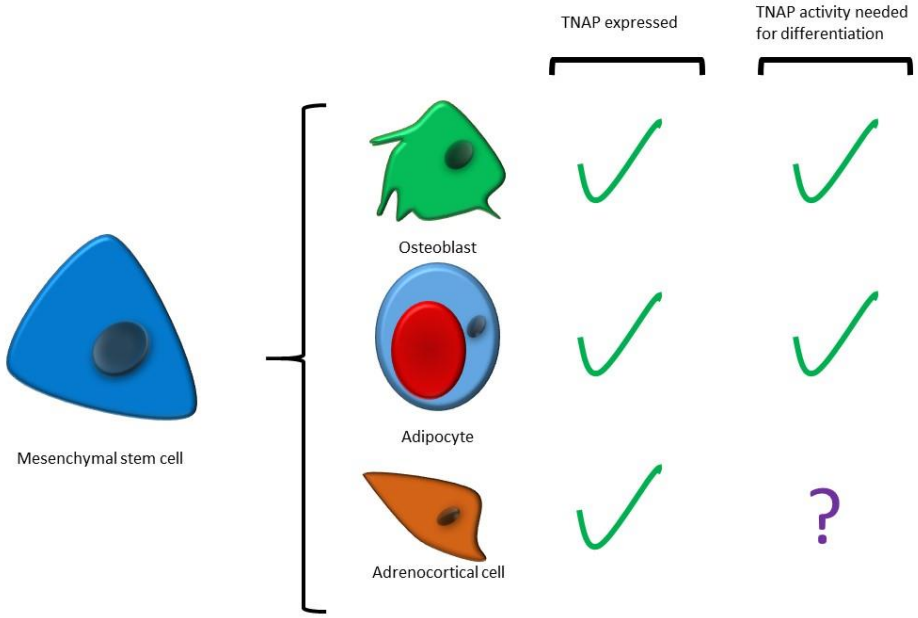

Figure 1.8: Mesenchymal stem cells are able to differentiate into numerous cells including osteoblasts, adipocytes and adrenocortical cells. It is further known that TNAP is expressed in all three of these cell types and its activity is necessary for the differentiation of osteoblasts and adipocytes. The importance of TNAP in the adrenocortical cells remains unclear.

1.11 The Adrenal Gland

The adrenal gland, located above the kidney, is composed of two embryonically distinct portions, the inner medulla and the outer cortex. The adrenal cortex itself is further divided into 3 zones, the zona glomerulosa, the zona fasciculata and the zona reticularis (Figure 1.9) (Wang and Rainey, 2012). The adrenal cortex is responsible for the synthesis of stress hormones such as cortisol. In the adrenal cortex, cholesterol is needed to synthesize corticosteroids.

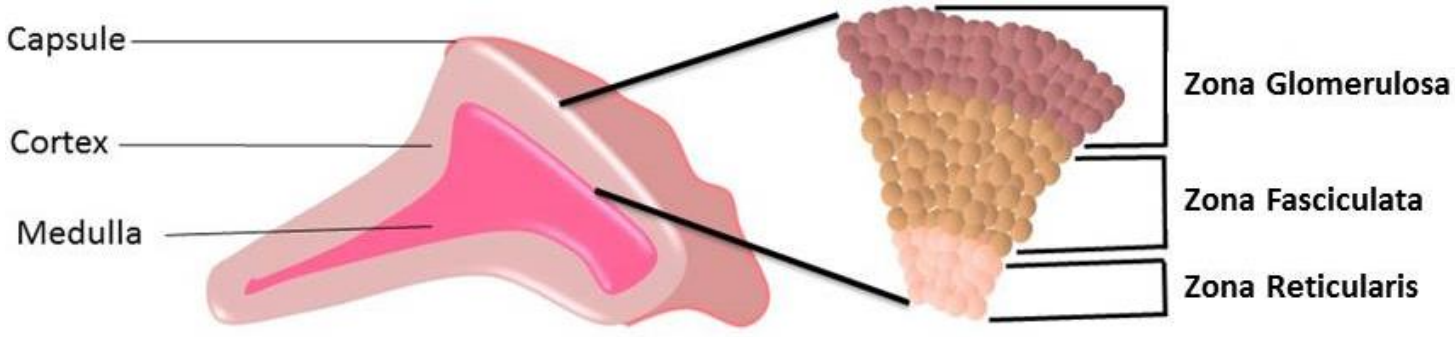

Figure 1.9: Schematic representation of the adrenal gland. The adrenal gland is composed of two embryonically distinct portions, the cortex and the medulla which are enclosed in a capsule. The adrenal cortex which is where cholesterol is stored in the form of cholesterol esters, is itself divided into three regions. The regions of the adrenal cortex are the zona glomerulosa, the zona fasciculata and the zona reticularis.

Steroid hormones are produced primarily in the cells of the adrenal gland and gonads. The accumulation of cholesterol esters within the adrenal cortex is an initial, vital step in the synthesis of steroid hormones. Cholesterol accumulates within the endoplasmic reticulum (ER) where it is converted into cholesterol esters (Kraemer et al., 2013). The cholesterol esters are stored within lipid droplets that are derived from budding of the ER membrane and which reside in the cytoplasm of the cells of the adrenal cortex (Listenberger and Brown, 2008).

1.11.1 Cholesterol accumulation in the adrenal cortex

In the adrenal gland, cholesterol may be synthesized *de novo* from acetate, but mostly the cholesterol comes from low density lipoprotein (LDL)-cholesterol obtained from

dietary cholesterol (Miller and Auchus, 2011). The cholesterol is stored in the form of cholesterol esters in lipid droplets in the cytoplasm of the cells of the adrenal cortex. Unesterified cholesterol accumulates within the endoplasmic reticulum of the adrenal cortex where fatty acyl coA: cholesterol acyltransferase converts it to cholesterol esters. The ER membrane then buds off to form cholesterol ester- containing lipid droplets (Kraemer et al., 2013).

1.11.2 Hydrolysis of cholesterol esters

Cholesterol esters need to be hydrolysed to free cholesterol (FC) to be biologically useful. As early as 1982, it was noted that the as yet unknown enzyme responsible for this process, termed neutral cholesterol ester hydrolase (nCEH), was identical in size and function to hormone sensitive lipase (which functions within the adipocyte to hydrolyse triglycerides) (Cook et al., 1982). In fact, overexpression of adipocyte derived HSL within macrophage foam cells was shown to increase the hydrolysis of cholesterol esters demonstrating the ability of HSL to generate FC (Escary et al., 1998). Knockdown of HSL within the adrenal cortex results in a reduction of cholesterol ester hydrolysis by as much as 98% (Kraemer et al., 2002). It is thought that HSL is tethered to lipid droplets through binding to the phosphorylated form of perilipin during lipolysis (Clifford et al., 2000). Therefore HSL is fundamental in lipid mobilization in both the adrenal cortex and adipose tissue.

1.11.3 Steroidogenesis

The process by which cholesterol is converted to biologically active steroid hormones is known as steroidogenesis. Steroidogenesis occurs in the mitochondria (Roberts et al., 1967). Steroid hormones are all synthesized from cholesterol and therefore have very similar structures, which are all based on the 4 ring structure (Miller and Auchus, 2011) (Figure 1.10).

There are four main adrenocortical steroids which are synthesized within the adrenal cortex, namely aldosterone (synthesized within the zona glomerulosa), dehydroepiandrosterone sulfate (DHEAS) (synthesized within the zona reticularis) and cortisol and corticosterone (synthesized within the zona fasciculata) (Miller and Auchus, 2011). The conversion of cholesterol to steroids is a stepwise process which involves numerous enzymatic reactions (Luu-The, 2013) (Figure 1.10).

If TNAP is indeed involved in the accumulation of cholesterol esters within the adrenal cortex it is possible that it affects the production of steroid hormones and therefore warrants future investigation.

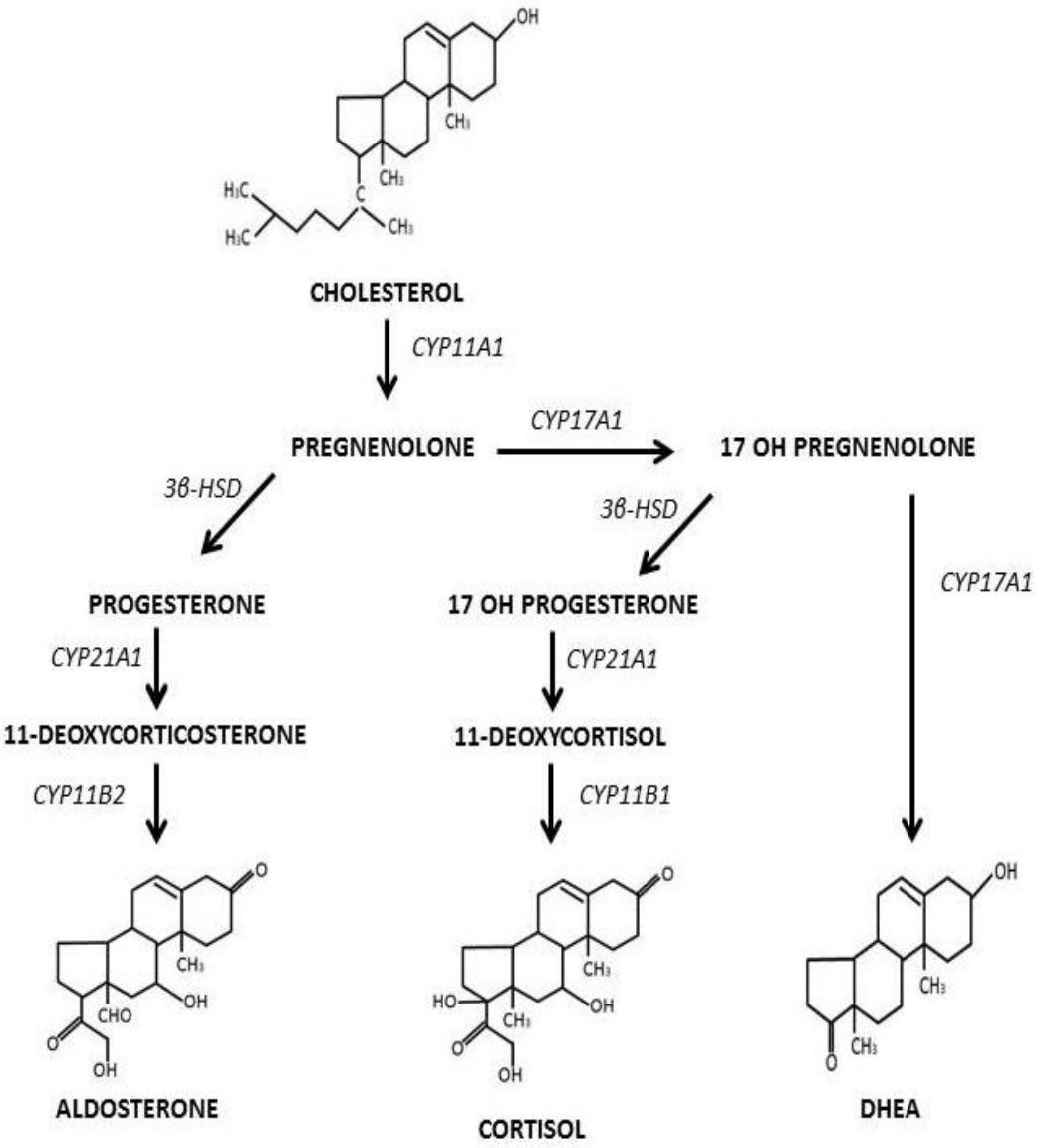

Figure 1.10: Schematic representation of the processing of cholesterol to adrenocortical steroids through enzymatic reactions (adapted from Turcu and colleagues (2015))

It can be concluded that data from the literature suggests that TNAP may act to modulate the accumulation of triglyceride in a number of different cell types via an unknown mechanism. The aims of this thesis (which will be elaborated in more detail below) are therefore to investigate the mechanism by which TNAP controls ICLA and

whether TNAP also functions in the accumulation of cholesterol ester-containing lipid droplets in steroidal cells.

1.11 Hypothesis, aims and objectives

We hypothesize that TNAP is a positive regulator of intracellular lipid accumulation in the adrenal cortex, as in the adipocyte. In addition we hypothesize that intracellular lipid accumulation within 3T3-L1 adipocytes is mediated through the ability of TNAP to generate phosphate which acts as a secondary messenger for gene expression.

Specifically we aim to:

- Determine at the sub-cellular level the mechanism(s) by which TNAP mediates ICLA during adipogenesis in the murine 3T3-L1 cell line

- Investigate whether TNAP is involved in the intracellular accumulation of cholesterol esters in the adrenal cortical cell line, Y1

These aims will be accomplished by meeting the following objectives:

- Determining the intracellular level of pyrophosphate during adipogenesis and its effect on ICLA in 3T3-L1 preadipocytes

- Determining the effect of exogenous phosphate on ICLA in 3T3-L1 preadipocytes in the presence of an inhibitor of TNAP activity

- Determining the effect of phosphate on the transcription of the gene coding for NRF2 during adipogenesis in 3T3-L1 preadipocytes

- Determining the level of expression of the TRAF2 gene during adipogenesis and the ability of the TRAF2 peptide to bind TNAP

- Determining TNAP activity during ICLA in the Y1 cell line and the effect of TNAP inhibition on this process

2 Methodology

2.1 Cell Culture

2.1.1 3T3-L1 preadipocytes

The 3T3-L1 preadipocytes are an embryonic murine preadipocyte cell line (Poulos et al., 2010), and were obtained from the American Type Culture Collection (ATCC). The cells were maintained in complete growth medium [high glucose DMEM (Lonza, Basel, Switzerland) supplemented with 10% Foetal bovine serum (FBS), 100 U/ml penicillin and 100 µg/ml streptomycin (Lonza)]. Cells were propagated in a humidified incubator at 5% CO_2. Complete growth medium was replenished twice weekly and the cells sub-cultured when confluency reached 80%. The 3T3-L1 cells were of unknown passage number, however all experiments were performed within 5 passages of each other.

2.1.2 Y1 adrenocortical cells

The Y1 cell line is derived from a tumour retrieved from a LAF_1 mouse which had been exposed to radiation. The tumour, was minimally differentiated and originated from the fasciculata zone. This cell line was utilized as it is able to accumulate cholesterol droplets within its cytoplasm (Rainey et al., 2004).

The Y1 murine adrenocortical cell line was obtained from the European Collection of Cell Cultures (ECACC). The cells were maintained in Hams F10 medium (Lonza, Basel, Switzerland) supplemented with 12.5% horse serum (PAA, Little Chalfont, United Kingdom), 2.5% FBS (Lonza), 100U/ml penicillin and 100 µg/ml streptomycin (Lonza). Cells were propagated in a humidified incubator at 5% CO_2. Growth medium was replenished twice a week and the cells sub-cultured prior to reaching 80% confluency. All cells used in all experiments had passage numbers of between 6 and 12.

2.2 Induction of intracellular lipid accumulation within cell culture models

2.2.1 Induction of triglyceride accumulation in the 3T3-L1 cell line

The 3T3-L1 preadipocytes were plated at a concentration of 3 x 10^6 cells/ml in complete growth medium in a 6 well plate. Differentiation was induced through the addition of transformation medium [complete growth medium supplemented with 500 µM 3-isobutyl-1-methyl-xanthine (Sigma, Massachusetts, USA), 255 nM dexamethasone (Sigma) and 1.83 µM insulin (Novo Nordisk, Bagsværd, Denmark)]. The cells were exposed to the transformation medium for the initial three days of the experiment. For the remainder of the experiment, the transformation medium was replaced with maintenance medium (high glucose DMEM with 1.83 µM insulin). Cells were monitored for 8 days, as substantial lipid accumulation was previously noted by this stage (Ali et al., 2005). Cells were harvested at days 1, 4 and 8 post induction of

differentiation, and compared to untreated cells (grown only in complete growth medium).

2.2.2 Induction of cholesterol accumulation in the Y1 adrenocortical cell line

The Y1 cells were plated at a density of 3 x 10^6 cells/ml and exposed to oleic acid-bovine serum albumin (BSA)-cholesterol to stimulate intracellular lipid accumulation as described by Brasaemle and colleagues (Brasaemle et al., 1997). Lipid accumulation was allowed to proceed for up to 8 days. Briefly the cell culture medium was supplemented with 400 mM of fatty acid in the form of oleic acid which was coupled to fatty acid-free BSA at a ratio of 6:1 mol:mol oleic acid to BSA and 130 mM of cholesterol. Lipid accumulation was allowed to proceed for up to 8 days.

2.3 Inhibition of TNAP activity

The activity of TNAP was inhibited using levamisole hydrochloride. Levamisole is specifically able to inhibit only TNAP and not the tissue specific alkaline phosphatases (Ali et al., 2006b). Levamisole inhibits TNAP activity through uncompetitive inhibition by binding to the residues His-434 and Tyr-371 (Kozlenkov et al., 2004) .

2.3.1 3T3-L1 cells

To inhibit TNAP activity in 3T3-L1 cells, cells were exposed to 5 mM levamisole hydrochloride (Sigma-Aldrich, Massachusetts, USA) 30 minutes prior to initiation of intracellular lipid accumulation, and throughout the experiment (Ali et al., 2005).

2.3.2 Y1 cells

To inhibit TNAP activity in Y1 adrenocortical cells, the cells were exposed to varying concentrations of levamisole, based on concentrations used on adipocytes (Ali et al., 2005). Based on optimal inhibition determined through these dose-response experiments a concentration of 5 mM was used to inhibit TNAP activity in Y1 cells in subsequent experiments. The cells were exposed to the levamisole 30 minutes prior to the initiation of intracellular lipid accumulation and throughout the experiment. The TNAP protein was extracted from cells as described below (section 2.4) and activity measured as described in section 2.6 (page 46).

2.4 Extraction of total protein from Y1 and 3T3-L1 preadipocytes

Crude protein extracts were obtained at baseline and on days 1, 4 and 8 following the initiation of intracellular lipid accumulation (section 2.2.1 and 2.2.2) as previously described (Ali et al., 2005, Brasaemle et al., 1997). Briefly cell culture medium was removed and the cells washed twice with cold phosphate buffered saline (PBS) (pH

7.2). The protein was extracted by adding 500 µl of extraction solution [tris base (1.57 mg/ml), Triton X-100 (1%) and phenylmethylsulphonyl fluoride (0.35 mg/ml)), pH 7.2] and incubating for 30 minutes. The detached cells were transferred to a microcentrifuge tube and centrifuged for 10 minutes at maximum (8000 x *g*) speed in a desktop centrifuge. The supernatant was harvested directly for the measurement of total cellular protein and TNAP activity.

2.5 Bradford Assay

Coomassie Brilliant Blue G-250 protein stain was prepared at a concentration of 100mg/50ml in absolute ethanol (Bradford, 1976). The Coomassie stain was adjusted through the addition of 100ml 85% (w/v) phosphoric acid. The stain was allowed to completely dissolve and then diluted 3 parts Coomassie/phosphoric acid to 7 parts water and filtered through 0.22 µm filter paper just before use.

An albumin standard curve was constructed ranging from 5 to 100 µg of protein in deionised water. Stain was added to both the standards and the unknown protein samples to a volume of 100 µl and allowed to incubate for 10 minutes. The standards and unknowns were measured on the Nanodrop spectrophotometer at an absorbance of 595 nm. The standard curve was generated using Excel (Microsoft, Redmond, Washington, US) by plotting concentration vs A_{595} measurements. Concentrations of the unknowns were determined through comparison to the standard curve. If the unknown readings fell out of range, they were diluted and re-measured and results adjusted according to the dilution factor.

2.6 Measurement of alkaline phosphatase activity in 3T3-L1 and Y1 murine cell lines

The TNAP activity was determined either by using an ADVIA 1800 chemistry analyser (Siemens, Berlin, Germany) according to manufacturer's instructions in the routine National Health Laboratory Services, Chemical Pathology Laboratory based at the Charlotte Maxeke Academic Hospital or alternatively using the alkaline phosphatase, diethanolamine detection kit (Sigma-Aldrich, St Louis, USA).

The ADVIA determines the activity of alkaline phosphatase through the cleavage of p-nitrophenyl phosphate (pNPP) to form a coloured by-product which is directly proportional to alkaline phosphatase catalytic activity. The protein content of the extracts was determined using the Bradford method (Bradford, 1976) (section 2.5), and used to correct all TNAP activity results. The TNAP activity was calculated as U activity/mg of protein and expressed as a percentage of the level of baseline activity.

For the alkaline phosphatase, diethanolamine detection kit, for each sample, 960µl of reaction buffer was combined with 20µl of 0.67M pNPP and equilibrated to 37°C. Cell lysate (20µl) was added to the solution for test samples and TNAP (20µl) was added to the control reaction and mixed immediately by inversion. Absorbance of the samples was measured at 405nm after 5 minutes on the Specord 250 plus spectrophotometer (Analytik-Jena, Germany) and normalised to the protein content of

the sample. The TNAP activity was calculated as A_{405nm}/mg of protein and expressed as a percentage of the level of baseline activity.

The same method of TNAP measurement was used throughout an individual experiment.

2.7 Growing 3T3-L1 and Y1 cells on a coverslip

In order to visualise intracellular lipid accumulation and immunocytochemistry results microscopically, 3T3-L1 cells were grown under appropriate conditions on sterile 22x22cm glass coverslips in phenol red free medium (to prevent cell autofluorescence). The cells were fixed (section 2.8) and used for Oil Red O staining/immunohistochemistry.

2.8 Fixing 3T3-L1 and Y1 cells for analysis

The cells were fixed through the addition of a 3% solution of formaldehyde in PBS to the cell monolayer for 30 minutes. The monolayer was then washed in 1x PBS to remove excess formaldehyde and submerged in 1x PBS for further processing.

2.9 Oil Red O staining of neutral lipids

The intracellular lipid droplet accumulation was measured using Oil Red O. Oil Red O is a fat soluble dye which binds to neutral lipids such as triglycerides and cholesterol esters.

The Oil Red O stain was prepared on the day of use from a stock concentration of 3 mg/ml in isopropanol. The working concentration was generated by mixing 3 parts of Oil Red O stock solution with 2 parts distilled water. The solution was incubated at room temperature for 10 minutes and filtered through 0.22 µm filter paper immediately prior to use.

The cell media was removed, and the lipids stained for 1 hour with the Oil Red O stain. The cells were then washed three times with distilled water. Lipid droplets were visualized under a 100x objective (Olympus, Tokyo, Japan) and the bound dye extracted with 200 µl isopropanol. The extracted stain was measured on a Nanodrop spectrophotometer (Thermoscientific, Massachusetts, USA) at a wavelength of 510 nm. The A_{510} measurement was normalised to cell number.

2.10 Immunocytochemistry – Enzyme Linked Fluorescence (ELF) 97 staining

The location of TNAP was detected using the ELF® 97 Endogenous Phosphatase Detection Kit. The ELF97 kit contains a substrate which, once dephosphorylated, fluoresces at 530mn (Molecular Probes, 2004). Fixed cells (section 2.8) were incubated in blocking solution (30 mM Tris, 150 mM NaCl, 1% BSA, 0.5% Triton® X-100, pH 7.5) for 30 minutes prior to staining, and subsequently washed three times for 5 minutes each in wash buffer (30 mM Tris, 150 mM NaCl, 1% BSA, 0.05% Triton X-100, pH 7.5). The cells were incubated for 15 minutes in a pre-reaction wash buffer (30 mM Tris, 150 mM NaCl, pH 7.5). The ELF 97 phosphatase solution was diluted 1:30 in immunohistochemistry reaction buffer and filtered through a 0.22 µm filter which was then applied to the cells. The reaction was allowed to proceed for 5 minutes following which the reaction was stopped through the addition of stop buffer (25 mM EDTA, 1.0 mM levamisole, 0.05% Triton X-100 in phosphate-buffered saline (PBS), pH 7.2) and washed thoroughly with stop solution for 10 minutes on a shaker. The cells were mounted onto a slide using the supplied immunohistochemistry mounting medium and the fluorescent product of alkaline phosphatase was visualised using a fluorescence microscope and indicates where in the cell alkaline phosphatase is active. The cell nucleus was stained with DAPI, and visualised at a wavelength of 461nm. Cells treated with levamisole, an inhibitor of TNAP activity were used as a negative control.

2.11 Nile Red staining of lipids

The location of lipid droplets within the cells was determined by staining with 50ug/ml Nile Red. Fixed cells (section 2.8) were exposed to Nile Red for 10 minutes, following which they were washed three times for 5 minutes on a shaking incubator. After washing the cells were mounted onto a slide and visualised (section 2.12). Fluorescent staining of lipids was required to determine whether TNAP (visualised through its fluorescent by-product ELF alcohol) was co-localised to the lipid droplet.

2.12 Microscopic imaging of Oil Red O and immunocytochemistry

Coverslips were inverted onto Fluoroshield Mounting Medium with DAPI (Abcam, Cambridge, UK) to allow for visualisation. Nile Red stained lipid droplets were visualised under the FITC filter (excitation – 485 nm; emission – 525 nm). The location of TNAP was established through the use of the ELF97 kit (Invitrogen, Massachusetts, USA) according to manufacturer's instructions (section 2.10). The resultant fluorescent product ELF alcohol plus DAPI-stained nuclei were visualised using the DAPI filter (excitation – 350 nm; emission – 460 nm).

Both images were captured using the BX41 microscope (Olympus, Tokyo, Japan) at 100x magnification. AnalySIS LB Research software (Olympus, Tokyo, japan) was used to generate and merge the images.

2.13 Inhibition of ANK in 3T3-L1 cells

The 3T3-L1 cells were exposed to 2.5mM probenecid (Merck, Darmstadt, Germany), an inhibitor of ANK (Prosdocimo et al., 2009). Probenecid was added to the cell medium 30 minutes prior to initiation of intracellular lipid accumulation and throughout the duration of the experiment. The cells were then induced to undergo intracellular lipid accumulation by the addition of transformation medium (section 2.2.1).

2.14 Intracellular pyrophosphate measurement in 3T3-L1

2.14.1 Harvesting cells

The 3T3-L1 preadipocytes were cultured as described above (section 2.1.1) and cell extracts harvested at day 0, 1, 4 and 8 post initiation of lipid droplet formation (section 2.2.1). Briefly, the cells were harvested using cell scrapers and washed in 1ml ice cold PBS. The cells were centrifuged at 1700 x *g* for 3 minutes to obtain a pellet, PBS discarded and the pellet resuspended in 0.5ml of 1M perchloric acid (PCA) in PBS to lyse the cells. The cells were centrifuged at 1700 x *g* for 5 min. The macromolecular precipitate was used to determine DNA concentration and the supernatant for pyrophosphate measurement.

2.14.2 Measurement of intracellular pyrophosphate

The pyrophosphate containing supernatant was neutralised to a pH of 7.5 with 0.1M KOH. The precipitated $KClO_4$ was removed by centrifugation (8000 x *g*; 5 min), and the supernatant assayed directly for pyrophosphate using the P_iPer Pyrophosphate Assay Kit (Invitrogen, Massachusetts, USA) (Figure 2.1) according to manufacturer's instructions.

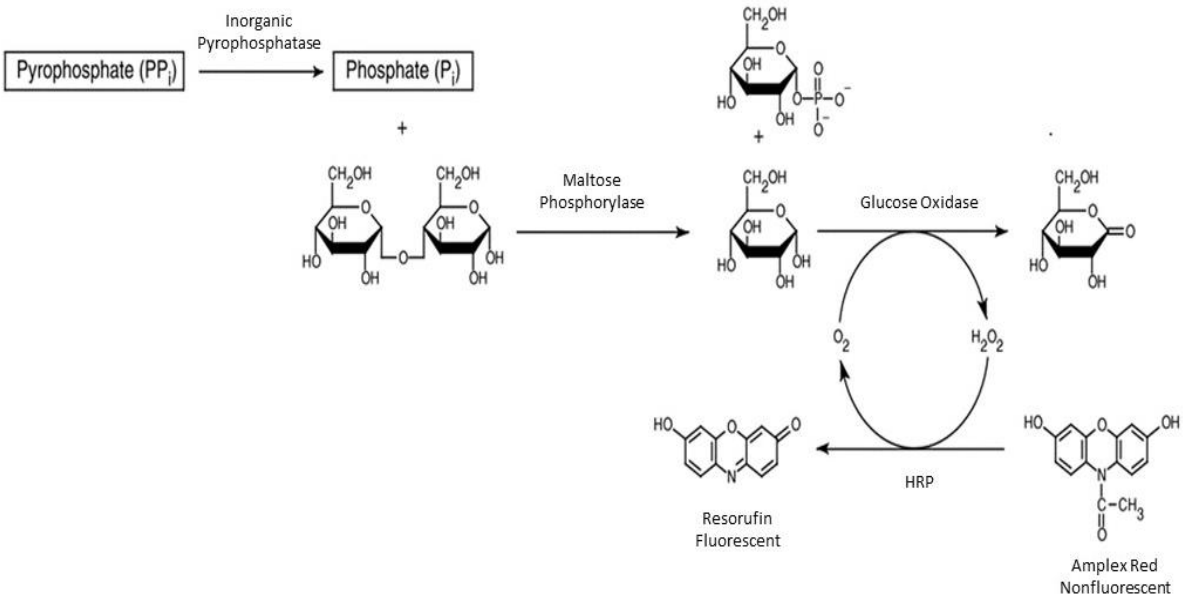

Figure 2.1: Schematic representation of the mechanisms through which pyrophosphate concentration is determined using the PiPer pyrophosphate Assay. Pyrophosphate within the sample is converted into two inorganic phosphate molecules by inorganic pyrophosphatase. Maltose phosphorylase is able to function in the presence of the phosphate molecules to convert glucose 1-phosphate to glucose. The glucose acts as a substrate for glucose oxidase, which generates hydrogen peroxide (H_2O_2) and gluconolactone. The horse radish peroxidase (HRP) acts as a catalyst for the reaction of Amplex Red and H_2O_2, which generates resorufin (a fluorescent product). The fluorescence within the sample can be measured at a wavelength of 587nm and is directly proportional to the pyrophosphate contained within the sample. Image obtained from (Molecular Probes, 2006)

Pyrophosphate was converted to phosphate by inorganic pyrophosphatase. One hundred µl of maltose phosphorylase (4 U/ml), which converts maltose, in the presence of inorganic phosphate, to glucose 1- phosphate and glucose, was added. Two µl of glucose oxidase (2 U/ml) was then added to the sample. Glucose oxidase converts the glucose to gluconolactone and hydrogen peroxide. Twenty µl of horseradish peroxidase (0.4 U/ml) was then added together with 100 µl of 50 µM 10-acetyl-3,7-dihydroxyphenoxazine which generates fluorescent resorufin (excitation wavelength -563nm; emission wavelength - 587nm). Absorbance was measured, and the resultant A_{587} values (which are directly proportional to the initial amount of pyrophosphate in the cell) were normalised to DNA concentration and expressed as a percentage of the untreated control.

As phosphate contamination within the samples would falsely elevate the results (as the measurement of pyrophosphate calls for it to be converted into phosphate to allow detection), background measurements of phosphate were determined in untreated cell extracts and deducted from the final PPi measurement.

2.15 Measurement of intracellular phosphate

Intracellular phosphate was determined using an ADVIA 1800 chemistry analyser (Siemens, Berlin, Germany) according to manufacturer's instructions in the routine National Health Laboratory Services, Chemical Pathology Laboratory based at the Charlotte Maxeke Academic Hospital. The ADVIA system works on the principle that inorganic phosphate ions reacts with molybdate forming a phosphomolybdate complex. The complex is then reduced with ascorbic acid, which generates a blue

complex which that can be measured spectrophotometrically (Murphy and Riley, 1962). The protein content of the extracts was determined using the Bradford method (Bradford, 1976) (section 2.5), and used to normalize phosphate concentration. Phosphate measurements were expressed as a percentage of the level of baseline phosphate concentration.

2.16 Determining if the role of TNAP is to generate phosphate in 3T3-L1 preadipocytes

The 3T3-L1 cells were treated with levamisole (section 2.3.1) for 30 minutes before the induction of intracellular lipid accumulation and through the experiment to ensure the continued suppression of TNAP. To determine whether phosphate is able to reconstitute lipid accumulation in the absence of TNAP activity, 10mM of sodium phosphate (Beck et al., 2003) was added extracellularly to the medium, whilst 10mM of sodium sulphate was added as a control. The concentration of 10 mM was based on experiments conducted by Beck and colleagues in the 3T3-E1 cell line (Beck et al., 2003) as well as toxic dose experiments (Appendix A2). Sodium sulphate and sodium phosphate were used to generate the free phosphate and sulphate. Lipid accumulation was then initiated (section 2.2.1).

The expression levels of TNAP (section 2.24) were assessed via quantification of ALPL mRNA. Activity assays of TNAP (section 2.6) and Oil Red O staining (section 2.9) were performed on day 0, 1 and 4 and the results compared to a control

experiment where the cells are allowed to proceed with adipogenesis normally in the absence of TNAP inhibition by levamisole.

2.17 Confirmation of phosphate induced lipid accumulation in 3T3-L1 cells

As the influx of phosphate into the cell may cause changes in other ions such as calcium and sodium, control experiments were undertaken to ensure that the effect noted was due solely to the re-introduction of phosphate ions and not through the action of other ions.

2.17.1 Inhibition of the sodium-dependant phosphate channels

Foscarnet inhibits the entry of phosphate into the cells through competitive inhibition of sodium phosphate co-transporters. Cells were treated with 300µM foscarnet as described by Beck and colleagues (Beck et al., 2000) and 5mM levamisole 30 minutes before the induction of adipogenesis (section 2.2.1) and addition of phosphate/sulphate (section 2.16). This serves to prevent the phosphate entering the cells, confirming the effect is caused by the extracellular phosphate entering the cells. Cells were monitored to determine whether lipid accumulation occurs in the absence of intracellular phosphate (section 2.9). Along with the sulphate control, a control with no foscarnet was included as a positive control for differentiation.

2.17.2 Inhibition of calcium

To ensure the effect is not caused by sequestering and depletion of calcium through the formation of calcium phosphate precipitation, 10mM of intracellular (BAPTA/AM) and 1mM extracellular (ethylene glycol tetracetic acid) calcium chelators were added to determine if they can mimic the effect of the phosphate. Cells were treated with the calcium chelators and 5mM levamisole 30 minutes before the induction of adipogenesis (section 2.2.1) and addition of phosphate/sulphate (section 2.16).

Cells were monitored to determine whether lipid accumulation occurs in the absence of calcium (section 2.9). Along with the sulphate control, a control with no calcium chelators was included as a positive control for differentiation.

.

Table 2.1: Summary of the control experiments used to confirm the role of phosphate in intracellular lipid accumulation in 3T3-L1 cells.

All control experiments were treated with 5mM levamisole 30 minutes before the induction of adipogenesis (section 2.2.1) and addition of phosphate (section 2.17), with the exception of the sulphate control where phosphate was omitted.

Experiment	**Purpose**	**Additional Reagent**
Inhibition of the sodium-dependant phosphate channels	Prevent the extracellular phosphate entering the cells, confirming the effect is caused by the extracellular phosphate entering the cells.	300 µM foscarnet (an inhibitor of sodium-dependant phosphate channels)
Inhibition of intracellular calcium	To ensure the effect is not caused by sequestering and depletion of intracellular calcium through the formation of calcium phosphate precipitation	10 mM of BAPTA/AM which functions intracellularly as a calcium chelator
Inhibition of extracellular calcium	To ensure the effect is not caused by sequestering and depletion of extracellular	1 mM ethylene glycol tetracetic acid which functions extracellularly as a calcium chelator

	calcium through the formation of calcium phosphate precipitation	
Positive Control	Confirmation of differentiation and intracellular lipid accumulation	None
Sulphate Control	Confirm that the effect seen is specific to the phosphate molecule and not a result of the carrier ion	10 mM Sodium Sulphate. A molecule with structural similarity to sodium phosphate.

2.18 Determining whether TNAP-generated phosphate induces NRF2 gene expression in 3T3-L1 preadipocytes

The ability of phosphate to enter the nucleus and induce NRF2 expression was determined by monitoring *NRF2* gene expression levels using real time PCR (section 2.24) within the murine 3T3-L1 preadipocytes. The cells were exposed to extracellular phosphate in the presence and absence of foscarnet (section 2.17.1), which inhibits the sodium-dependent phosphate channels and thereby blocks phosphate entering the cell through these channels. β-Actin mRNA measurement was used as an endogenous control allowing for relative quantification of mRNA levels. Intracellular phosphate concentration was determined to confirm the inhibition of phosphate entering the cells in the presence of foscarnet (section 2.15).

2.19 Determining if TRAF 2 binds TNAP

Two techniques were used to determine the ability of TRAF 2 to bind TNAP, namely the band shift assay and immunocoprecipitation. Both experiments were performed to increase the likelihood of detecting any interactions which may exist.

2.19.1 Band shift assay

The TRAF 2 (Abcam, Cambridge, UK) and TNAP (Thermo Fischer, Waltham, Massachusetts) peptides were bought commercially and the ability of TRAF 2 to bind TNAP was determined using band shift assays. The TNAP and TRAF 2 were incubated together at 37˚C for 1 hour then run on a 10% native (non-denaturing, non-reducing) PAGE gel (BioRad, Hercules, California, U.S.A.). If binding occurs the two proteins should run together at a higher molecular weight causing the band to shift upwards from either protein run alone.

2.19.2 Co-immunoprecipitation

Co-immunoprecipitation was performed on crude protein extracts (section 2.4) isolated from 3T3-L1 cells 8 days after initiation of adipogenesis, as this is when maximal ALPL expression was seen. Co-immunoprecipitation was carried out using the Pierce co-immunoprecipitation kit (Pierce, Waltham, Massachusetts, USA).

For immune co-precipitation, 50 µg of either antibody or protein was coupled to a resin solid phase. Four co-immunoprecipitation experiments were carried out to determine the binding of TRAF 2 to TNAP in both pure protein samples and crude cellular extracts. As it is unknown where TNAP might bind TRAF 2, the possibility exists that they may share a binding site with anti-TNAP and/or anti-TRAF 2 antibodies. If this were the case then competition between the antibody and proteins of interest may

occur and the interaction may be missed. It was therefore decided to perform the immuno co- precipitation with varying binding options as described below:

1. Purified TNAP was coupled to the resin and purified TRAF 2 was passed over the resin
2. Purified TRAF 2 was coupled to the resin and purified TNAP was passed over the resin
3. Anti-TNAP antibody was coupled to the resin and a pre-incubated mixture of purified TNAP-TRAF 2 was passed over the resin
4. Anti-TRAF 2 antibody was coupled to the resin and a pre-incubated mixture of purified TNAP-TRAF 2 was passed over the resin

A 50µl volume of resin was added to a spin column and washed twice through the addition of 200 µl 1x coupling buffer and spinning for 1 minute at 1000 x *g*. Three µl of sodium cyanoborohydride was then added in a fume hood to the resin. The relevant proteins were then mixed with 200 µl of 1x coupling buffer and added to the resin.

The resin/protein/cyanoborohydride mixture was then incubated on a rotator at room temperature for 120 minutes. Following incubation, the resin was washed twice with 1 x coupling buffer (1 min; 100 x *g*). Two hundred µl of quenching buffer was then added to the resin as well as an additional 3 µl sodium cyanoborohydride and the slurry incubated for 15 minutes with gentle shaking. A further 2 washes were performed (1 x coupling buffer; 1 min; 100 x *g*) followed by 6 washes with 150µl of wash solution (1 min; 1000 x *g*).

For the crude protein experiments, the medium was removed from the cell monolayer and washed with 1x modified Dulbecco's PBS (Gibco). The cells were then incubated on ice with ice-cold IP lysis buffer for 5 minutes, mixing intermittently. The lysate was then centrifuged (13000 x *g*; 10 minutes) and the resultant supernatant used for protein quantification and the remainder precleared by passing over control resin. Once precleared the lysate was used for co-immunoprecipitation experiments.

Co-immunoprecipitation was carried out at 4°C. Single proteins were diluted in 200 µl IP lysis/wash buffer (experiment 1 and 2 above). Bait and prey proteins (TNAP and TRAF 2) were mixed together and diluted in 200 µl IP lysis/wash buffer (experiment 3 and 4 above). The protein mixtures were then added to the previously prepared resins and incubated for 2 hours at 4ºC.

Following incubation, the resin was washed thrice with 200 µl IP/wash buffer and once with 100µl of 1x conditioning buffer. The proteins were then eluted with 10 µl of elution buffer and analysed using Western blotting (section 2.21)

2.20 Determining the effect of over-expression of TRAF 2 on intracellular lipid accumulation

2.20.1 TRAF 2 ORF clone preparation

A *TRAF 2* ORF expression clone was purchased from Genecopoeia (Maryland, U.S). The clone consists of the murine TRAF 2 gene (NM_009422.3) being incorporated into the OmisLink expression vector under the control of a CMV promoter (Figure 2.2).

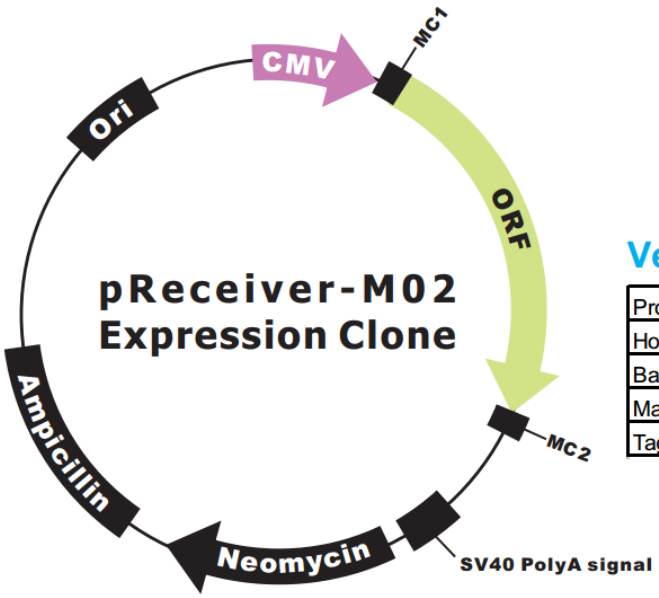

Vector Features

Promoter	CMV
Host Cell	Mammalian
Bacterial selection antibiotic	Ampicillin
Mammalian selection marker	Yes
Tag	N/A

Figure 2.2: Plasmid map of the vector pReceiver-MO2 expression clone. The sequence for the expression of both TRAF2 and NRF2 was incorporated by Genecopia into this vector under the control of the CMV promotor and the resultant plasmids were used for downsteam transfection experiments.

The clone was transformed into ultracompetent *E.coli* (Stratagene, La Jolla, California, US) through heat shock. Thus, competent *E. coli* were incubated on ice together with

1µg plasmid. The plasmid-cell mixture was then exposed to a temperature of 42°C for 45 seconds. One hundred µl of super optimal broth with catabolite repression (SOC) medium (Qiagen) was added to the mixture and the *E. coli* were allowed to grow for 1 hour at 37°C, following which it was transferred to Luria-Bertani medium (10g NaCl, 5 g yeast extract, 10 g tryptone; to 1L in distilled water) supplemented with 100 µg/ml ampicillin and incubated overnight at 37°C.

Plasmid preparation was carried out using the Qiagen endotoxin free midi plasmid prep kit (Qiagen), as per the manufacturer's instructions. Briefly, the overnight culture was harvested through centrifuging for 15 min (6000 x *g*; 4°C) and the resultant bacterial pellet was resuspended in 10ml buffer P1. Ten ml of the lysis reagent, buffer P2 was added and the suspension mixed through inversion and incubated at room temperature for 5 minutes. Following incubation, 10ml of the chilled neutralisation solution buffer P3 was added and mixed through inversion. The lysate was then added to the QIAfilter cartridge and incubated for 10 minutes at room temperature. The lysate was then filtered through the cartridge through pressure applied by the plunger. Two and a half ml of buffer ER was added to the lysate, mixed by inversion and incubated at 4°C for 30 minutes. The lysate solution was then added to an equilibrated QIAGEN-tip 500 and allowed to pass through by gravity. The QIAGEN-tip was then washed twice with 30 ml buffer QC and the plasmid DNA eluted into 15 ml buffer QN in a 30 ml endotoxin-free tube. The DNA was precipitated through the addition of room temperature isopropanol (10.5 ml) and centrifugation (15000 x *g*; 30 min; 4°C). Following precipitation, the supernatant was discarded and the pellet washed by centrifugation (15000 x *g*; 10 min) with 5 ml of endotoxin-free room-temperature 70% ethanol. The supernatant was discarded, the pellet air dried and the pellet

resuspended in 500 µl endotoxin-free buffer TE. The plasmid was then used for transfection.

2.20.2 Transfection of TRAF 2 into the 3T3-L1 cell line

One µg of endotoxin-free plasmid was transfected into 3T3-L1 cells plated out in 6-well plates at a concentration of 5 x 10^6 per well using X-tremeGENE 9. Cells were transfected 24 hours after plating out. Three µl of room temperature X-tremeGENE was combined with 1 µg plasmid in a final volume of 100 µl of serum free DMEM and incubated for 20 minutes at room temperature. The XtremeGENE/plasmid complex was then added in a dropwise fashion to the cell cultures. Cells which did not have plasmid added were treated with transfection reagent only.

2.20.3 Confirmation of increased gene expression of TRAF 2 in transfected 3T3-L1 cells

Confirmation of TRAF 2 gene expression in the presence of the TRAF 2 expressing plasmid was confirmed through real time PCR (section 2.24).

2.21 Western blot analysis

The binding of TNAP and TRAF 2 was assessed via Western blotting.

Equal volumes of protein were combined in a 1:1 ratio with native buffer and loaded onto a precast 10% SDS-Polyacrylamide gel (BioRad, Hercules, California, U.S.A.) (Laemmli, 1970). The gel was run for 1 hour at 100V.

Proteins were transferred to a PVDF membrane for 30 min at 25V using the BioRad semidry blotter. The PVDF membrane was then blocked in 5% milk in Tris buffered saline supplemented with 0.5% Tween 20 (TBST), and incubated overnight in a 1:1000 dilution of each primary antibody (anti-TNAP and anti-TRAF 2) (Towbin et al., 1979).

The membrane was then washed three times for 5 minutes each in TBST and probed with the secondary horse radish peroxidase labelled antibody (diluted 1:2000) for 2 hours. The membrane was then subjected to three additional wash steps (TBST; 5 min) and detected in the ChemiDoc imaging system (BioRad) using the Pierce ECL Western Blotting Substrate (Thermo Fisher Scientific, Massachusetts, USA).

2.22 Determining the location of TNAP in Y1 cells

Murine Y1 adrenal cells were cultured on a coverslip (section 2.7) and induced to accumulate lipid by the addition of oleic acid coupled to bovine serum albumin and cholesterol (section 2.2.2) for 1, 4 and 8 days. The cells were fixed with 3% formaldehyde (section 2.8) and the lipid content of the droplets stained with Nile Red

(section 2.11). To determine where TNAP is located in the cells the slides were exposed to ELF 97 (section 2.10) and visualized under a fluorescence microscope to determine if the TNAP and lipid droplets co-localize (section 2.12).

2.23 Determining the role TNAP plays in cholesterol accumulation

The Y1 mouse adrenal cells were induced to accumulate lipids (section 2.2.2) in the presence and absence of 5mM levamisole (a potent, specific inhibitor of TNAP) to establish if cholesterol accumulation is impaired in the absence of TNAP activity (section 2.3.2). The accumulation of lipids was determined through staining the cells with Oil Red O (section 2.9) and the lipid droplets visualized (section 2.12). The stained lipids were extracted and quantified (section 2.9). The values were normalized to cell number. Protein was extracted from the cells (section 2.4) and used to measure TNAP activity using the ADVIA autoanalyser (Siemens), to ensure that TNAP is present during the course of intracellular lipid accumulation and decreased following treatment with the inhibitor (section 2.6). The TNAP activity was normalized to protein concentration [determined by the Bradford assay (section 2.5)].

2.24 Analysis of gene expression

Gene expression of TNAP, NRF2, and TRAF 2 was determined through relative real time PCR, with β-actin used as the control gene.

2.24.1 RNA extraction

Total RNA was extracted using the RNeasy extraction kit (Qiagen, Venlo, Netherlands) from cells at baseline and at days 1, 4 and 8 of lipid accumulation.

To harvest RNA, cells were detached from the bottom of the culture plate and centrifuged to form a pellet (12000 x *g*; 1 minute) and 350 µl of buffer RLT was added to the pellet. The pellet was homogenised in the buffer through pipetting action resulting in cell lysis. The lysate was then pelleted to remove cellular debris (12000 x *g*; 3 min) and the supernatant transferred to a clean microcentrifuge tube. One volume of 70% ethanol was added to the lysate and mixed thoroughly. The mixture was then spun through an RNeasy spin column (8000 x *g*; 15s) and the flow-through discarded.

The column was washed twice with 500 µl of buffer RPE through centrifugation (8000 x *g*; 15s – first spin and 8000 x *g*; 2 min – second spin). The RNA was then eluted from the membrane by the addition of 30µl of RNase free water and centrifugation (8000 x *g*; 1 min).

2.24.2 cDNA synthesis

Extracted RNA was reverse transcribed to cDNA using the Transcriptor Reverse Transcriptase cDNA synthesis kit (Roche, Basel, Switzerland), and was used as a template for real time PCR, using relative (ΔΔCt) quantification (Livak and Schmittgen, 2001).

To synthesise cDNA, 4 µg RNA was incubated with 50pmol/l anchored-oligodT primers for 10 min at 65°C. Following denaturation, 5 x Transcriptor Reverse Transcriptase Buffer, 20U of protector RNase inhibitor, 1mM deoxynucleotide (dNTP) mix, 5mM DTT and 22U of Transcriptor Reverse transcriptase (RT) was added to the primer/RNA mix and cDNA synthesis carried out at 50°C for 50 minutes. The RT was then inactivated at 85°C for 5 minutes and the resultant cDNA stored at -20°C until needed as a template for PCR.

2.24.3 Real time PCR

Real-time PCR was used to determine relative increase or decrease in gene expression during experiments. Untreated cells and cells allowed to undergo standard lipid accumulation acted as control samples for comparison.

Gene expression was determined through relative real-time PCR on the Step One Plus machine (Applied Biosystems, Waltham, Massachusetts, USA) using the ΔΔCt

method (Livak et al., 1995). Taqman technology was employed. All primers and probes for Real-time PCR were designed by TIB Molbiol (Berlin, Germany) (Table 2.2; Table 2.3) and ordered from Roche (Basil, Switzerland).

Real time PCR was undertaken using 2x Taqman® fast universal PCR mastermix (Applied Biosystems, Massachusetts, USA). All reactions were set up in 25 µl volume and contained β-actin control primers and probe and the primer and probe for the relevant gene of interest (12.5 µl Mastermix, 50 ng cDNA, 18 µM of each forward and reverse primer and 5 µM of each probe). The PCR was run on the Step one plus (Applied Biosystems) and β-actin acted as the normalisation control.

All real-time reactions were run using the following conditions: an initial denaturation of 95°C for 5 minute, cycling for 35 cycles (58°C for 30 seconds; 95°C for 10 seconds).

Table 2.2 : List of Primers used for relative quantitation PCR.

Gene	Primer	Gene position	sequence
TNAP	TNAP F	NM_007431 696-714	5'-ggATATCgACgTgATCATgggTg-3'
	TNAP R	NM_007431 1034-1014	5'-ggAATgCTTgTgTCTgggTTT-3'
Rodent β actin	RodAct F	NM_007393 558-577	5'-ACCCACACTgTgCCCATCTA-3'

	RodAct R	NM_007393 899-880	5'-gCCACAggATTCCATACCC-3'
TRAF 2 (exons 6-8)	TRAF 2 F	NM_009422 657-674	5'- CTCgggAgACgTTTCAgg – 3'
	TRAF 2R	NM_009422 761-741	5'- gCAggTTCTCAgTCTCCACCA – 3'
NRF2 (Nfe212)	NRF2 F	NM_010902 240-257	5'- gACTTggAgTTgCCACCg – 3'
	NRF2 R	NM_010902 524-503	5'- ACTggTgTCTggATgrGC – 3'

Table 2.3: List of Probes used for Real time PCR

Gene	Gene position	Sequence	λmax/nm (absorption)	λmax/nm (emission)
TNAP	NM_007431 918-946	FAM–CCgAAgAACAgAACTgATgTggAATACgA-BBQ	494	518
Rod Act	NM_007393 584-605	YAK – CATCCTgCgTCTggACCTggC - BBQ	530	549
TRAF 2	NM_009422 685-705	FAM – AgCATgCAgCAAATgCCgggT - BBQ	494	518

NRF2 (Nfe212)	NM_010902 277-306	FAM-AggACATggATTTgACATCCTTTggA - BBQ	494	518

2.25 Statistical Analysis

Interday comparisons were performed using the paired Student t-test. Intraday comparisons were performed using the unpaired Students t-test using Microsoft Excel (Washington, United States).

2.26 Ethics

An ethics waiver was granted by the Human Research Ethics Committee (Medical). The ethics waiver number was W-CJ-120213-1 (Appendix A1).

3 Intracellular inorganic pyrophosphate is a positive mediator of intracellular lipid accumulation in murine 3T3-L1 cells

3.1 Background

Obesity is a condition that results from an imbalance between energy intake and energy expenditure and is characterized by the expansion of adipose tissue by both hyperplasia and hypertrophy of adipocytes (Drolet et al., 2008, Calder et al., 2011). Hyperplasia occurs through the conversion of immature adipocytes (preadipocytes) into mature adipocytes. This process of maturation of the preadipocyte, termed adipogenesis, is characterized by the intracellular accumulation of membrane-bound, triglyceride-containing lipid droplets (Shoham and Gefen, 2012, Lowe et al., 2011). Various factors have been identified, including hormones, enzymes and growth factors, as regulators of adipogenesis (Lowe et al., 2011), however the full molecular pathway has yet to be elucidated.

Tissue non-specific alkaline phosphatase (TNAP) is a known positive regulator of intracellular lipid accumulation in both human preadipocytes (Ali et al., 2006b, Ali et al., 2006a) and the 3T3-L1 murine preadiopocyte cell line (Ali et al., 2005), via an unknown mechanism. This enzyme, together with ectonucleotide pyrophosphatase phosphodiesterase 1 (ENPP-1) and progressive ankyloses protein homolog (ANKH), are essential for the control of pyrophosphate concentration in bone (Wang et al., 2008). Adenosine triphosphate (ATP) is hydrolysed to form adenosine monophosphate (AMP) and inorganic pyrophosphate through ENPP-1 activity (Hessle et al., 2002). The pyrophosphate in turn is transported out of the cell through ANK where TNAP catalyses the hydrolysis of pyrophosphate to phosphate; pyrophosphate inhibits whilst phosphate stimulates bone mineralizaton (Hessle et al., 2002, Ho et al., 2000).

Polymorphisms in the genes encoding ANKH, ENPP-1 and TNAP have previously been shown to be associated with obese phenotypes in humans (Meyre et al., 2005, Korostishevsky et al., 2010). The mechanism through which these peptides may contribute to the obese phenotype has yet to be established. Given that all these peptides are also expressed in adipose tissue (Uhlen et al., 2015) we hypothesized that they function in preadipocytes, as in osteoblasts, to regulate the level of pyrophosphate. The effect of pyrophosphate on intracellular lipid accumulation (ICLA) in preadipocytes is not known. However, through the use of the ANK pyrophosphate transporter inhibitor probenecid, it is possible to increase levels of intracellular pyrophosphate. Therefore, the main aim of the current study was to determine the effect of probenecid-mediated ANK inhibition on intracellular lipid accumulation in 3T3-L1 preadipocytes. Secondary aims of this study were to determine the intracellular levels of pyrophosphate during adipogenesis and what effect inhibition of TNAP had on those levels.

3.2 Methods

3.2.1 Determining the impact of high intracellular pyrophosphate concentration on intracellular lipid accumulation in the murine preadipocyte cell line 3T3-L1

To determine the impact of high intracellular pyrophosphate levels on intracellular lipid accumulation and TNAP activity, 3T3-L1 cells were cultured (section 2.1.1) and induced to accumulate lipids (section 2.2.1) in the presence and absence of 2.5mM probenecid, a potent inhibitor of the pyrophosphate transporter ANK (section 2.13). Lipid accumulation (section 2.9) and TNAP activity (measured with the alkaline phosphatase, diethanolamine detection kit - section 2.6) was determined before induction and on days 1, 4 and 8 of lipid accumulation. Intracellular pyrophosphate was measured in the presence and absence of functional ANK using the P_iPer Pyrophosphate Assay Kit (Invitrogen, Massachusetts, USA) (section 2.14).

3.2.2 Determining the effect of TNAP on intracellular pyrophosphate concentration during intracellular lipid accumulation in the 3T3-L1 cells

To determine how intracellular pyrophosphate concentration is altered over the course of adipogenesis and the effect TNAP activity has on the intracellular pyrophosphate concentration, cells were cultured in the presence and absence of 5mM levamisole (an inhibitor of TNAP) (section 2.3.1). Intracellular pyrophosphate concentrations were determined before induction and on days 1, 4 and 8 of lipid accumulation (section 2.14). Levamisole mediated TNAP inhibition was confirmed through measurement of TNAP activity (section 2.6) as was inhibition of intracellular lipid accumulation (section 2.9).

3.2.3 Morphological measurements

To determine morphological measurements, the cells were fixed and stained as described above. Each measurement was made at the widest diameter and size determined using the AnalySIS LB software (Olympus, Tokyo, Japan)

3.2.4 Statistical Analysis

Statistical analysis was performed as described in section 2.25.

3.3 Results

3.3.1 Intracellular pyrophosphate levels during adipogenesis in 3T3-L1 cells in the presence or absence of probenecid.

Pyrophosphate levels were measured in cells undergoing adipogenesis in the presence or absence of probenecid. In baseline cells i.e. those at day 0, intracellular pyrophosphate levels were set at 100% and the pyrophosphate levels of all other cells at all time points were expressed as a % of the baseline levels.

In the non-treated cells, intracellular pyrophosphate levels decreased over the course of intracellular lipid accumulation (Figure 3.1) reaching a level of 34.1 ± 10.48 % of baseline levels by day 8 of intracellular lipid accumulation ($p=0.008$).

As ANK functions to transport pyrophosphate out of the cell, we aimed to determine whether inhibition of ANK resulted in the expected accumulation of intracellular pyrophosphate (Figure 3.1). On inhibition of ANK, pyrophosphate levels increased within 24 hours of intracellular lipid accumulation to 154.6 ± 1.51% of the level in cells at baseline ($p=0.01$), however by day 8, the pyrophosphate levels were no longer significantly different from the baseline levels (90.1 ± 22.5%; $p=0.71$). However, at all time points intracellular pyrophosphate levels were significantly ($p<0.05$ at all time points) higher in probenecid-treated compared to non-treated cells (Figure 3.1).

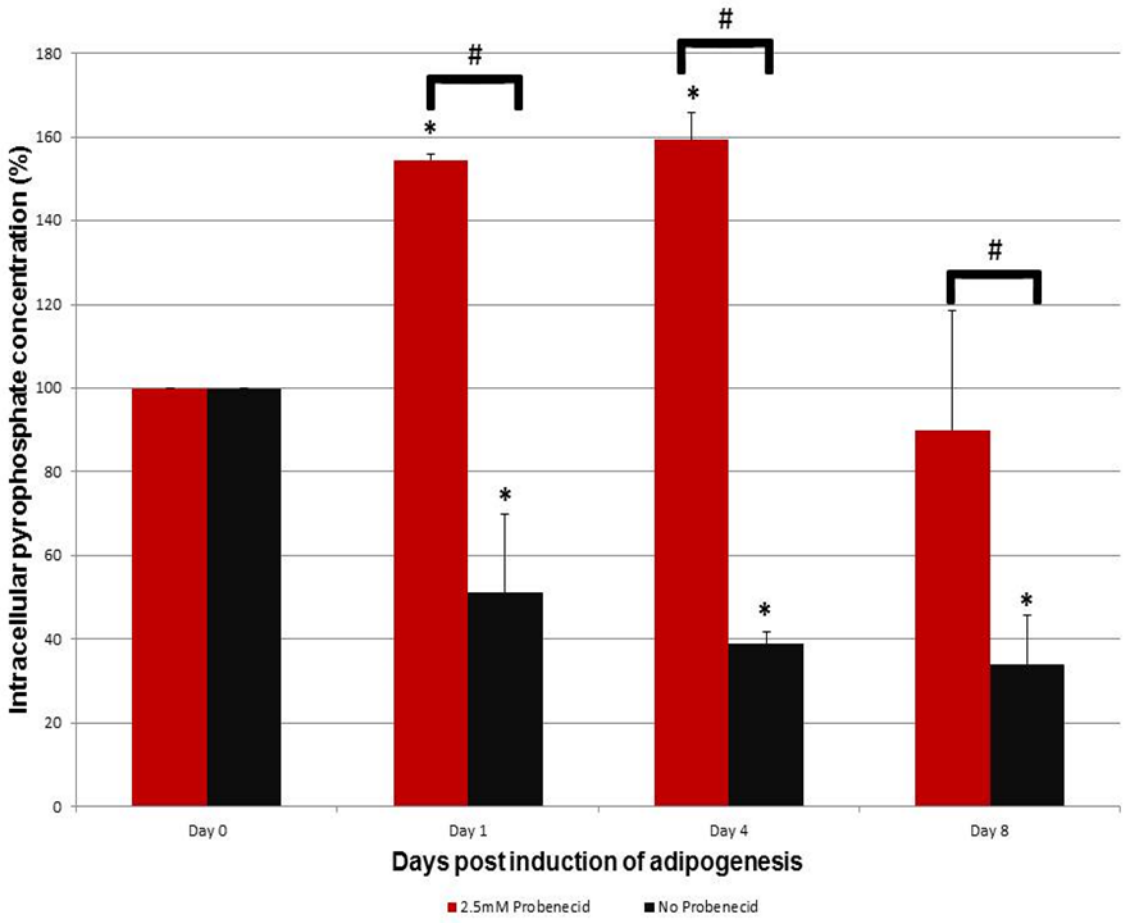

Figure 3.1: Intracellular pyrophosphate concentration in the presence and absence of probenecid during intracellular lipid accumulation in 3T3-L1 cells. Pyrophosphate levels were measured on days 0, 1, 4 and 8 after the induction of intracellular lipid accumulation in 3T3-L1 cells; *$p<0.05$ versus cells at day 0; $^{\#}p<0.05$ for probenecid-treated versus non-treated cells. Experiments were conducted in triplicate and error bars represent ± SD.

3.3.2 The activity of TNAP is increased in cells without a functional ANK transporter

The enzyme TNAP catalyses the hydrolysis of pyrophosphate to phosphate, and is known to be expressed in adipocytes. We therefore aimed to determine whether TNAP activity was altered in cells with elevated intracellular inorganic pyrophosphate

levels. The activity of TNAP was therefore measured in 3T3-L1 cells in the presence or absence of probenecid. As shown in Figure 3.1, probenecid leads to elevated levels of intracellular pyrophosphate. The TNAP activity in cells not treated with probenecid confirmed previous results (Ali et al., 2005), with TNAP attaining maximal levels (212.9 ± 44.05 %; $p=0.03$ vs baseline levels) on day 8 of intracellular lipid accumulation. Within the probenecid treated cells, TNAP activity rose sharply over the initial 24 hours reaching levels of 291.5 ± 57.8% of levels seen in cells at baseline ($p=0.038$), but by day 8 TNAP activity had returned to levels not significantly different from baseline (107 ± 9.91 %; $p=0.122$) (Figure 3.2). When TNAP activity was compared between probenecid-treated and non-treated cells, activity was significantly higher ($p<0.05$) in the treated cells at days 1 and 4 but this situation was reversed by day 8 with TNAP activity now significantly higher ($p<0.05$) in the non-treated cells (Figure 3.2).

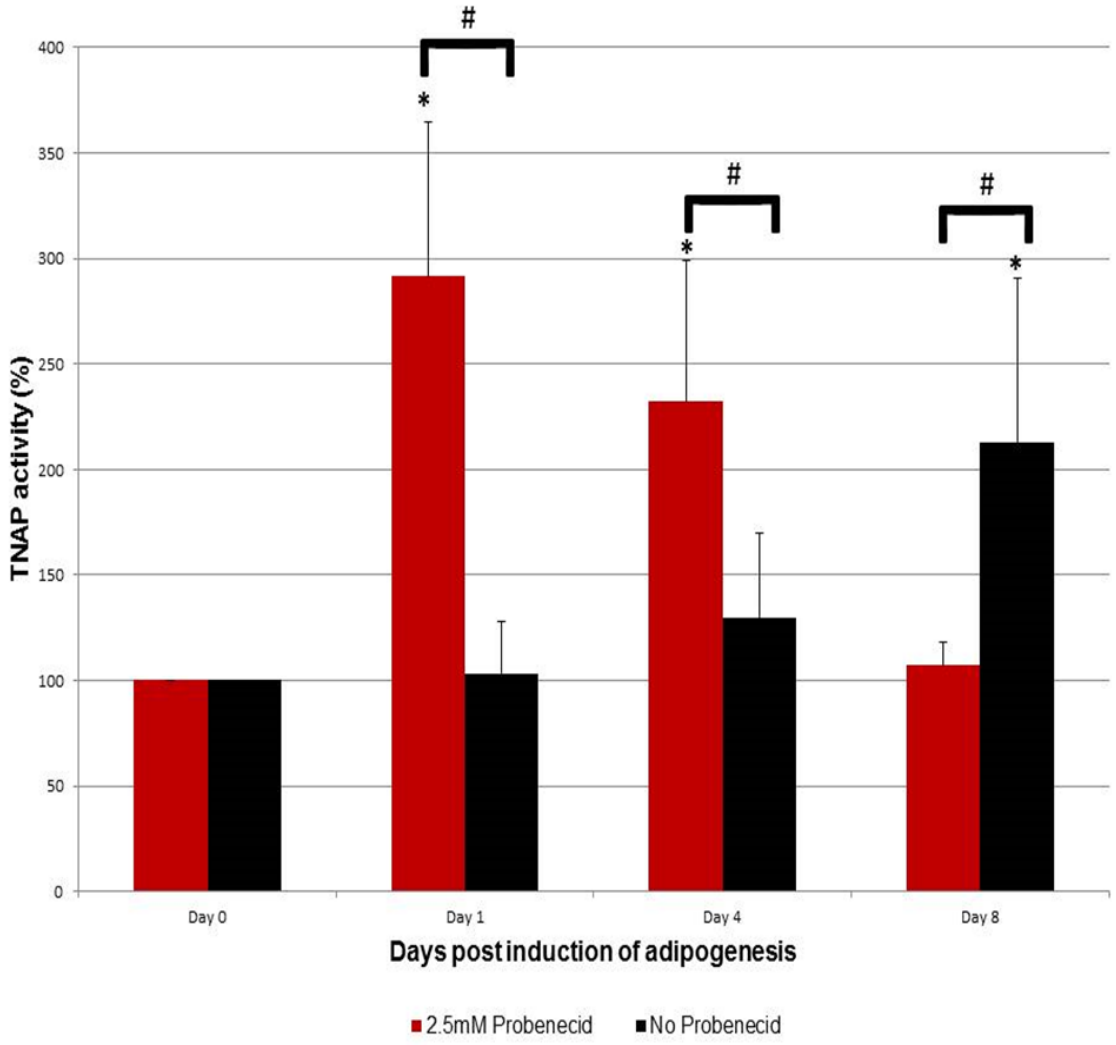

Figure 3.2: Activity of TNAP after the induction of intracellular lipid accumulation in 3T3-L1 cells in the presence and absence of probenecid. The activity of TNAP was measured on days 0, 1, 4 and 8 after the induction of intracellular lipid accumulation in 3T3-L1 cells; *$p<0.05$ versus cells at day 0; $^{\#}p<0.05$ for probenecid-treated versus non-treated cells. Experiments were conducted in triplicate and error bars represent ± SD.

3.3.3 Inhibition of ANK enhances lipid accumulation

Both ANK insufficiency (Korostishevsky et al., 2010) and increased TNAP activity (Ali et al., 2006b) have been associated with increased adiposity. We therefore determined the level of lipid accumulation seen in cells exposed to probenecid compared to normal

controls. Intracellular lipid accumulation increased in a linear fashion from day 0 to day 8 in both probenecid-treated and non-treated cells. However, the lipid levels were significantly higher ($p<0.05$) in cells treated with probenecid when compared to cells not exposed to probenecid, by day 4 (Figure 3.3). In both treatment-types, intracellular lipid levels were significantly higher than baseline ($p<0.05$) at all time points. Intracellular lipid accumulation in cells exposed to probenecid reached a maximal level of 507.4 ± 30.39% by day 8 ($p=0.002$ vs day 0), compared to 337.6 ± 16.17% at day 8 ($p=0.001$ vs day 0) for untreated cells (Figure 3.3).

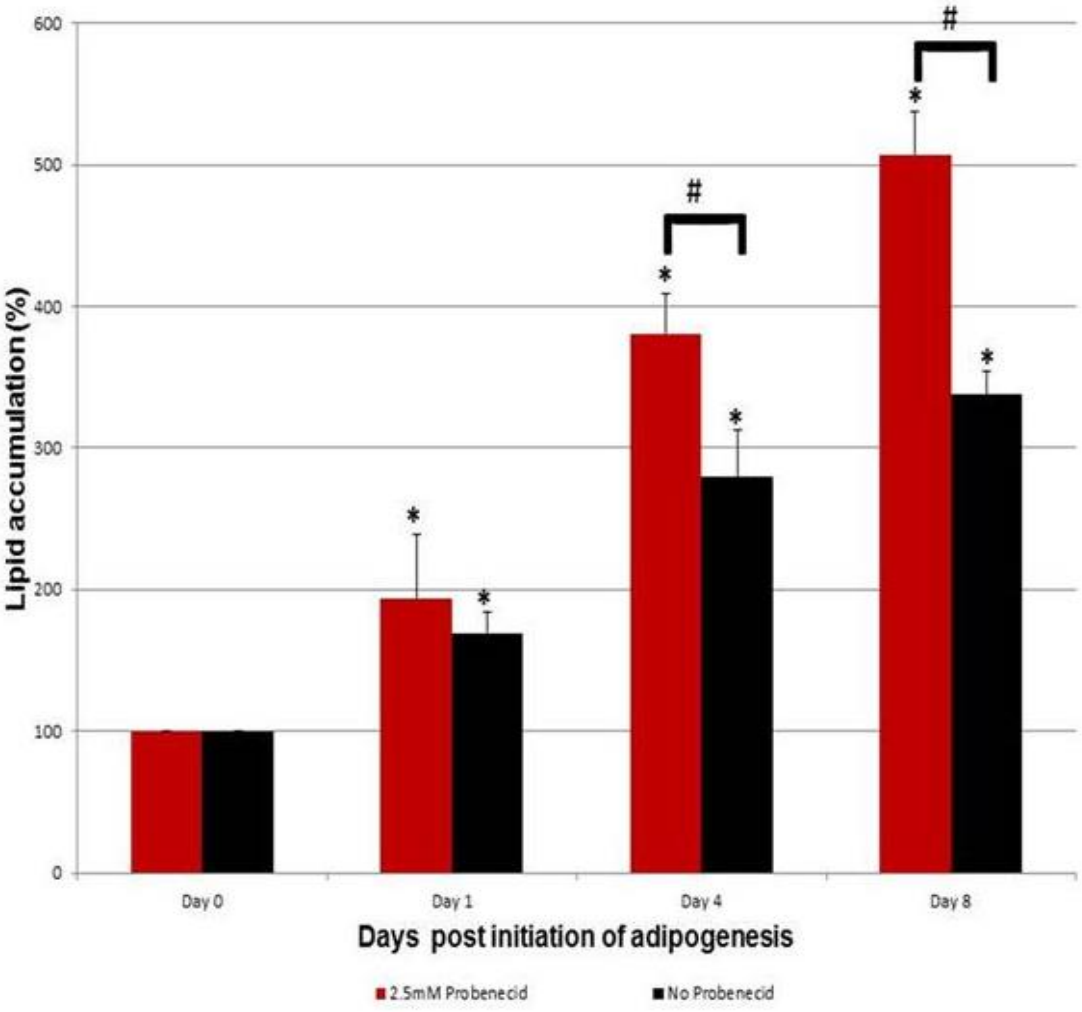

Figure 3.3: Intracellular lipid accumulation in 3T3-L1 cells in the presence or absence of the ANK inhibitor probenecid. Intracellular lipid accumulation was determined through Oil Red O staining and spectrophotometric measurement of the extracted stain; *$p<0.05$ versus cells at day 0; $^{\#}p<0.05$ for probenecid-treated versus non-treated cells. Experiments were conducted in triplicate and error bars represent ± SD.

3.3.4 The effect of TNAP on intracellular inorganic pyrophosphate levels

Inorganic pyrophosphate is known to be converted to inorganic phosphate by the action of TNAP. Therefore, in order to determine whether TNAP activity was responsible for lowering the intracellular inorganic pyrophosphate concentration

during adipogenesis, as shown in Figure 3.1, we measured the changes in intracellular inorganic pyrophosphate levels in cells induced to undergo intracellular lipid accumulation in the presence and absence of the TNAP inhibitor levamisole. Under normal conditions (in the absence of levamisole), intracellular inorganic pyrophosphate levels dropped below baseline levels over the duration of intracellular lipid accumulation, however when TNAP activity was inhibited with levamisole (Figure 3.4A) intracellular inorganic pyrophosphate levels remained constant at baseline levels (Figure 3.4B) and at each time point were significantly higher ($p<0.05$) than in cells not treated with levamisole. The inhibition of TNAP was coupled to a dramatic decrease in intracellular lipid accumulation as previously reported (Ali et al., 2005) (Figure 3.4C).

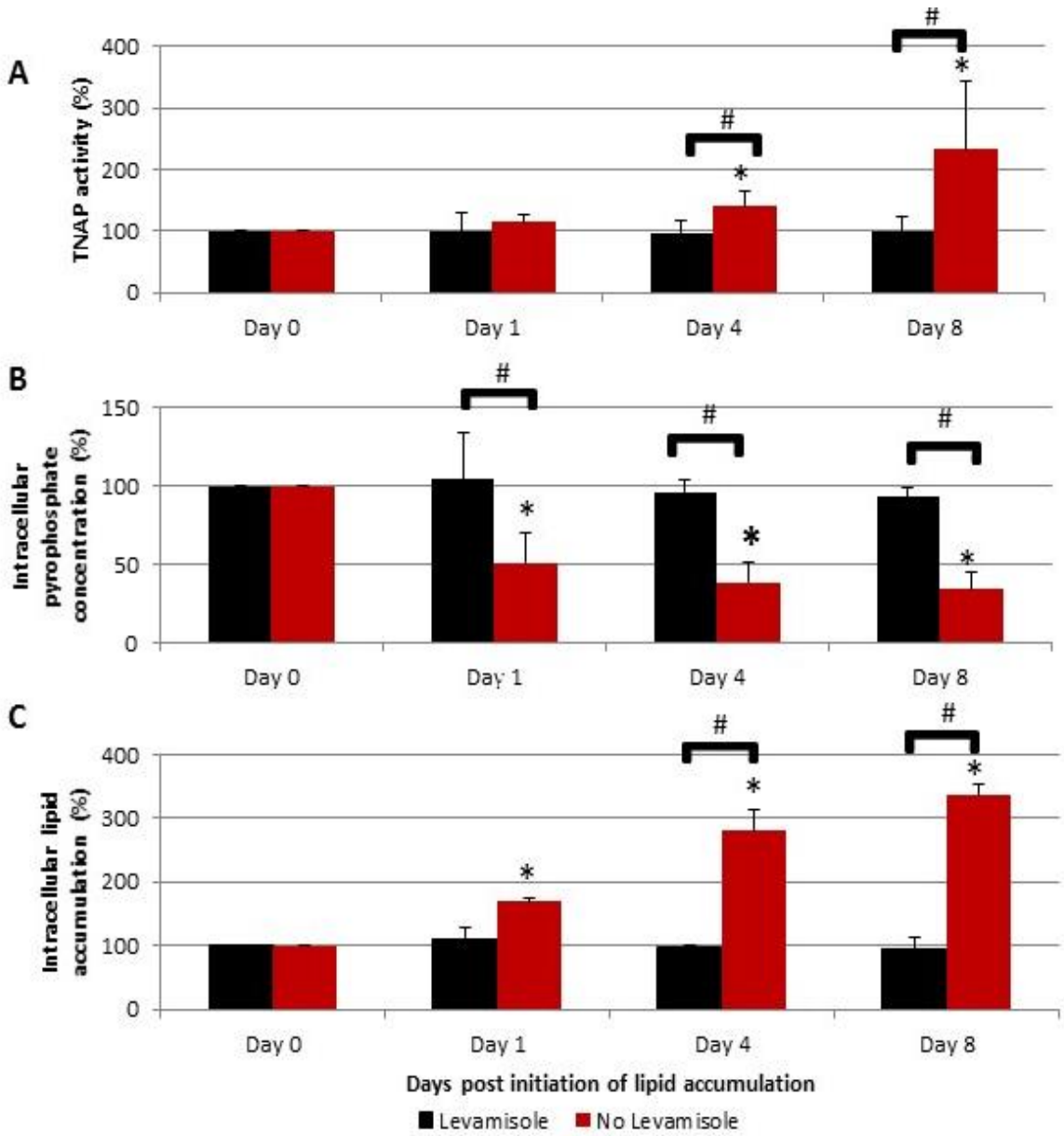

Figure 3.4: The effect of TNAP inhibition (A) on intracellular pyrophosphate levels (B) and intracellular lipid accumulation (C). Intracellular inorganic pyrophosphate was measured in cells induced to undergo intracellular lipid accumulation in the presence and absence of levamisole, a TNAP inhibitor; *$p<0.05$ versus cells at day 0; #$p<0.05$ for levamisole-treated versus non-treated cells. Experiments were conducted in triplicate and error bars represent ± SD.

3.3.5 Cells treated with ANK have altered morphology

A morphological comparison of adipocytes (day 8) treated with probenecid to those allowed to undergo adipogenesis under normal conditions showed that probenecid exposed adipocytes exhibited increased cell diameter (97.3 ± 35.0 µm) when compared to non-exposed adipocytes (35.8 ± 11.1 µm; p=0.0006) (Figure 3.5). Similarly, the nuclei within the probenecid treated cells had a larger diameter than in the non-treated cells (52.0 ± 29.9 µm vs 16. 8 ± 6.1 µm; p=0.04) whereas the lipid droplets were significantly smaller in diameter in the probenecid treated cells (5.1 ± 2.8 µm vs 10.1 ± 4.3 µm; p=0.04).

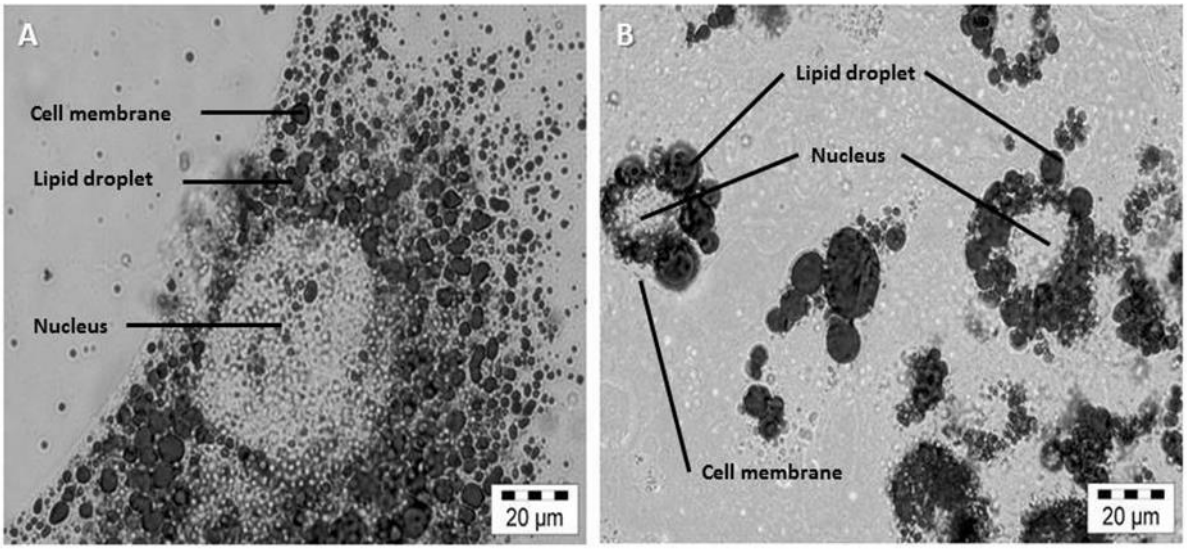

Figure 3.5: Comparison of the morphological features of 3T3-L1 adipocytes in ANK inhibited and non-inhibited cells. Cells treated with probenecid (A) are larger than those not treated (B).

3.4 Discussion

This study demonstrated that inhibition of ANK through treatment with probenecid resulted in an increase in intracellular lipid accumulation in the presence of high concentrations of pyrophosphate (Figure 3.1; Figure 3.3). The increased inorganic pyrophosphate was paralleled by an increase in TNAP activity (Figure 3.2). Treatment of cells with the TNAP inhibitor levamisole led to a drop in both TNAP activity and lipid accumulation but to a higher level of intracellular pyrophosphate when compared to untreated cells (Figure 3.4A-C). Inhibition of the ANK pyrophosphate transporter resulted in adipocyte hypertrophy; however, the lipid droplet size was significantly smaller when compared to cells which were not treated with probenecid (Figure 3.5).

3.4.1 Inhibition of ANK increases intracellular pyrophosphate levels in 3T3-L1 preadipocytes

In cells which were not exposed to probenecid, within 24 hours there was a decrease in the intracellular concentration of pyrophosphate (Figure 3.1). This initial decrease may be attributed to the activity of the ANK pyrophosphate transporter and TNAP may also be responsible especially at days 4 and 8 where its activity is increased (Figure 3.2). Another explanation may be a drop in activity of the pyrophosphate generating enzyme ENPP-1. Expression of ENPP-1, whilst upregulated in the initial 16 hours of adipogenesis, is thereafter rapidly down regulated reaching levels below baseline within 24 hours post initiation of adipogenesis (Liang et al., 2007).

Pyrophosphate is important in various cellular functions. Within the mitochondria it plays a role in bioenergetics, and is known to be able to mediate the functioning of enzymes such as glucose-6-phosphatase (Mansurova, 1989). It is therefore unlikely that throughout adipocyte differentiation no pyrophosphate is being formed. Whilst it is known that ENPP-1 is downregulated, the status of other pyrophosphate generating enzymes within the context of adipogenesis remains unknown. It is therefore probable that there is a constant generation of pyrophosphate, throughout adipogenesis, which adds to the intracellular pyrophosphate pool. The generated pyrophosphate would then presumably be cleared through a combination of TNAP activity (TNAP activity is known to increase throughout ICLA (Ali et al., 2005)) and being shuttled out of the cell into the extracellular milieu through ANK mediated transport (Ho et al., 2000).

Probenecid is a weak organic acid which is a known inhibitor of the ANK pyrophosphate transporter (Ho et al., 2000). As expected, probenecid-mediated inhibition of ANK resulted in a rapid accumulation of intracellular pyrophosphate. However by day 8 of lipid accumulation, the pyrophosphate levels have fallen to baseline levels. Within the probenecid treated cells, the mechanism through which pyrophosphate is cleared is expected to be through TNAP mediated hydrolysis of pyrophosphate particularly over the first 4 days where TNAP activity is very high (Figure 3.2). It is possible that the decrease in pyrophosphate seen on day 8 (at which point TNAP activity is low) is a result of an increase in ANK expression to compensate for the high intracellular pyrophosphate levels. This increase in ANK expression may be sufficient to compensate for the inhibitory effect of probenecid. Alternatively, in

response to the high pyrophosphate levels, pyrophosphate-generating enzymes such as ENPP-1, may be downregulated.

3.4.2 TNAP activity is increased in response to high intracellular pyrophosphate concentrations

Within osteoblasts TNAP functions to catalyse the hydrolysis of pyrophosphate to phosphate, and acts to control the intracellular pyrophosphate/phosphate balance within these cells (Kim et al., 2010b, Hessle et al., 2002). Adipocytes and osteoblasts share a common mesenchymal progenitor (Takada et al., 2007), and it is likely that they share common pathways, including those involved in phosphate regulation.

The TNAP activity in probenecid treated cells is seen to increase dramatically (Figure 3.2), tracking the levels of intracellular pyrophosphate noted within the probenecid treated cells (Figure 3.1). The dramatic increase in TNAP activity is likely in response to the high pyrophosphate levels in an attempt to normalize the pyrophosphate levels within the adipocyte. Potentially, the high intracellular pyrophosphate levels cause, either directly or indirectly, an increased expression of ALPL mRNA and its subsequent translation to protein. This is supported by work in endochondral and osteoblast organoid cultures which shows that TNAP activity is increased in the presence of probenecid in a dose dependant fashion (Zimmermann, 2008).

In the absence of probenecid, the level of TNAP activity rose throughout adipogenesis, confirming results by Ali *et. al.* (Ali et al., 2005). Phosphate generated by TNAP is able to induce the expression of more TNAP, through an indirect mechanism (Orimo and Shimada, 2008). This phenomenon may explain why over the course of adipogenesis in the absence of probenecid, there is a cumulative increase in the levels of TNAP in the absence of high levels of pyrophosphate. However, it should be noted that the control of TNAP expression in adipocytes is a matter of conjecture and factors other than phosphate may also be involved in the increased expression of TNAP during ICLA.

The level of TNAP activity seen within the probenecid treated cells appears to track the amount of pyrophosphate within the cell. It is possible that the removal of TNAPs substrate (via the mechanisms described above) may have resulted in the decrease in activity of TNAP observed by day 8 in the treated cells. Thus, it is possible that in non-probenecid treated cells TNAP activity is modulated by factors other than pyrophosphate whilst in probenecid-treated cells TNAP activity is forcibly modulated by the high levels of pyrophosphate.

3.4.3 Probenecid increases intracellular lipid accumulation.

Probenecid treatment of preadipocytes resulted in a consistently higher level of intracellular lipid accumulation when compared to the untreated control cells (Figure 3.3). This difference reached significance within 4 days of initiation of lipid

accumulation. Both pyrophosphate and phosphate are known to mediate the expression of genes (Ronchetti et al., 2013, Beck, 2003). We therefore hypothesise that either the pyrophosphate itself, or its TNAP-generated by-product phosphate, is important in adipocyte differentiation and intracellular lipid accumulation. The ability to completely inhibit differentiation through levamisole mediated inhibition of TNAP activity (Figure 3.4), (Ali et al., 2005) strongly implicates TNAP as a modulator of ICLA during adipogenesis. The TNAP may function to induce ICLA through either alleviating an inhibitory block caused by pyrophosphate, or alternatively to generate phosphate which may act as a secondary messenger. We find that in the presence of high pyrophosphate levels, ICLA is enhanced, strongly suggesting that TNAPs role within adipogenesis is to generate Pi and that pyrophosphate does not block ICLA. This being so, the increased levels of lipid accumulation noted within the probenecid treated cells may be due to increased TNAP-generated phosphate which enters the nucleus and acts as a transcription factor for genes necessary for ICLA. Inhibiting TNAP activity prevents any ICLA from occurring (Ali et al., 2005) (Figure 3.4), and therefore it is likely that TNAP's function within ICLA occurs in the early stages of adipogenesis. This is supported by data showing that when TNAP was inhibited by levamisole, ICLA remained at baseline levels throughout the full course of the experiment (Figure 3.4). In the absence of levamisole, TNAP activity at day 1 was still at baseline levels but ICLA was activated. It is possible that there was upregulation in TNAP activity at a level below that which was detectable with our assay, however an alternative explanation would be that baseline levels of TNAP are sufficient to allow ICLA to proceed but ICLA cannot be initiated without the full induction of adipogenesis through the addition of insulin, IBMX and dexamethasone.

It is interesting to note that inorganic pyrophosphate is a known inhibitor of the lipoprotein lipases (Krauss et al., 1973), and these enzymes are important in facilitating the uptake of triglyceride-derived free fatty acids into adipocytes, where they are converted back into triglycerides by re-esterification with glycerol, for storage in the intra-cellular lipid droplets. It is therefore feasible that by inhibiting ANK we are decreasing the extracellular inorganic pyrophosphate concentration and allowing for the uptake of a greater amount of free fatty acids into the adipocytes resulting in enhanced intracellular lipid accumulation. It is interesting to note that in bone mineralization, pyrophosphate also functions in the extracellular matrix (Hessle et al., 2002).

3.4.4 High intracellular pyrophosphate levels are associated with hypertrophy and small lipid droplets in 3T3-L1 cells.

As pyrophosphate and phosphate are known to regulate gene expression (Beck, 2003, Ronchetti et al., 2013), it is possible that the greater nuclear size observed in cells treated with probenecid is due to greater nuclear activity. Furthermore, the probenecid treated cells were hypertrophic and had greater numbers of smaller lipid droplets compared to the cells not treated with probenecid. This suggests that the high cellular PPi levels block lipid droplet fusion, thus producing large numbers of small lipid droplets. This phenomenon requires further investigation. It is interesting to note that a study has shown that polymorphisms in the ANKH gene are associated with obesity (Korostishevsky et al., 2010), and the current data suggests that this may be mediated by the effects of ANKH on adipocytic lipid deposition and cell morphology. It is

important to note that the changes described here are representative of those seen within early adipogenesis. Within the initial stages of adipogenesis preadipocytes undergo mitotic clonal expansion prior to the expression of adipogenic genes (Tang et al., 2003). It is possible, therefore that the addition of probenecid may have some effect on the cytoskeleton during clonal expansion which may result in the cellular hypertrophy and decreased lipid droplet size. In addition, isobutylmethylxanthine (a cAMP phosphodiesterase inhibitor), dexamethasone, insulin and FBS are needed to allow the cells to undergo differentiation (Patel and Lane, 2000). It is therefore possible that the addition of one of these reagents may trigger TNAP activation. However this would need to be confirmed through further cell culture experimentation.

3.5 Conclusions

In conclusion, inhibition of the ANK pyrophosphate transporter results in an increase in ICLA within the murine 3T3-L1 preadipocyte, potentially through increased levels of intracellular pyrophosphate. This increase in lipid accumulation is proposed to be mediated through an increase in TNAP activity (a known positive mediator of intracellular lipid accumulation). The mechanism by which TNAP increases intracellular lipid accumulation is not known, however it is clear from this work that TNAP does not function by alleviating pyrophosphate-associated inhibition of ICLA. It is therefore possible that TNAP functions within ICLA to generate phosphate from pyrophosphate, and phosphate is a known transcription factor that functions in bone to increase mineralization (Beck et al., 2003). Furthermore, inhibition of ANK causes both cellular hypertrophy and storage of lipids in a larger number of small lipid droplets.

These data suggest that pyrophosphate (or phosphate) may play a role in the control of lipid droplet fusion, a process that is known to produce the characteristic unilocular lipid droplet of mature adipocytes (Yang et al., 2012).

4 Tissue non-specific alkaline phosphatase functions to control intracellular lipid accumulation through the generation of intracellular inorganic phosphate

4.1 Background

Adipose tissue contains both immature (preadipocytes) and mature adipocytes. The process of maturation of the preadipocyte is termed adipogenesis, during which various mechanisms work together to allow the differentiation of the preadipocyte into a mature adipocyte. During differentiation, genes which code for proteins that give rise to the mature cell phenotype, including the accumulation of lipid droplets in the cytoplasm of the cell, become expressed via a process that is controlled by a number of transcription factors. These factors include CCAAT enhancer binding protein alpha (C/EBPα) and peroxisome proliferator-activated receptor gamma (PPARϒ). The expression of these transcription factors occurs rapidly on stimulation of differentiation (Shoham & Gefen, 2012, Lowe et al., 2011, Tang, 2003). Tissue non-specific alkaline phosphatase (TNAP), is a known positive mediator of intracellular lipid accumulation (Ali et al., 2005).

Tissue non-specific alkaline phosphatase is a homodimeric metalloenzyme which is expressed ubiquitously throughout the body (Harris, 1989, Balcerzak et al., 2003). The function of TNAP within many of the tissues in which it is expressed is largely unknown, with the exception of bone, where TNAP is important for bone mineralization

(Balcerzak et al., 2003, Hessle et al., 2002). Within bone TNAP catalyzes the hydrolysis of pyrophosphate resulting in the release of inorganic phosphate. Inorganic phosphate is known to stimulate bone mineralization whilst inorganic pyrophosphate inhibits this process (Johnson et al., 2000). Within bone it is known that the balance between inorganic phosphate and pyrophosphate is maintained by the action of TNAP and ectonucleotide pyrophosphatase/phosphodiesterase 1 (ENPP-1) (which produces pyrophosphate from ATP) and the p*rogressive ankylosis* gene (ANK). ANK is a transmembrane protein that acts to transport pyrophosphate out of the cell and into the extracellular milieu (Ho et al., 2000). Inorganic phosphate is transported into the cell by sodium dependent channels (Beck et al., 2003).

Within adipocytes, it has been demonstrated that the knockdown of TNAP by siRNAs results in the cessation of ICLA in the 3T3-L1 mouse preadipocyte cell line (Ali et al., 2005) and in human mammary gland preadipocytes, ICLA was blocked by the TNAP inhibitor histidine (Ali et al., 2006). Adipocytes and osteoblasts are both of mesenchymal origin, and it has been shown that it is possible to reprogram adipocytes into osteoblasts (Takahashi 2011). Thus, these two cell types must share some common molecular pathways that control cellular differentiation and/or maturation and which may involve TNAP function.

The inhibition of ANK results in an increase in ICLA (Chapter 3), demonstrating the TNAP does not function within the preadipocytes during adipogenesis to alleviate an inhibitory concentration of pyrophosphate. It is therefore likely that is through the ability of TNAP to generate phosphate that is mediates its effect on intracellular lipid

accumulation. Evidence that inorganic phosphate may act in this fashion comes from experimental studies in osteoblasts, where it has been shown that intracellular inorganic phosphate acts as a signaling molecule in the regulation of osteoblast differentiation (Beck, 2003, Beck et al., 2003). Inorganic phosphate acts as a transcription activator in osteoblasts (Beck, 2003) and has been shown to be able to completely replace TNAP in the differentiation of osteoblasts (Beck et al., 2003). This demonstrates that one major function of TNAP in osteoblasts is to produce inorganic phosphate (Bellows et al., 1992) . Therefore, the aim of the present study was to determine whether TNAP activates intra-cellular lipid accumulation in 3T3-L1 preadipocytes by the generation of inorganic phosphate.

4.2 Methods

4.2.1 Determining whether TNAP activity can be replaced with extracellular phosphate during intracellular lipid accumulation.

To determine if TNAP activity can be replaced by phosphate, 3T3-L1 mouse preadipocyte cells were induced to undergo intracellular lipid accumulation in the presence and absence of 5 mM levamisole, a TNAP inhibitor (section 2.3.1).

Phosphate was added to complete growth medium at a concentration of 10 mM, to determine if phosphate is capable of reconstituting intracellular lipid accumulation in

the presence of the TNAP inhibitor levamisole, which blocks TNAP activity and hence inhibits intracellular lipid accumulation (section 2.16).

The accumulation of lipids was determined through staining the cells with Oil Red O (section 2.9), and the lipid droplets were visualized (section 2.12). Protein was extracted from the cells (section 2.4) and used to measure TNAP activity using the ADVIA autoanalyser (Siemens) (Section 2.6), to ensure that TNAP is present during the course of intracellular lipid accumulation and decreased following treatment with the inhibitor.

Measurement of TNAP activity and Oil Red O staining were performed at baseline (day 0) and on day 8 (as this was when maximal lipid accumulation occurred). Measurement of intracellular inorganic phosphate levels where performed on day 0, 1, 4 and 8 (section 2.15).

4.2.2 Control experiments

All control experiments contained a differentiation control where TNAP was not inhibited and a control without added chelators or channel inhibitors

All control experiments were undertaken in the presence of 5 mM levamisole (section 2.3.1) and the addition of extracellular phosphate (section 2.16) with the exception of

the sulphate control. In all cases differentiation was monitored through intracellular lipid accumulation (section 2.2.1), and the inhibition of TNAP activity was confirmed through TNAP activity assays (section 2.6)

To ensure the effect noted is due to the presence of phosphate and not the carrier ion, sodium, a sulphate control was included. Sulphate was selected due to it having a similar structure to phosphate (section 2.16).

To ensure the ability of phosphate to mediate ICLA is not caused by sequestering and depletion of calcium through the formation of calcium phosphate precipitation, 10mM of intracellular (BAPTA/AM) and extracellular (ethylene glycol tetra acetic acid) calcium chelators were added to determine if they can mimic the effect of the phosphate (section 2.17.2).

To ensure that the effect of differentiation was in fact due to the phosphate entering the cells the sodium dependant phosphate channels were inhibited with foscarnet (section 2.17.1) preventing the entry of phosphate into the cells.

4.3 Results

4.3.1 Intracellular phosphate levels are elevated during adipogenesis

Within 24 hours of induction of intracellular lipid accumulation, there is a significant increase in the levels of intracellular phosphate (246.01 ± 50.90 %; $p= 0.038$) compared to levels on day 0 (phosphate levels set at 100%). The phosphate remained significantly raised throughout the experiment. When TNAP activity and therefore ICLA were inhibited through the use of levamisole, there was an increase in the level of intracellular phosphate at day 1 which just missed significance ($p= 0.051$ vs day 0), whilst by day 4 phosphate levels were very close to day 0 levels ($p= 0.19$ vs day 0) and at day 8 levels were greater than day 0 but again did not reach statistical significance against day 0 ($p= 0.074$) (Figure 4.1). On days 1 and 4 phosphate levels were significantly higher ($p<0.05$) in cells not treated with levamisole when compared to those treated with the TNAP inhibitor, whilst on day 8 phosphate levels were very similar in the treated and non-treated cells.

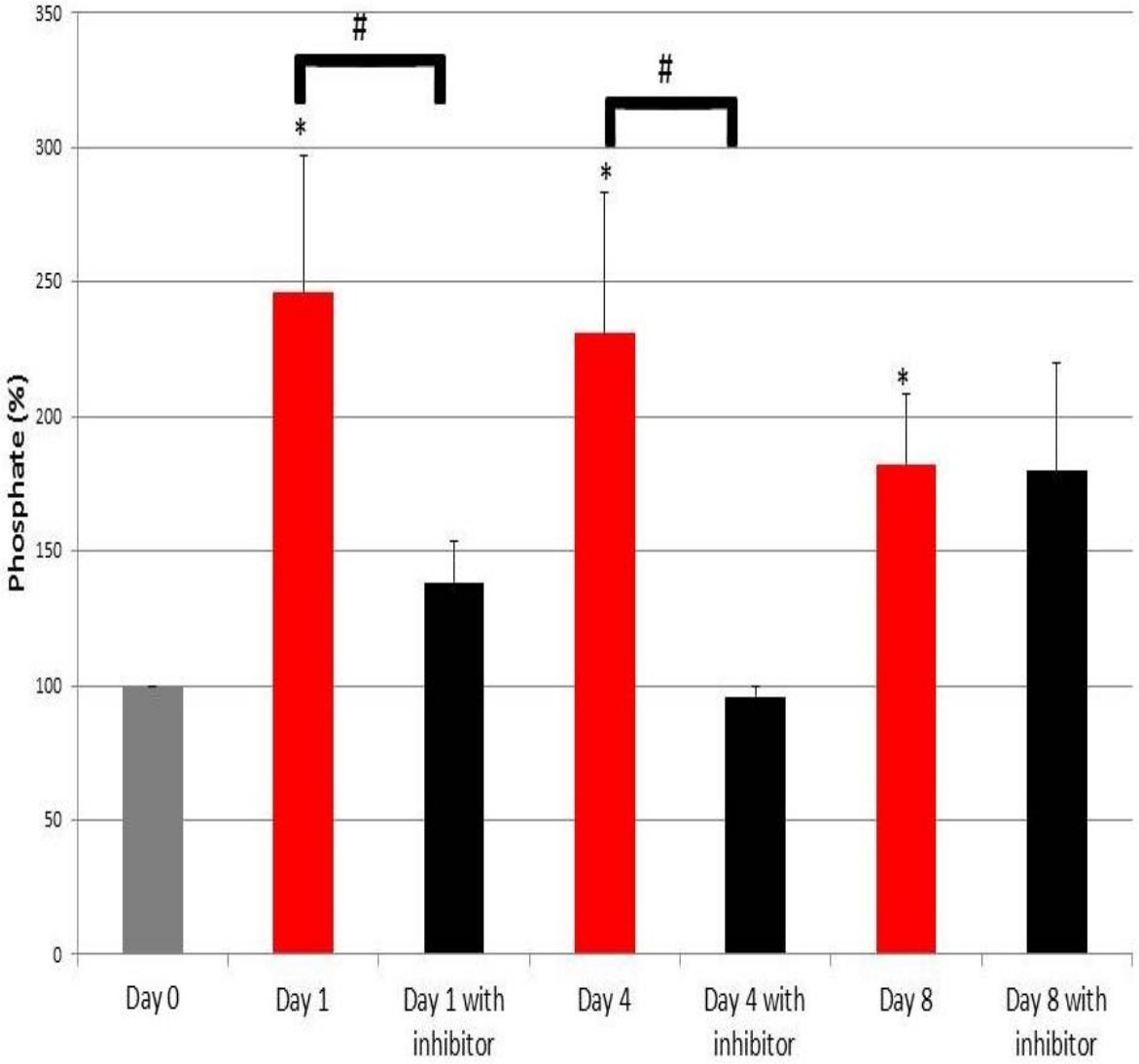

Figure 4.1: Intracellular phosphate levels in the presence and absence of levamisole; *p<0.05 vs day 0; #p<0.05 treated vs non-treated cells. Experiments were conducted in triplicate and error bars represent ± SD.

4.3.2 Intracellular lipid accumulation in cells deficient in TNAP activity is reconstituted in cells exposed to extracellular phosphate

In cells inhibited with levamisole there was no intracellular lipid accumulation by day 8. When phosphate was added to cells treated with levamisole, the level of intracellular lipid accumulation was similar to that seen in cells not treated with levamisole (284.01 ± 62.52% vs 275.86 ± 35.52% respectively; p= 0.83). The addition of sulphate as a control was not able to reconstitute lipid levels to those seen in the cells not treated with levamisole (284.01 ± 62.52 vs 144.63 ± 14.81; p= 0.018). In cells not treated with the transformation cocktail, no lipid accumulation was observed (Figure 4.4).

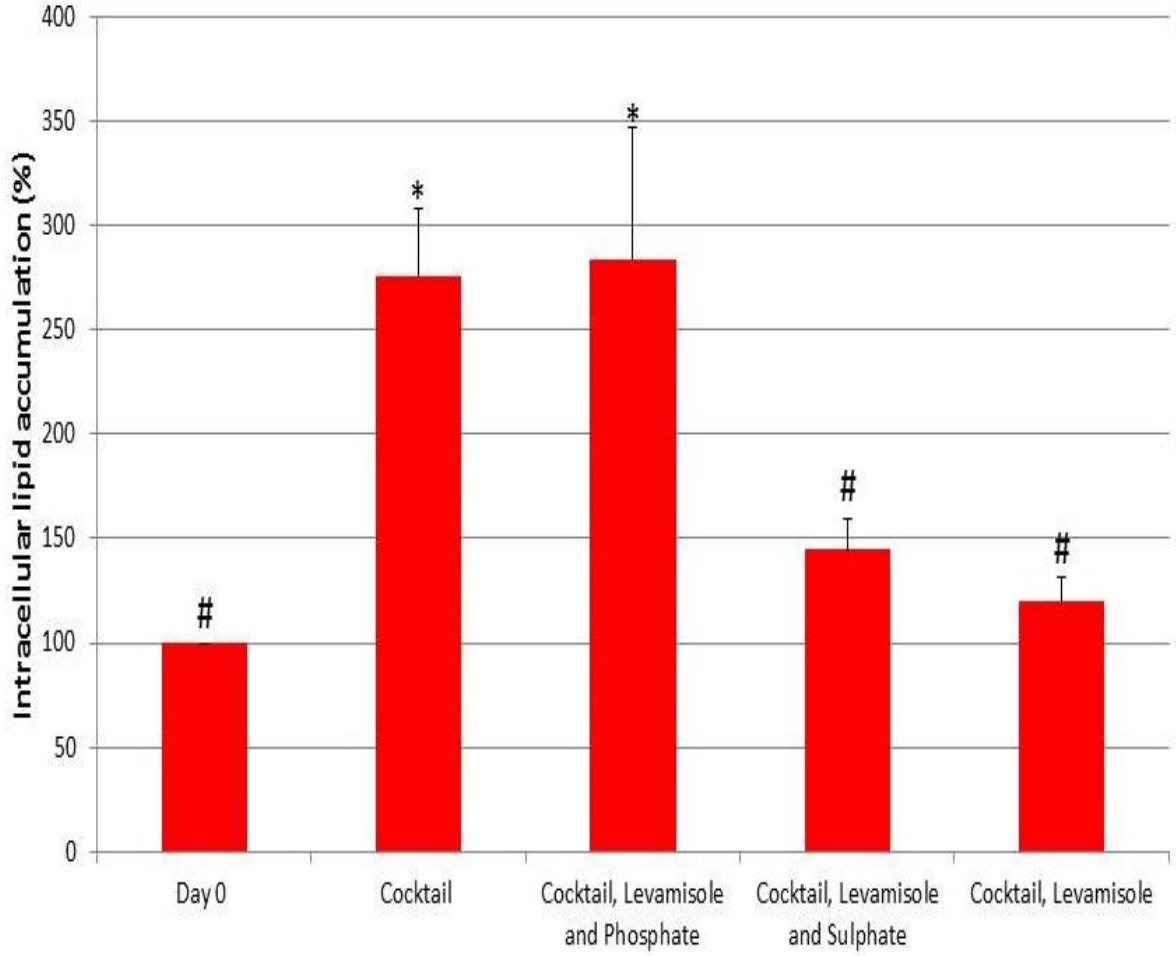

Figure 4.2: Intracellular lipid accumulation was induced through the addition of transformation cocktail. Levamisole treatment inhibited lipid accumulations to baseline levels (day 0). In the presence of levamisole, lipid levels were reconstituted by the addition of 10mM phosphate, but not 10 mM sulphate; *$p<0.05$ vs baseline; #$p<0.05$ vs cocktail-only treated cells. Experiments were conducted in triplicate and error bars represent ± SD.

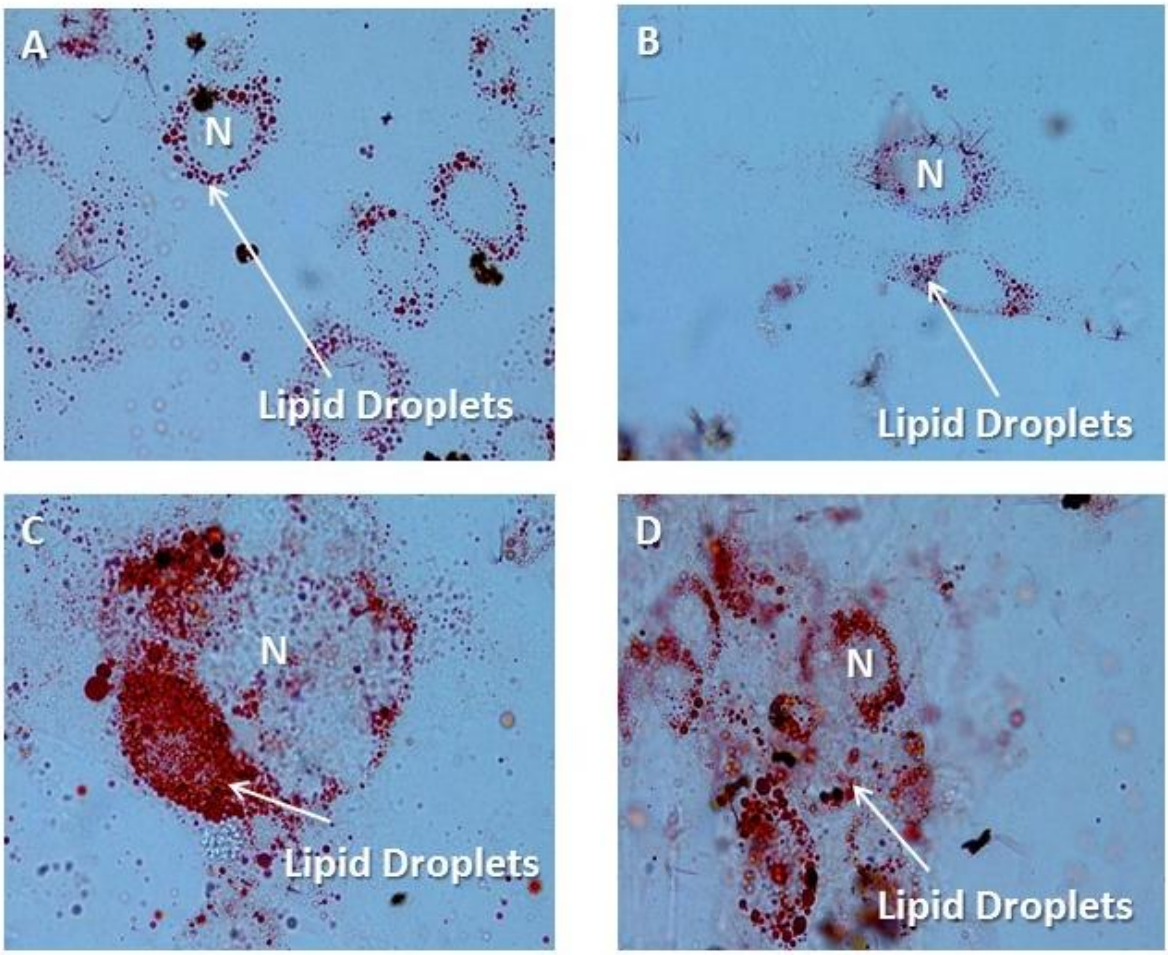

Figure 4.3: The ability of phosphate to reconstitute intracellular lipid accumulation was determined through the addition of extracellular phosphate to cells lacking TNAP activity (through levamisole inhibition). Lipid accumulation was inhibited in cells treated with levamisole and sulphate (A) and cells treated with levamisole alone (B). The addition of phosphate to levamisole treated cells (C), resulted in a reconstitution of lipid accumulation to levels similar to that seen in an adipogeneiss control (lacking levamisole; D); 100x magnification

4.3.3 TNAP activity in the presence of levamisole and phosphate

To confirm that there was reduced TNAP activity in the cells after levamisole treatment, TNAP activity was measured after 8 day of exposure to levamisole. TNAP

activity was significantly lower ($p<0.05$ in all cases) in all cells treated with levamisole when compared to the cells not treated with levamisole (Figure 4.4).

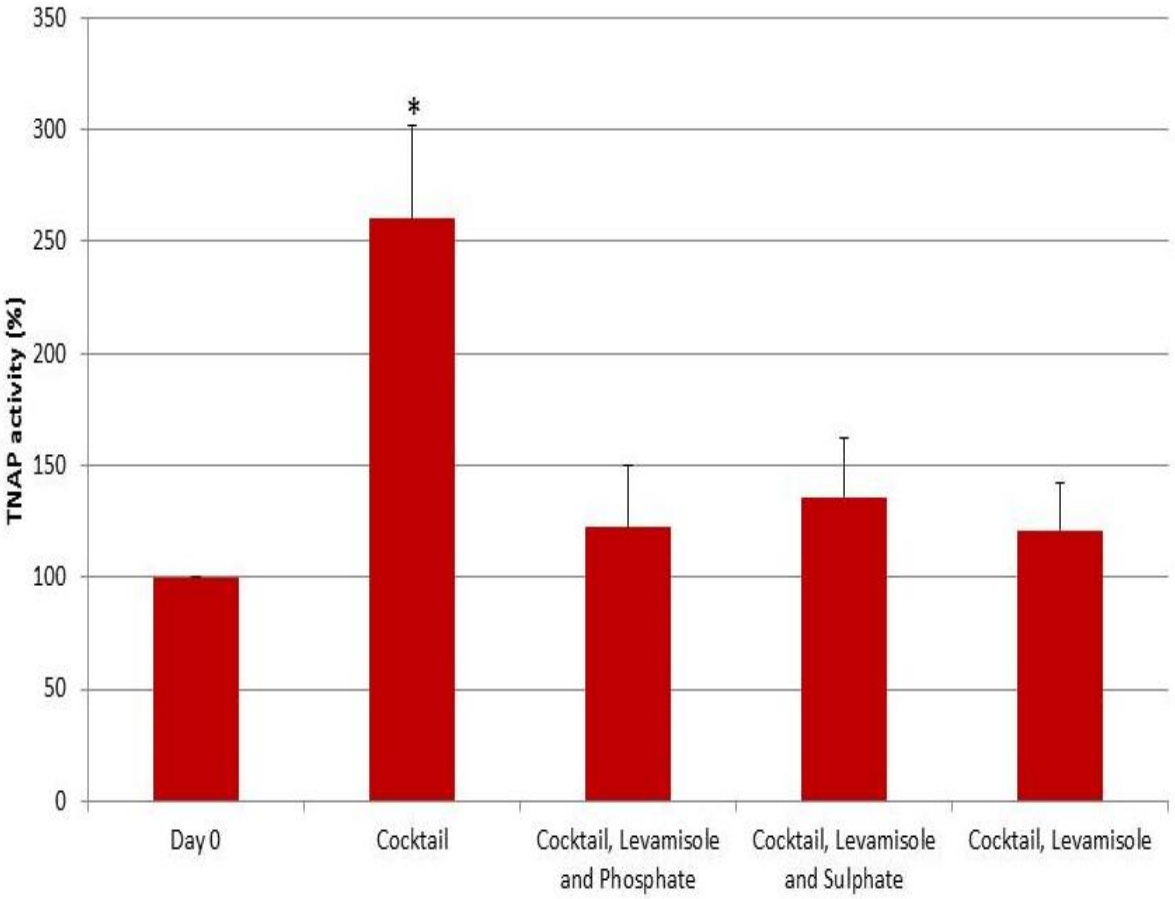

Figure 4.4: Inhibition of TNAP activity with levamisole was confirmed after 8 days of incubation and compared to cells allowed to undergo adipogenesis without the addition of an inhibitor. Cells treated with levamisole had TNAP activity significantly decreased from those without levamisole whilst phosphate had no effect on TNAP activity; *$p<0.05$ vs all other treatments and day 0. Experiments were conducted in triplicate and error bars represent ± SD.

4.3.4 Effect of intracellular and extracellular calcium chelators on phosphate-mediated lipid accumulation

Intracellular lipid levels on day 8 of incubation were not significantly different in cells treated with cocktail, levamisole and phosphate (284.01 ± 62.52%) when compared to cells treated with intracellular BAPTA/AM (278 ± 55.22; p=0.78) or extracellular ethylene glycol tetraacetic acid [EGTA] (250 ± 36.25%; p=0.42) calcium chelators in the presence of cocktail, levamisole and phosphate (Figure 4.5).

4.3.5 Effect of inhibition of the sodium-dependant phosphate channel on phosphate-mediated lipid accumulation.

In cells treated with the sodium dependant phosphate channel inhibitor foscarnet, intracellular lipid accumulation on day 8 of incubation was significantly lower when compared to the cells not treated with foscarnet (131.70 ± 21.01 vs 284.01 ± 62.52, respectively; p = 0.025) and was not significantly different to levels seen in the cells treated with levamisole and cocktail (100%; p = 0.12) (Figure 4.5).

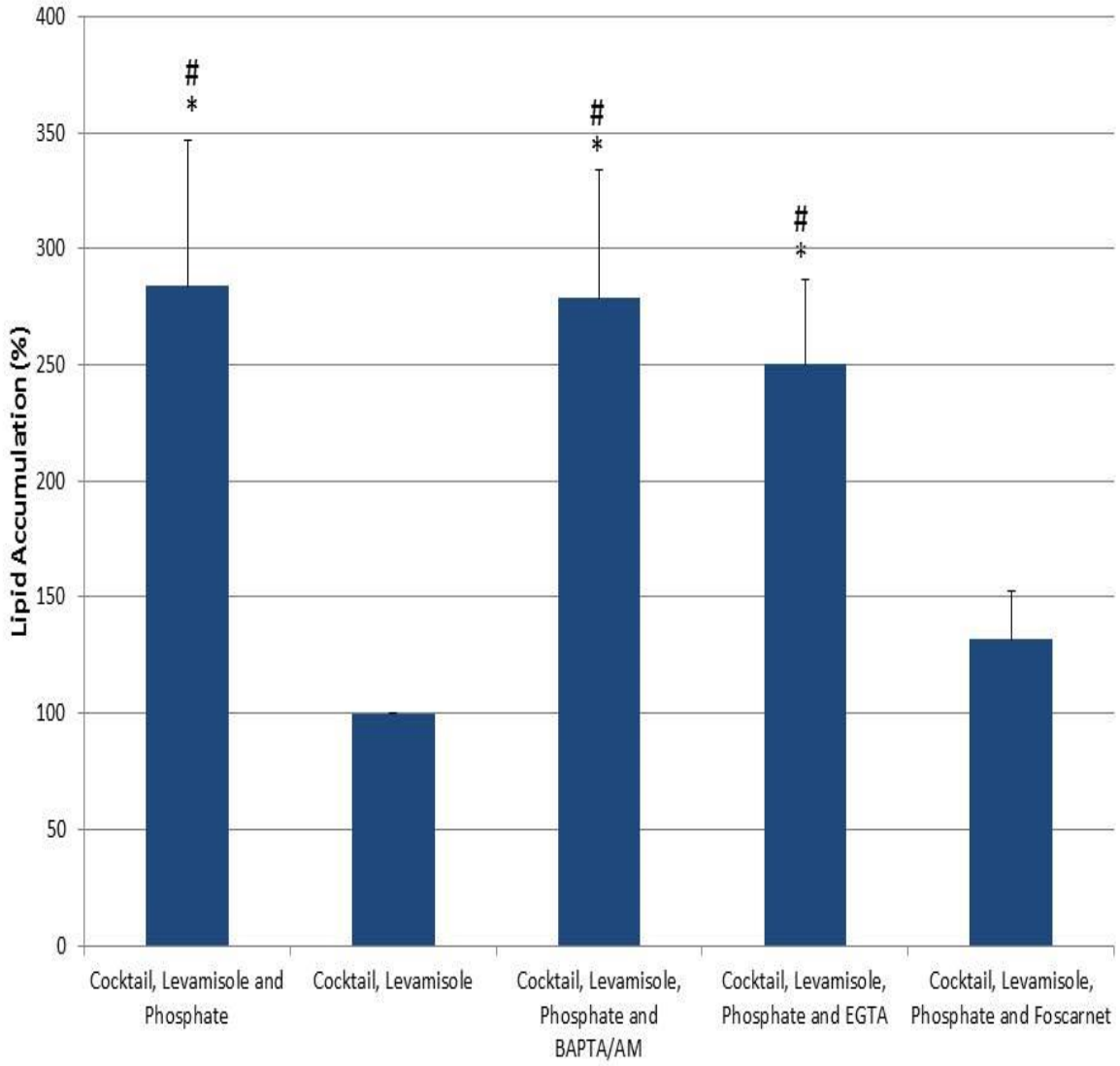

Figure 4.5: To confirm that phosphate is able to reconstitute intracellular lipid accumulation, and the effect is not caused through effects of calcium, 3T3-L1 were treated with an intracellular calcium chelator (BAPTA/AM) and an extracellular calcium chelator (EGTA). To ensure the effect was mediated through the entry of phosphate into the cells, the cells were treated with an inhibitor of Na^+ dependant phosphate channels (foscarnet). The resultant intracellular lipid accumulation was determined though Oil Red O staining and compared to levels seen in cells treated with phosphate and those seen in the levamisole control. Statistical significance from cocktail plus levamisole is indicated by a *$p<0.05$ and statistical difference from the foscarnet control is designated by $^{\#}p<0.05$). Experiments were conducted in triplicate and error bars represent ± SD.

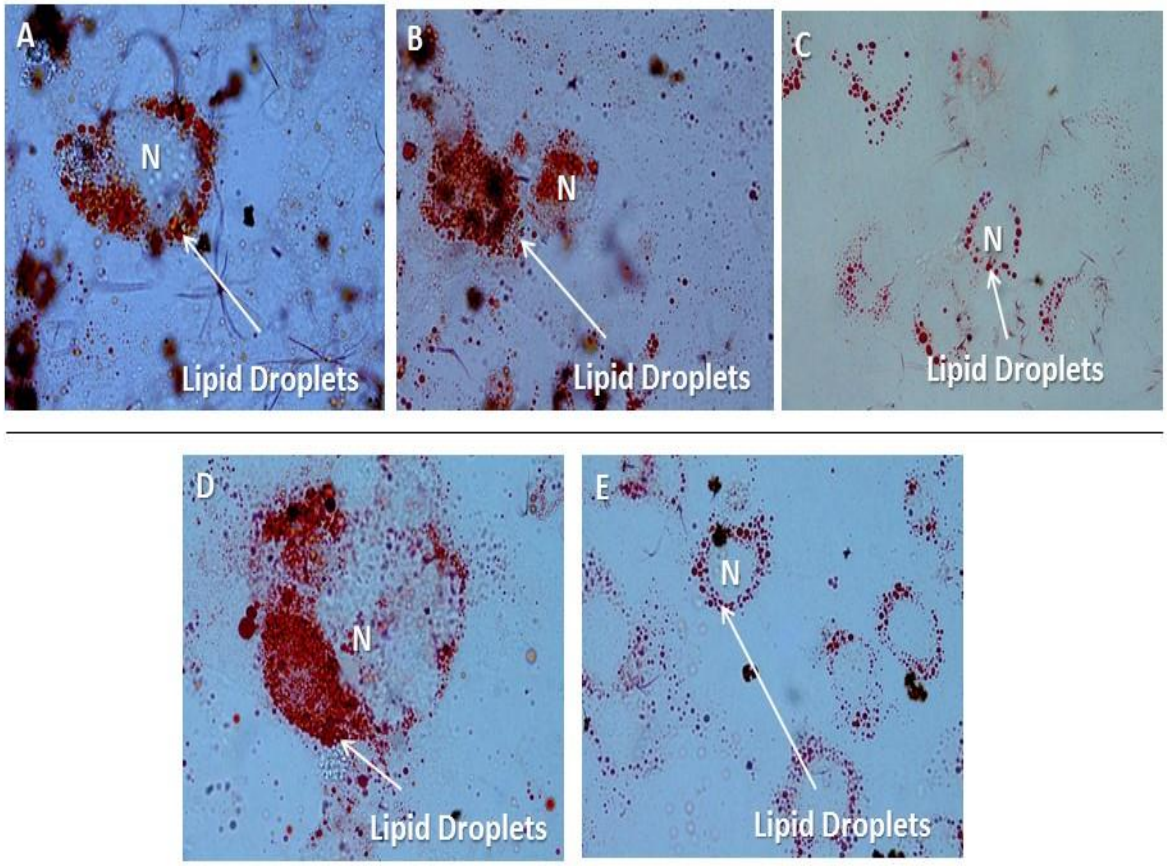

Figure 4.6: Microscopic visualisation of Oil Red O stained lipids in phosphate control experiments at 100x magnification. Phosphate-mediated lipid accumulation was noted in the absence of extracellular calcium (A – cells treated with an extracellular calcium chelator, EGTA) or intracellular calcium (B - cells treated with an intracellular calcium chelator, BAPTA/AM). In cells treated with foscarnet (an inhibitor of sodium dependant phosphate channels – C) thereby preventing phosphate from entering the cells, phosphate-mediated lipid accumulation was reduced. The lipid accumulation was compared to levels seen in cells treated with phosphate D) and those seen in the levamisole control (E).

4.4 Discussion

This study demonstrated that during the course of intracellular lipid accumulation (ICLA) intracellular phosphate concentration increased above baseline levels. Cells induced to undergo adipogenesis in the absence of TNAP activity were unable to accumulate lipids. However, the addition of 10mM extracellular phosphate was able to reconstitute lipid accumulation. This effect was shown to be specific to the addition of phosphate.

4.4.1 Phosphate is increased during adipogenesis

Tissue nonspecific alkaline phosphatase is an essential positive mediator of ICLA within the preadipocytes. Inhibition of this activity through treatment with levamisole, a potent inhibitor of TNAP activity is able to induce the cessation of adipogenesis and the associated lipid accumulation (Ali et al., 2005, Ali et al., 2006a, Ali et al., 2006b). It was hypothesized that the function of TNAP within the preadipocytes may be mediated through the generation of phosphate. Quantitation of intracellular phosphate showed that during the course of adipogenesis, there is a rise in intracellular phosphate concentration, most notably within the initial 4 days of lipid accumulation (Figure 4.1). When TNAP activity is inhibited there is no significant increase in the levels of phosphate above the baseline levels.

On days 1 and 4 of ICLA, phosphate levels are significantly higher in cells not treated with levamisole when compared to those treated with the TNAP inhibitor (Figure 4.1). This suggests that the rise in phosphate levels above baseline is due to TNAP but it cannot be ruled out that other sources of phosphate may also contribute to this. On day 8, phosphate levels in the levamisole treated cells are very similar to those in the non-treated cells and higher (though not statistically so) than on day 0. This suggests that the intracellular phosphate pool on day 8 may be contributed to by other non-TNAP related sources that are activated by the low phosphate levels caused by levamisole.

4.4.2 Phosphate is able to increase intracellular lipid accumulation in preadipocytes lacking TNAP activity

In cells where TNAP activity is inhibited with levamisole, no lipid accumulation is seen (Chapter 3 and Figure 4.2), however, the addition of phosphate to the extracellular milieu is able to completely reverse this effect (Figure 4.2). Sulphate was added to cells inhibited with levamisole as a control, and both phosphate and sulphate had the same carrier ion, sodium, to rule out any carrier ion effects. Sulphate was chosen as the control anion because of its structural similarity to phosphate (Beck et al., 2003). Within the sulphate control minimal lipid accumulation was noted, which suggests that phosphate is specifically able to stimulate lipid accumulation in the 3T3-L1 cells. Furthermore, in the cells treated with the differentiation cocktail, levamisole and phosphate, TNAP activity was maintained at baseline levels (Figure 4.3) suggesting that any lipid accumulation occurring in these cells is not due to TNAP but phosphate

and that phosphate may be the mechanism by which TNAP induces lipid accumulation.

4.4.3 Phosphate does not function to deplete calcium by causing calcium phosphate precipitation.

Calcium has well documented anti-adipogenic effects at high concentrations (>2.5mM) (Jensen et al., 2004) in 3T3-L1 cells. High intracellular calcium within human preadipocytes has also been shown to result in the inhibition of adipogenesis (Shi et al., 2000). Calcium functions within preadipocytes to activate calcineurin (a calcium dependant serine/threonine protein phosphatase), the activation of which results in the downregulation of the pro-adipogenic genes, PPARγ and C/EBPα (Neal and Clipstone, 2002). Calcium and phosphate are able to form a precipitate within the cell (Bellows et al., 1992). It is therefore possible that the mechanism through which phosphate works within adipogenesis, is to form a precipitate with calcium, thereby inhibiting calcineurin action. To determine whether the mechanism by which TNAP-generated phosphate functions in adipogenesis is to sequester calcium via calcium phosphate precipitation, thereby preventing the anti-adipogenic actions of calcium, calcium chelators were added to the cells. Neither the intracellular (BAPTA/ AM) nor the extracellular (EGTA) calcium chelators had any effect on the ability of phosphate to increase intracellular lipid accumulation (Figure 4.5). This suggests that phosphate is not functioning by causing calcium phosphate precipitation and thus blocking calcium effects.

4.4.4 Inhibition of sodium-dependant phosphate channels prevented intracellular lipid accumulation

Intracellular lipid accumulation was not increased when phosphate was prevented from entering the cell by use of the sodium-dependent phosphate channel inhibitor foscarnet. This is further proof that phosphate is specifically able to enhance lipid accumulation in the 3T3-L1 cells in the absence of TNAP activity.

4.4.5 Proposed mechanism of action of TNAP-generated phosphate in adipogenesis

It is clear that phosphate is able to completely reconstitute intracellular lipid accumulation in the murine 3T3-L1 cell line in the absence of TNAP activity, and therefore TNAP may function within adipogenesis to generate phosphate. The phosphate generated by TNAP functions intracellularly, and may be needed for gene expression.

The role of phosphate as a signalling molecule has previously been established in numerous cell types including the osteoblast and the chondrocyte (Beck, 2003, Beck et al., 2000, Khoshniat et al., 2011). Phosphate is able to regulate the expression of transcriptional regulators such as nuclear factor (erythroid-derived 2)-like 2 (NRF2) (Beck et al., 2003), which is known to induce the expression of the pro-adipogenic gene CCAAT/enhancer-binding protein β (C/EBPβ) in adipogenesis (Hou et al., 2012).

It is therefore likely that TNAP mediates intracellular lipid accumulation in 3T3-L1 preadipocytes through the generation of phosphate which acts intracellularly, potentially in mediating the expression of transcription factors such as NRF2.

5 Tissue non-specific alkaline phosphatase-generated phosphate mediates the expression of NRF2

5.1 Background

In osteoblast precursor cells (MC3T3-E1), it has been shown that inorganic phosphate promotes nuclear factor (erythroid-derived 2)-like 2 (NRF2) gene expression (Beck et al, 2003). This protein is a cap-n-collar basic leucine zipper transcription factor that has been shown to increase adipogenesis (Hou et al. 2012), and causes severe metabolic syndrome in ob/ob mice deficient in NRF2 (Xue et al. 2013). This factor has also been shown to regulate the transcription of c/EBPβ and PPARϒ, which are terminal factors responsible for adipogenesis (Chen et al. 2013). Deficiency of NRF2 in mouse preadipocytes and embryonic fibroblasts results in impaired adipogenesis (Hou et al. 2012) (Pi et al. 2010).

The NRF2 knockdown mouse displays a decrease in fat mass, and does not become obese when exposed to high fat diets (Pi, 2010). The *ob/ob* mice with an adipocyte-specific knockout of the NRF2 gene showed reduced body weight, but developed insulin resistance and hyperglycemia (Xue et al. 2013). It is thought that NRF2 plays a role as a key transcription factor in the control of adipogenesis, lipogenesis, insulin sensitivity and glucose homeostasis (Chen et al. 2013).

As NRF2 has been implicated in adipogenesis, and it has been shown in osteoblasts that TNAP-generated phosphate can induce expression of NRF2, we aimed to determine if the function of TNAP within adipocytes is to stimulate the expression of NRF2 via phosphate generation thereby resulting in the progression of adipogenesis.

5.2 Methods

5.2.1 Cell culture and differentiation

The 3T3-L1 cells were cultured (section 2.1.1) and induced to accumulate lipids in the absence of TNAP activity (measured with the alkaline phosphatase, diethanolamine detection kit - section 2.16) with added phosphate to compensate for the lost TNAP activity. Progression of differentiation and intracellular lipid accumulation was monitored by detecting gene expression through real time PCR (section 2.24) and lipid accumulation through Oil Red O staining of neutral lipids (section 2.9).

5.2.2 Determining the ability of phosphate to induce NRF2 gene expression in 3T3-L1 preadipocytes

The ability of inorganic phosphate to enter the nucleus and activate NRF2 activity was determined by monitoring *NRF2* gene expression (with real time PCR (section 2.24) within mouse preadipocytes in the presence and absence of extracellular phosphate in cells treated with levamisole to inhibit TNAP activity (section 2.3.1). As induction of gene expression is expected to occur rapidly upon phosphate treatment, monitoring on gene expression was restricted to the initial 48 hours of phosphate treatment.

5.3 Results

5.3.1 NRF2 gene expression is inhibited when TNAP activity is inhibited

The 3T3-L1 preadipocytes were induced to accumulate lipids in the presence and absence of TNAP activity (through treatment with levamisole) as previously shown (Figure 5.1).

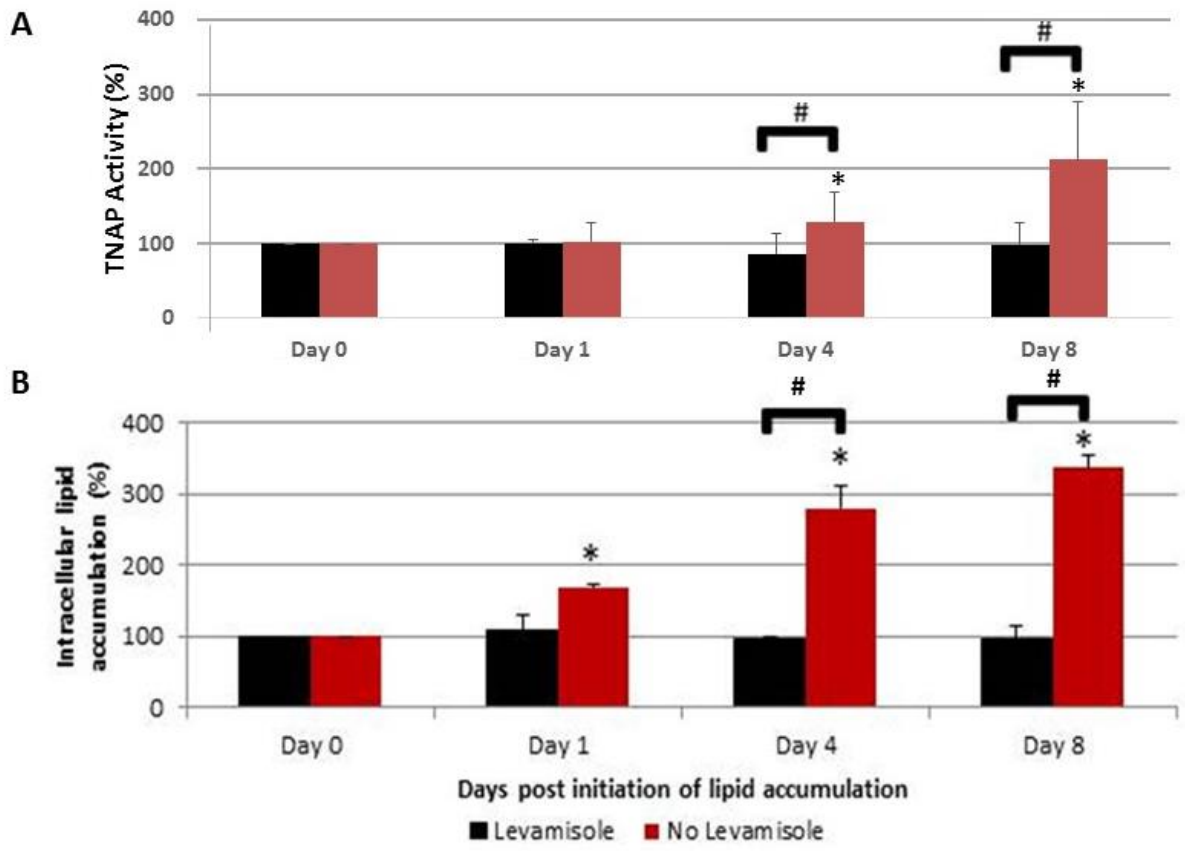

Figure 5.1: Intracellular lipid accumulation was inhibited in the presence of levamisole in the 3T3-L1 cell line (A). Levamisole induced inhibition of TNAP activity was confirmed (B). Experiments were conducted in triplicate and error bars represent ± SD.

The NRF2 gene expression was monitored through relative quantification using β-actin as the reference gene and results were expressed as a percentage of the baseline expression. B-actin was chosen as the reference gene based on the outcome of a study by Zhang and colleagues determining suitable reference genes for measuring gene expression in 3T3-L1 cells. They identified that β-actin acts as a stable reference gene during adipogenesis within these cells (Zhang et al., 2014). The NRF2 gene expression levels were higher than baseline throughout intracellular lipid accumulation reaching levels of 319.21 ± 27.88 % ($p = 0.005$ vs baseline) by 8 days of lipid accumulation. In cells lacking TNAP activity there was no increase in the levels of NRF2 mRNA above baseline levels (Figure 5.2).

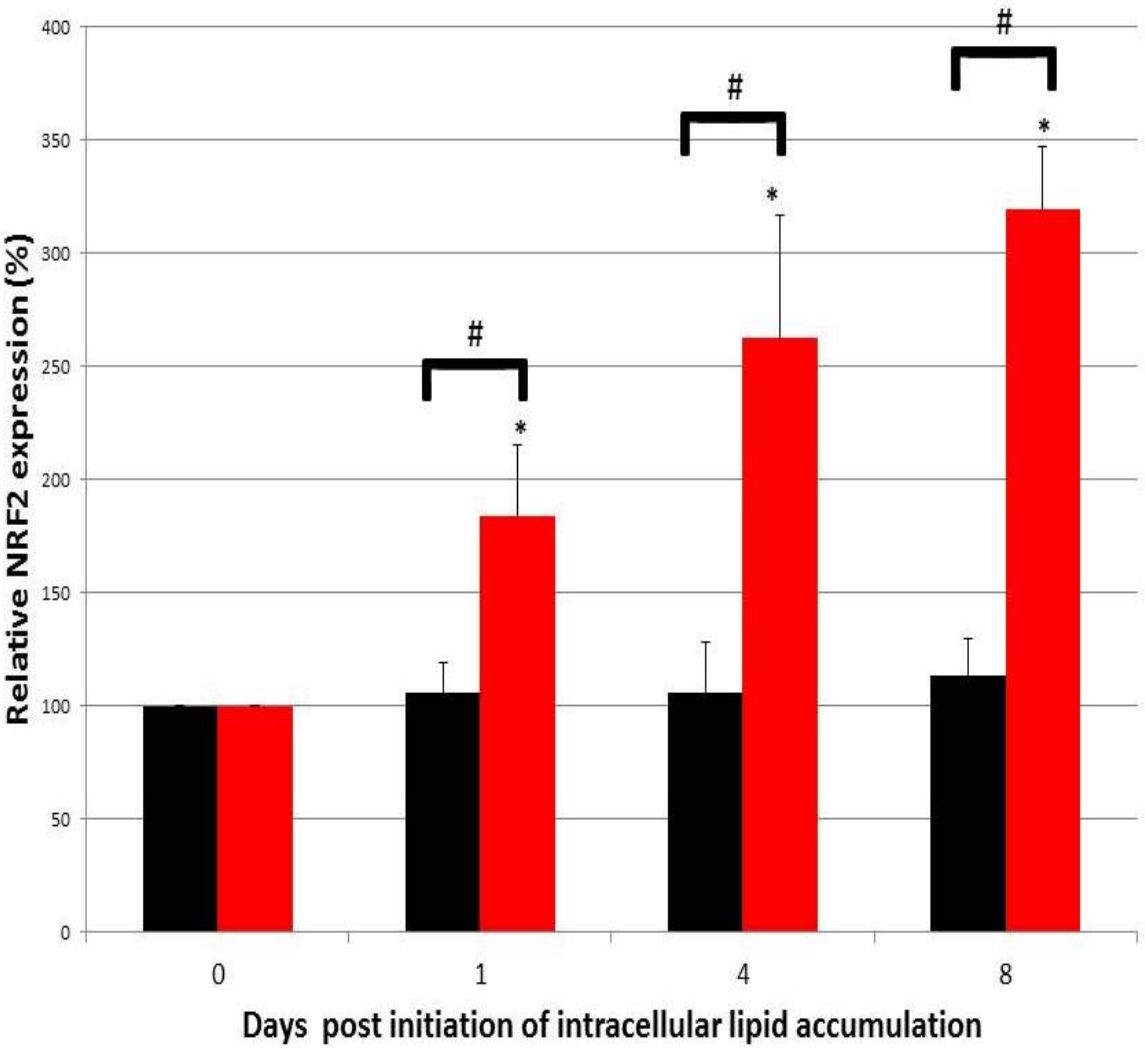

Figure 5.2: NRF2 mRNA is increased in 3T3-L1 cells in the presence of intracellular lipid accumulation (red bars), however it remains unchanged when TNAP activity is inhibited (black bars); #p<0.05 intra-day comparisons; *p<0.05 versus baseline. Experiments were conducted in triplicate and error bars represent ± SD.

5.3.2 NRF2 gene expression is upregulated in the presence of extracellular phosphate

In order to ascertain whether NRF2 expression was induced by TNAP-generated phosphate within the context of adipogenesis, 3T3-L1 cells were exposed to the TNAP

inhibitor levamisole and 10mM extracellular phosphate was added to the extracellular milieu. The NRF2 mRNA was measured before the addition of phosphate and at 1, 8, 24 and 48 hours after the addition of phosphate and compared to cells not exposed to extracellular phosphate. In cells exposed to phosphate NRF2 levels were increased within 1 hour of exposure when compared to cells not exposed to phosphate (216.64 ± 19.24% vs 98.28 ± 3.79%, respectively; $p = 0.004$) (Figure 5.3). Furthermore, in cells exposed to phosphate NRF2 expression was higher than baseline at all time points whilst in cells not exposed to phosphate NRF2 expression remained at baseline levels (Figure 5.3).

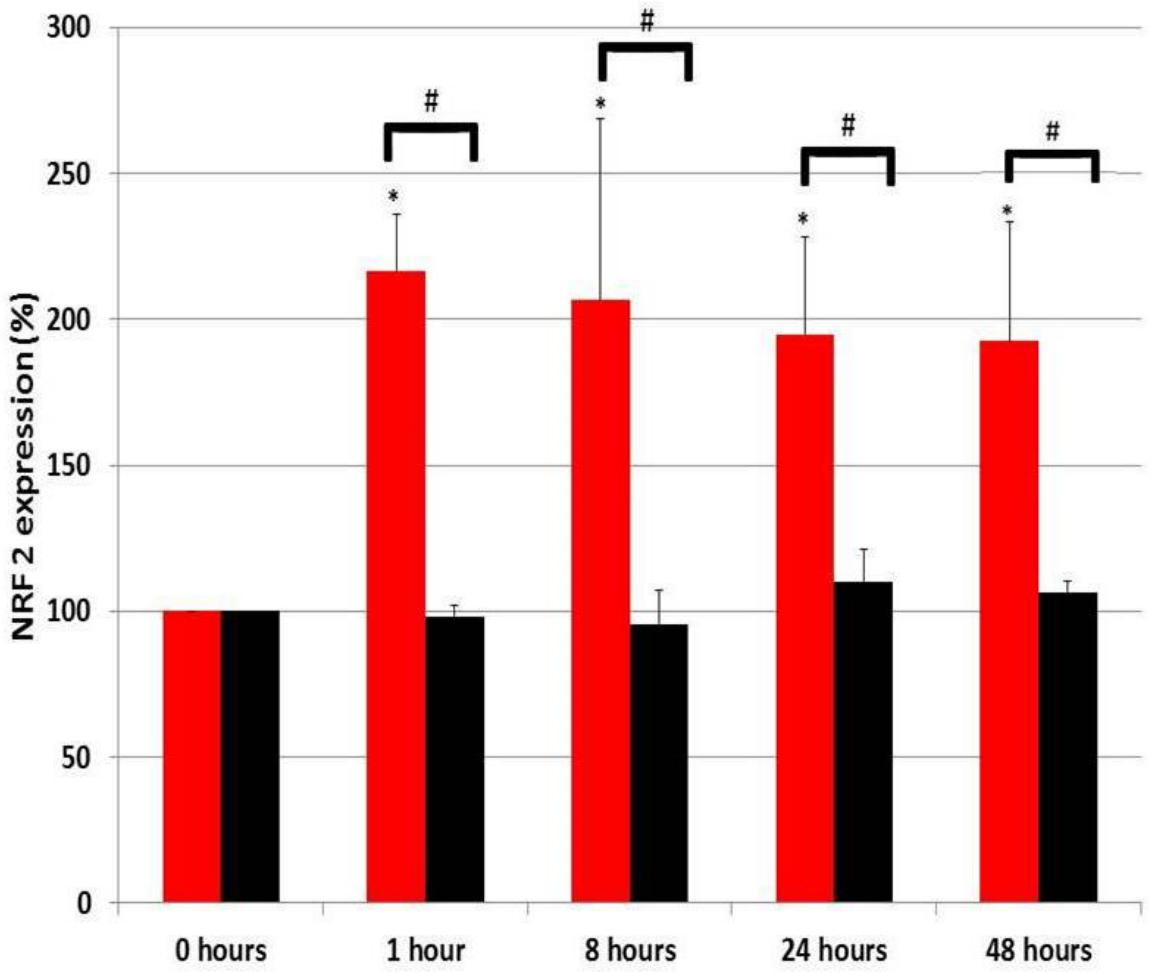

Figure 5.3: Phosphate upregulates NRF2 expression in 3T3-L1 preadipocytes. In cells lacking TNAP activity the addition of phosphate (red bars) induced a greater than 200% increase in the levels of NRF2 gene expression when compared to cells not exposed to extracellular phosphate (black bars); #p<0.05 intraday comparisons; *p<0.05 versus baseline. Experiments were conducted in triplicate and error bars represent ± SD.

5.3.3 Expression of NRF2 in 3T3-L1 cells in the absence of TNAP activity partially reconstitutes intracellular lipid accumulation

To determine whether TNAP functions to increase lipid accumulation within preadipocytes via activation of NRF2 expression, cells lacking TNAP activity (through treatment with levamisole) were transfected with NRF2 expressing plasmids (NRF 2

expression was confirmed through real-time PCR (Appendix A4)). Inhibition of TNAP activity was confirmed on Day 8 of lipid accumulation and compared to that seen in the positive control (137.9 ± 27.1 vs 246.5 ± 39.7; p= 0.011) (Figure 5.4). Intracellular lipid accumulation was determined through Oil Red O staining and compared between the cells transfected with NRF2 plasmids (in the absence of TNAP activity) and cells allowed to undergo intracellular lipid accumulation in the presence of an empty vector (positive control).

The plasma half-life of levamisole is reported to be 3-4 hours, however, according to the Drug Enforcement Administration (DEA) 70% of levamisole is cleared by the kidneys within 3 days (Drug Enforcement Administration, 2013). It is therefore likely that within the context of cell culture, the drug will remain functional for a longer period of time, however, the exact half-life would need to be confirmed. We replenished the levamisole every 48 hours, and it is therefore feasible that the drug levels were reduced below amounts needed to completely inhibit TNAP activity. This may account for the background level of ICLA seen within levamisole treated cells. It may therefore be of use to confirm these results using RNA interference (RNAi) or generating an ALPL deficient cell line in the future.

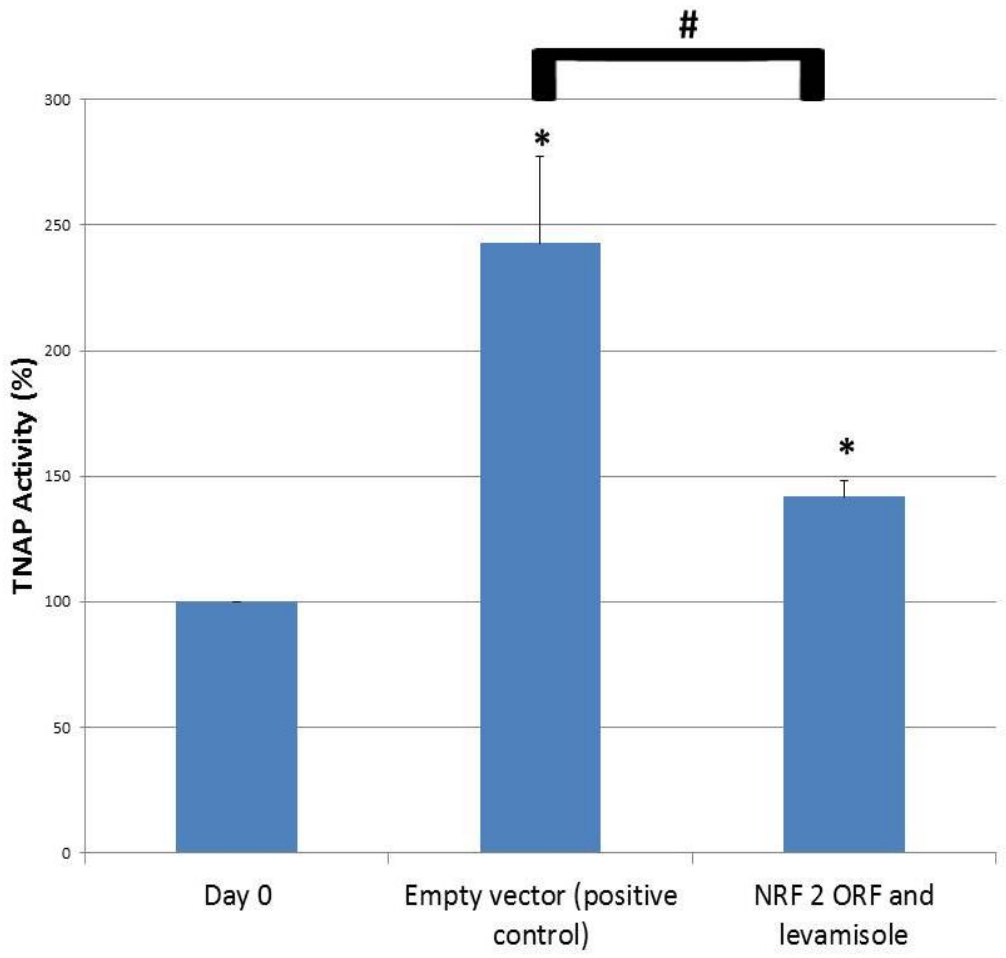

Figure 5.4: TNAP activity was successfully inhibited in the presence of levamisole in cells transfected with NRF 2 expressing plasmids. Experiments were conducted in triplicate and error bars represent ± SD.

The NRF2 plasmid was able to partially reconstitute lipid accumulation within the preadipocytes when compared to the positive control (193.72 ± 16.51 vs 326.46 ± 47.64, respectively; p = 0.019) reaching levels significantly higher than those seen in the negative (untreated) control (cells exposed to levamisole with no NRF2 plasmid) (p = 0.010) (Figure 5.5).

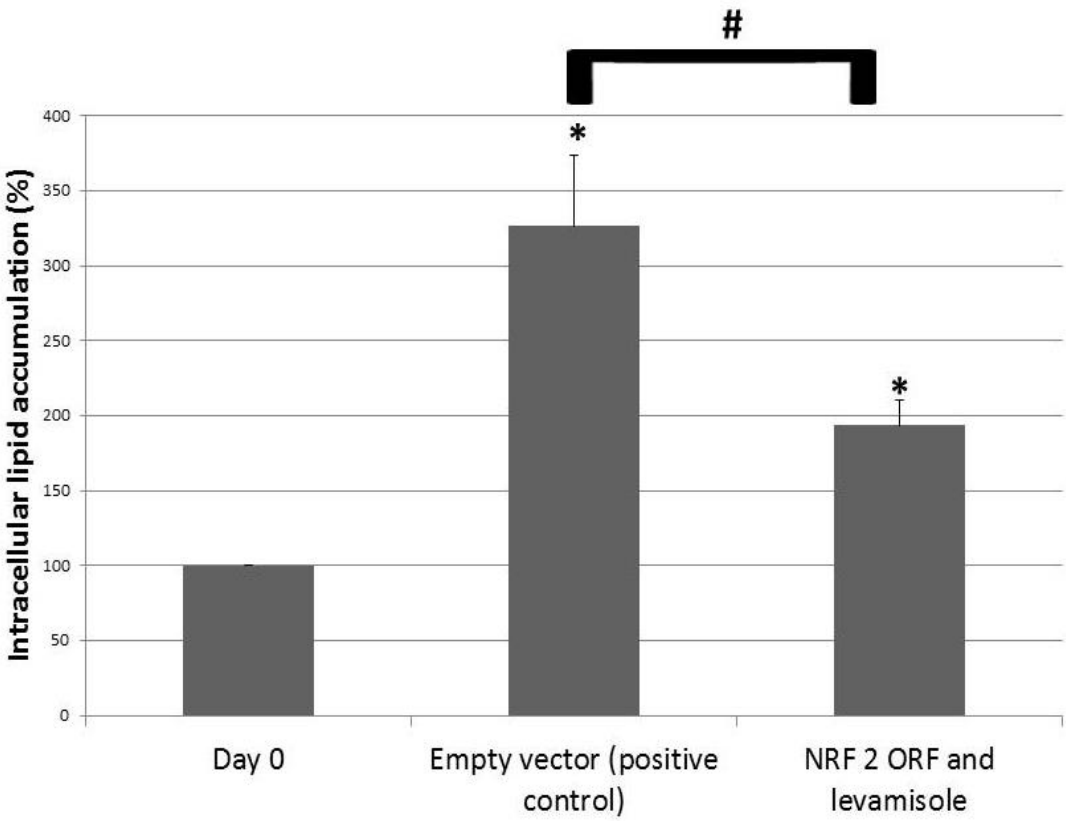

Figure 5.5: NRF2 expression partially restores intracellular lipid accumulation in the absence of TNAP activity. Intracellular lipid accumulation was monitored through the staining of intracellular lipids with Oil Red O and spectrophotometrically quantified; $^{\#}p<0.05$ intraday comparisons; $*p<0.05$ versus baseline. Experiments were conducted in triplicate and error bars represent ± SD.

5.4 Discussion

These experiments show that NRF2 mRNA expression is upregulated in adipogenesis in 3T3-L1 cells. When TNAP activity is inhibited so is the expression of NRF2. To determine whether this effect was due to the lack of TNAP-generated phosphate, cells were exposed to levamisole, to block TNAP activity, and to extracellular phosphate and the levels of NRF2 gene expression measured. Within 1 hour of exposure to extracellular phosphate, there was a significant increase in NRF2 mRNA expression, indicating that TNAP-generated phosphate mediates the transcription of NRF2 mRNA. Whether this occurs through the direct action of phosphate or through an indirect mechanism is unclear.

NRF 2 is a known transcription factor which is well studies in the context of oxidative stress. Under non-stress conditions NRF 2 binds to a Keap1/E3 ligase complex. The E3 ligase ensures that NRF 2 remains ubiquitinated under non-stressed conditions (Itoh et al., 1999, Kobayashi et al., 2004). In the context of oxidative stress, the keap1 adapter protein is modified, inactivating the E3 ligase complex and thereby preventing NRF 2 ubiquitination (Vriend and Reiter, 2015). NRF 2 is thus free to accumulate within the cell, unbound, where it is phosphorylated. Phosphorylated NRF 2 enters the nucleus, heterodimerises with small MAF proteins and induces the transcription of proteins involved in the antioxidant response pathway under the control of AREs (Vriend and Reiter, 2015, Itoh et al., 1997). Within osteoblasts TNAP-generated phosphate is able to mediate NRF2 gene expression, the transcription of which is directly due to phosphate action (Beck et al., 2003). It is therefore possible that it is

through this direct interaction of TNAP-generated phosphate with the promotor of NRF2, that NRF2 mRNA is increased during adipogenesis.

It is known that oxidative stress increases NRF2 within the cell (Nguyen et al., 2009). Interestingly, it has been reported that reactive oxygen species (ROS) are able to promote adipocyte differentiation through increasing the level of mitotic clonal expansion (Lee et al., 2009). Treatment of 3T3-L1 cells with hydrogen peroxide (H_2O_2) enhances the DNA binding activity of C/EBPβ as well as the progression of the cells through the cell cycle, from S to G_2/M (Lee et al., 2009). In addition, ROS appears to be essential for the conversion of mesenchymal stem cells to adipocytes through blocking the transcriptional activation cAMP response element-binding protein (CREB) through NAD(P)H oxidase 4 (Nox 4) activity (Kanda et al., 2011). It would therefore be interesting to study the effect of ALPL expression on oxidative stress in 3T3-L1 preadipocytes.

In order to determine whether the expression of NRF2 is the sole mechanism through which TNAP modulates intracellular lipid accumulation, cells deficient in TNAP activity were induced to accumulate lipid in the presence and absence of a plasmid vector expressing NRF2. In the presence of NRF2 expression, there was a partial recovery of intracellular lipid accumulation; however this did not reach the levels seen in the positive control.

This data implicates TNAP-generated phosphate in mediating the expression of NRF2. In addition, as the expression of NRF2 was insufficient to completely restore lipid accumulation in the absence of TNAP activity, it suggests that phosphate may be involved in the up- or down-regulation of additional genes in the preadipocyte to activate adipogenesis. It is important to note that although NRF2 has been shown to be upregulated and important for the initiation of adipogenesis (through the initiation of expression of genes such as PPARγ C-EBPα and C-EBPβ) (Hou et al., 2012, Pi et al., 2010) conflicting results have been reported showing that NRF2 results in a decrease in the differentiation capacity of the preadipocytes (Shin et al., 2007) and its nuclear expression is decreased in murine bone marrow ST2 cells (Chartoumpekis et al., 2011b). However the same group found that NRF 2 expression is indeed upregulated in obese mice, NRF 2 knockout mice are resistant to obesity, and that it may also function to repress the expression of fibroblast growth factor 21 (FGF21) – a protein with known metabolic actions (Chartoumpekis et al., 2011a). The contrasting results seen may be due to differing effects that NRF may have in different cell lines, and may be influenced by differential responses to controlling both adipogenesis and the antioxidant response pathway (Chartoumpekis et al., 2011b). In addition, a study by Xu and colleagues demonstrated that constitutively expressing NRF 2 (through the knockout of keap1) resulted in decreased lipid accumulation in adipose tissue (Xu et al., 2012), suggesting that whilst NRF 2 expression may be needed to initiate lipid accumulation, prolonged exposure may have the opposite effect

Interestingly, constitutive expression of NRF 2 within the keap1 knockout mice was shown to increase hepatic steatosis (Xu et al., 2012), a process in which TNAP activity has also been implicated (Chirambo, 2010).

These experiments suggest that TNAP may increase intracellular lipid accumulation during adipogenesis by the generation of phosphate which in turn activates the transcription of genes, including NRF2, which leads to the initiation of lipid droplet formation. However, it is also possible that TNAP may function in other ways to modulate lipid accumulation including the dephosphorylation of proteins (Kellett and Hooper, 2015) or other forms of interaction and further studies are required to test this hypothesis.

6 TRAF 2 attenuates intracellular lipid accumulation in the 3T3-L1 preadipocyte through a TNAP-independent mechanism

6.1 Background

The expansion of adipose tissue in obese subjects occurs via adipocyte hypertrophy and hyperplasia (Calder et al., 2011). The latter occurs via maturation of immature adipocytes (preadipocytes) into mature adipocytes, a process termed adipogenesis.

Tissue non-specific alkaline phosphatase is expressed in a number of tissues. An important role for TNAP in the regulation of adipogenesis (Ali et al. 2005) has been shown, with the inhibition of TNAP resulting in the cessation of adipogenesis in the 3T3-L1 mouse preadipocyte cell line. The main function of TNAP within the body is to hydrolyse pyrophosphate to phosphate (Harris, 1990), and the role of TNAP-generated phosphate within adipogenesis has been shown within chapter 2 of this thesis. However, TNAP has been shown to possess the ability to interact with other proteins, and alter the phosphorylation status of proteins (Kellett and Hooper, 2015). Therefore, the possibility that TNAP may function within adipogenesis via a protein-protein interaction needs to be investigated.

Tissue non-specific alkaline phosphatase was predicted to interact with TRAF2 within the human using the STRING algorithms (Szklarczyk et al., 2015). The STRING program consists of a database of protein-protein interactions which have previously been predicted or proven experimentally. The STRING interactions may represent a

direct interaction or alternatively a functional association with another protein (Szklarczyk et al., 2015). The STRING software predicted the direct interaction of murine TNAP with TNF receptor-associated factor 2 (TRAF2). This interaction was predicted based on the co-immunoprecipitation experiments carried out on human TNAP by Hu and colleagues, which demonstrated that human TRAF 2 and TNAP bound to each other (Hu et al., 2004).

The TRAF intracellular proteins were originally identified as signalling adaptors. The TRAF 2 peptide contains a C-terminal TRAF domain which takes part in protein-protein interactions. It is involved in the initiation of nuclear factor kappa light chain-enhancer of activated B cells (NF-κβ) and mitogen activated protein kinase (MAPK) signalling cascades (Lee & Lee 2002).

As TNAP activity is essential for intracellular lipid accumulation, and it is predicted to interact with TRAF 2 it is possible that TRAF 2 plays a role in lipid accumulation in the adipocyte. This work therefore aims to determine whether there is an interaction between TNAP and TRAF2 using both *in silico* and laboratory-based methods, and whether TRAF 2 plays a role in the accumulation of intracellular lipids within the preadipocyte.

6.2 Methods

6.2.1 *In silico* prediction of TNAP binding

Tissue non-specific alkaline phosphatase binding interactions were predicted by the protein-protein interaction engine (PIPE) computer algorithms (based on known peptide interactions) (Pitre et al., 2006).

6.2.2 Cell Culture and differentiation

The 3T3-L1 cells were cultured as previously described (section 2.1.1) and induced to accumulate lipids (section 2.2.1).

6.2.3 Real Time PCR

Real-time PCR was used to determine relative increase or decrease in TRAF 2 gene expression during adipogenesis. The RNA from 3T3-L1 preadipocytes was extracted at days 0, 1, 4 and 8 following the addition of the transformation cocktail (section 2.24.1), reversed transcribed (section 2.24.2) and the resultant cDNA was used as the template for TRAF2 expression (section 2.24.3)

6.2.4 Binding assays

To determine whether TNAP binds to TRAF 2, band shift assays as well as immune co-precipitation was undertaken.

6.2.4.1 Band Shift assays

Native (non-denaturing, non-reducing) PAGE gels were run to determine if commercially available TRAF 2 and TNAP bind to each other (see section 2.19.1). When binding occurs the two proteins should run together at a higher molecular weight causing the band to shift upwards when compared to either protein run alone.

6.2.4.2 Immuno co-precipitation

In addition to the band shift assay, TNAP and TRAF2 binding was investigated through immune co-precipitation as described in section 2.19.2.

6.2.5 Overexpression of TRAF 2 open reading frame plasmid during adipogenesis

The TRAF 2 open reading frame clone was obtained from Genecoepia, and transfected into 3T3-L1 cells (section 2.20.2) to allow for over-expression of the TRAF

2 protein. Adipogenesis was induced (section 2.2.1) and the effect of TRAF 2 over-expression on adipogenesis was examined through Oil Red O staining (section 2.9), mRNA expression studies (section 2.24) and measuring TNAP activity (measured with the alkaline phosphatase, diethanolamine detection kit - section 2.6).

6.3 Results

In silico analysis was carried out to predict TNAP binders using protein-protein interaction engine (PIPE). PIPE computer algorithms are based on known peptide interactions (Pitre et al., 2006). This database identified three proteins which might potentially interact with TNAP, namely mitogen activated protein 3 kinase 14 (MAP3K14), tumour necrosis factor alpha receptor associated factor 2 (TRAF 2) and tumour necrosis factor alpha receptor associated factor 3 (TRAF3). Messenger RNA analysis of MAP3K14 and TRAF3 expression within 3T3-L1 cells was examined, however no differences over the course of adipogenesis were seen and they were not examined further (data not shown).

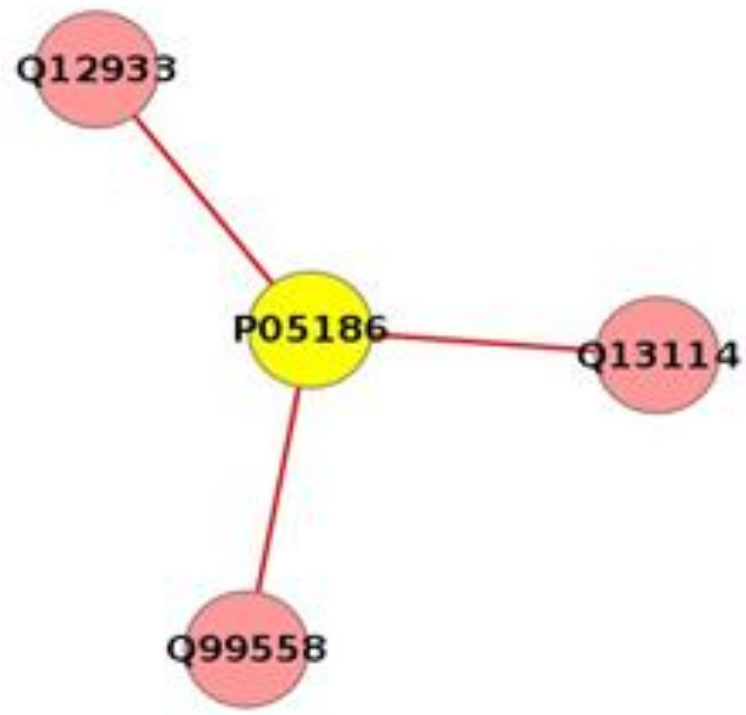

Figure 6.1: Predicted binding of tissue non-specific alkaline phosphatase (P05186) to TRAF 2 (Q99558), TRAF 3 (Q12933) and MAP3K14 (Q99558) using PIPE.

As TRAF2 was implicated as a potential TNAP binder by both PIPE and STRING we hypothesised that it may have a role in preadipocyte lipid droplet formation. To investigate this possibility, changes in TRAF 2 mRNA were investigated over the duration of intracellular lipid accumulation.

6.3.1 TRAF 2 mRNA is down-regulated during intracellular lipid accumulation in the 3T3-L1 preadipocyte cell line

The TRAF 2 mRNA expression levels were monitored during intracellular lipid accumulation in the 3T3-L1 murine preadipocyte cell line. Figure 6.2 shows that in the presence of TNAP activity and therefore adipogenesis, TRAF2 mRNA was significantly downregulated to levels reaching 15.27 ± 10.27% ($p= 0.014$) of baseline (levels prior to induction of intracellular lipid accumulation) after four days of intracellular lipid accumulation. The TRAF 2 mRNA levels were also significantly lower than baseline levels at day 1 and day 8. When TNAP was inhibited with levamisole, no differentiation occurred and there was no downregulation of TRAF 2 mRNA from baseline levels. Furthermore, at days 1, 4 and 8 lipid accumulation in cells treated with levamisole was significantly higher than levels seen in the absence of levamisole (Figure 5.1).

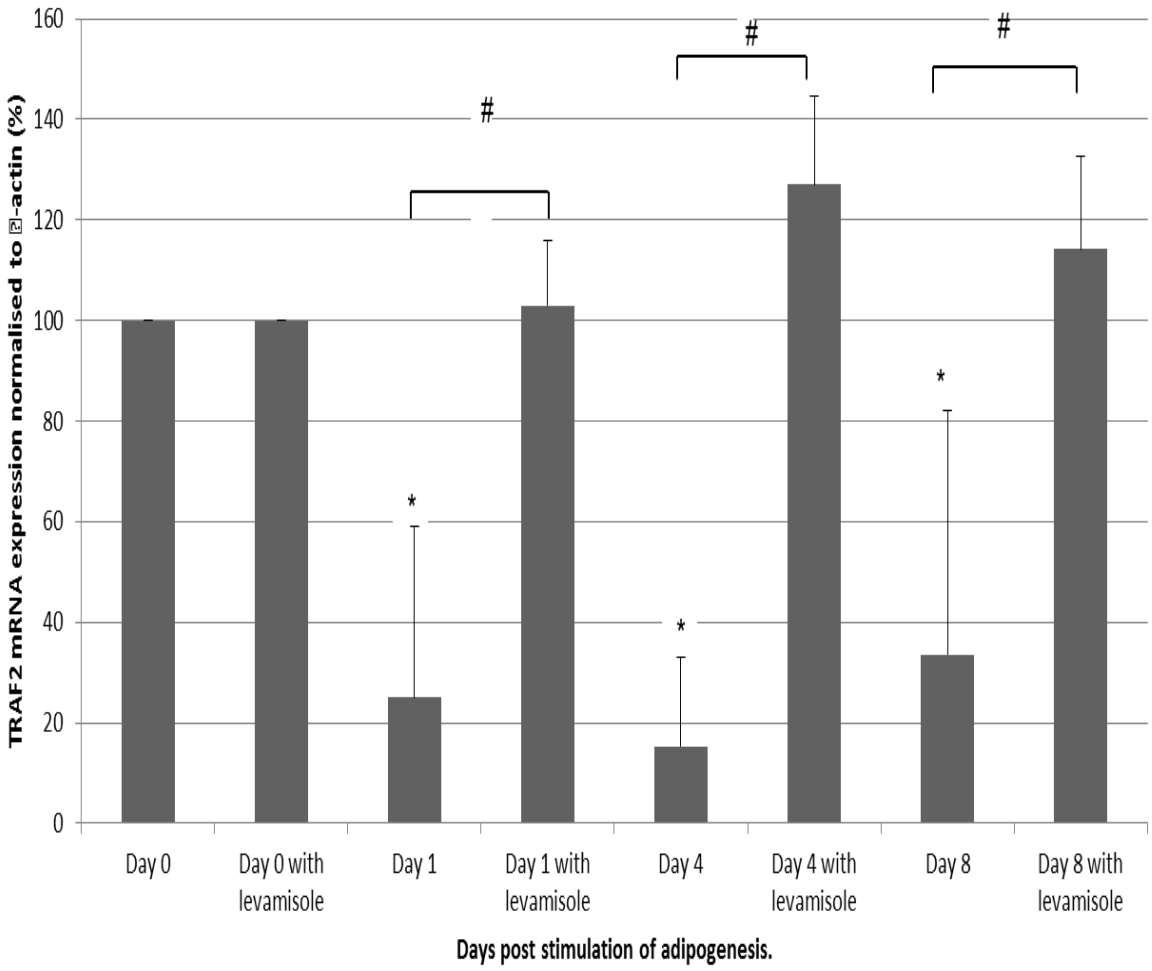

Figure 6.2: Relative mRNA expression of TRAF 2 normalised to β-actin over the course of adipogenesis. Following induction of adipogenesis mRNA expression was measure on day 0,1,4 and 8 in the absence and presence of 5mM levamisole (TNAP inhibitor). During adipogenesis, the expression of TRAF 2 mRNA was downregulated from baseline ($^{\#}p<0.05$ intraday comparisons; $^{*}p<0.05$ versus baseline) for the entire 8 days of the assay compared to no change in TRAF 2 expression when adipogenesis was inhibited. Experiments were conducted in triplicate and error bars represent ± SD.

6.3.2 Overexpression of TRAF 2 in 3T3-L1 preadipocytes decreases intracellular lipid accumulation

The overexpression of TRAF 2 (Appendix A4) within the 3T3-L1 preadipocyte was able to reduce intracellular lipid accumulation when compared to the control (transfected with an empty vector) (147.88 ± 11.28% vs 326.46 ± 47.64%; p=0.028 (day 8)), and when compared to the untreated control (day 0 - lipid levels set at 100%) lipid accumulation was slightly but statistically significantly increased (p=0.018) (Figure 6.3). Lipid accumulation in the cells transfected with an empty vector was also significantly higher than the day 0 control (p=0.0012).

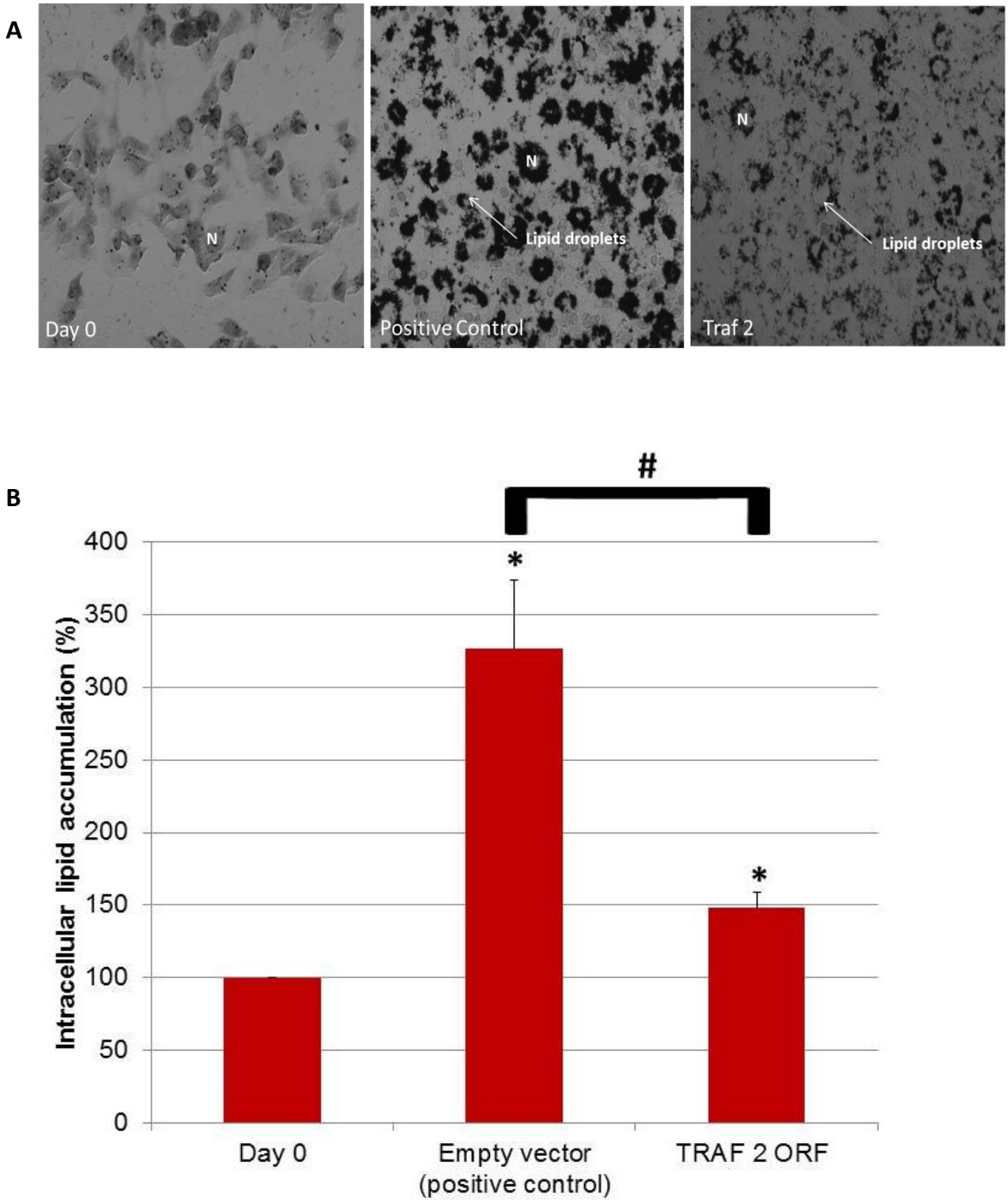

Figure 6.3: TRAF 2 overexpression significantly inhibited intracellular lipid accumulation in 3T3-L1 cells induced to undergo differentiation. Lipids were stained with Oil Red O, visualised (40x magnification) (A) and quantified (B). ($^{\#}p<0.05$ intraday comparisons; $^{*}p<0.05$ comparison to baseline). Experiments were conducted in triplicate and error bars represent ± SD.

6.3.3 TRAF 2 does not bind to TNAP

To determine whether TRAF binds to TNAP two methods were employed, band shift assays and immuno co-precipitation. Co-incubation of TRAF 2 and TNAP and running on an acrylamide gel under non-reducing, non-denaturing conditions did not exhibit an upward shift (indicating increased size due to complex formation) when compared to TNAP run on its own. The molecular weight of TRAF 2 is 53 KDa, whereas the molecular weight of the TNAP monomer is 57 KDa (Silvent et al., 2014), thus even taking into account any potential variations in molecular weights from post-translational modifications, relative charges of the molecules and experimental factors such as the addition of the His tag, one would still expect a significant shift, which should be visible within the gel.

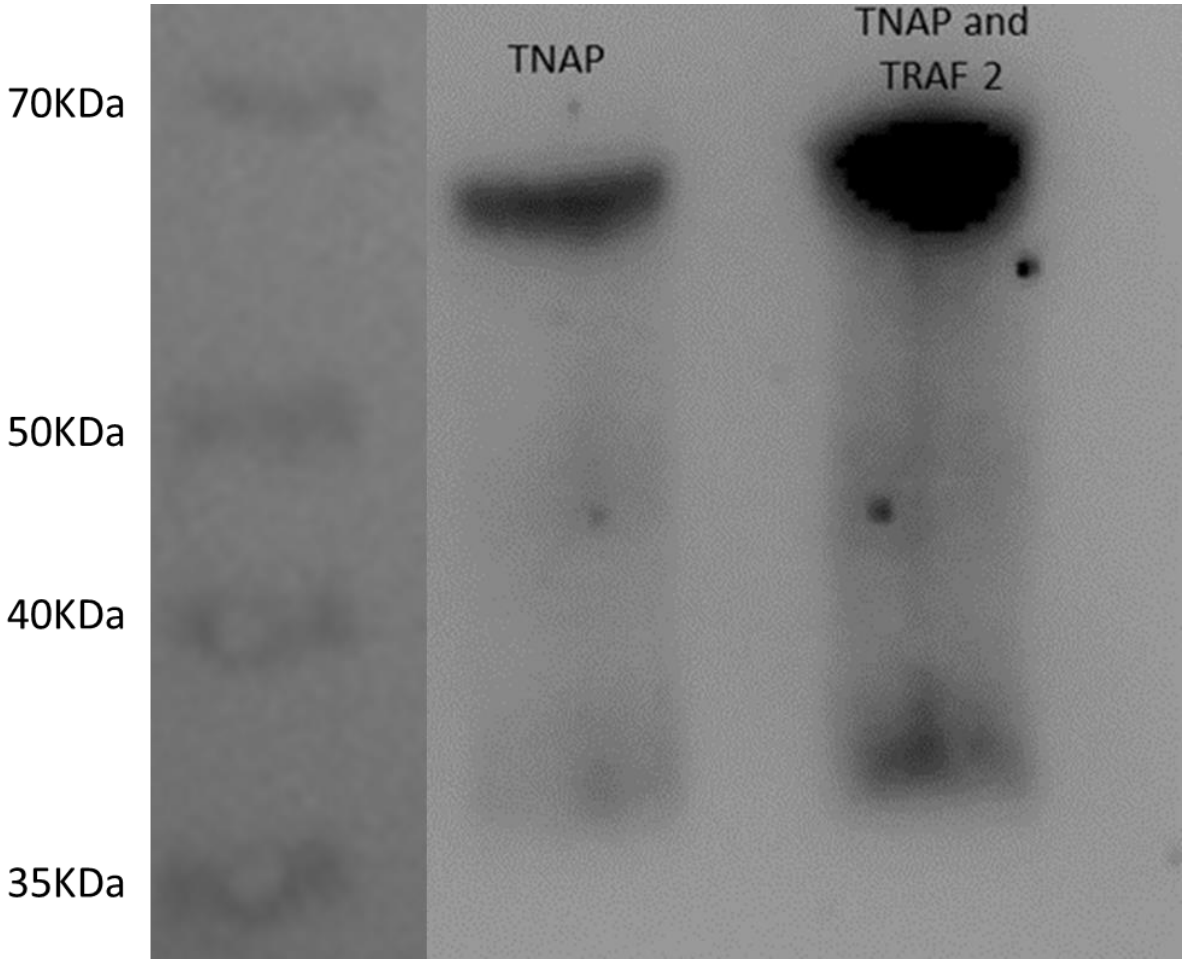

Figure 6.4: Western blot of band shift assay to determine TRAF 2/TNAP binding. TRAF 2 and TNAP were incubated together and run on a native PAGE gel next to TNAP alone. There was no noticeable upward shift in the TRAF2/TNAP lane indicating no binding of TNAP to TRAF 2.

Several variations on the immunoprecipitation experiments were employed using both capture antibodies and antigens as described in section 2.19.2. These variations were employed to try to minimise the possibility of the capture antibodies binding to the same area where TNAP and TRAF 2 may bind to each other. The binding of the antigen to the resin-capture antibody complex was confirmed using Western blotting. However, neither TNAP nor TRAF 2 were captured by the respective TRAF 2 or TNAP-resin complex. Binding of TNAP to TRAF 2 may not occur in a 1:1 molar ratio as laid out in this experiment, however with the large amounts of both proteins co-incubated,

it would be expected that at least a portion of the proteins would form heterodimers, which was not observed.

TNAP and TRAF2 proteins were run alongside each other on a native gel to determine whether these proteins, run alone ran at the expected size and visualised using Western blotting (Figure 6.5). Whilst TNAP ran at the expected size of its monomer 57 kDa, TRAF2 appeared to form aggregates and did not leave the well.

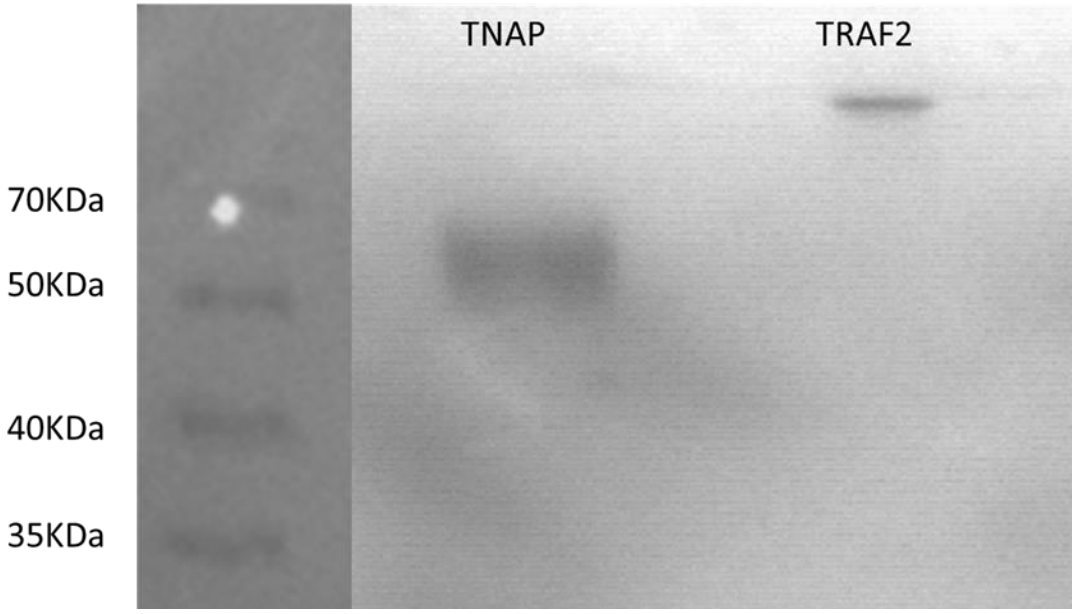

Figure 6.5: Western blot of TNAP and TRAF 2 separated on a blue native gel.

If TNAP and TRAF 2 were to be functional partners, it would be expected that they would be expressed simultaneously within the preadipocyte. The mRNA expression

patterns of both proteins was therefore compared during adipogenesis to determine the relative abundance of each protein (Figure 6.6).

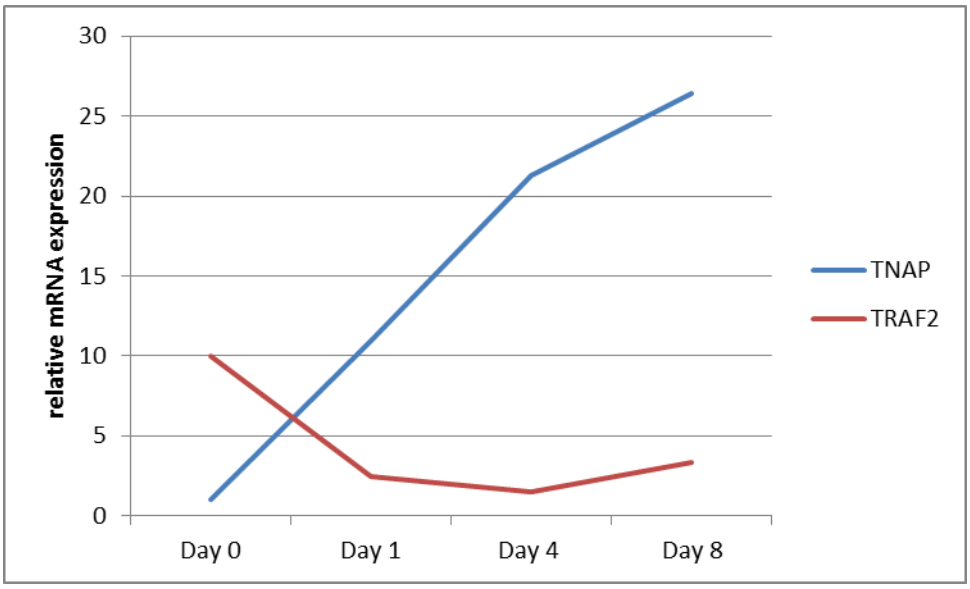

Figure 6.6: Relative mRNA expression levels of TNAP and TRAF2 during intracellular lipid accumulations (all values were normalised to β-actin).

Whilst mRNA data is often considered to be a prediction of relative protein levels within a cell, it is important to note that there is not always an exact correlation. A study by Guo et al, investigated the relative mRNA and protein expression levels of 71 different genes and found that in only half of the observations, was mRNA highly correlated with protein levels (Guo et al., 2008). Thus the data represented in figure 6.6 may not accurately represent the actual protein levels within the cell at a given time and only serves to show one possible scenario.

6.4 Discussion

In silico analysis using PIPE identified TRAF 2 as a potential binder of TNAP. The expression of TRAF2 during intracellular lipid accumulation was determined to be down regulated as adipogenesis proceeded. To determine the role of TRAF 2 in intracellular lipid accumulation, TRAF 2 was overexpressed, which resulted in a decrease in lipid accumulation. Despite the prediction of TNAP-TRAF2 binding, immune co-precipitation and band shift assays showed no evidence of this binding occurring.

Both the STRING algorithm and the PIPE algorithm predicted that TNAP should bind to TRAF2. The STRING software predicts binding of TNAP to TRAF 2 by quoting experimental data generated by Hu and colleagues. However within the article, it appears that the protein identified whilst also known as TNAP (for TRAFs and NIK-associated protein) (Hu et al., 2004), is not in fact tissue non-specific alkaline phosphatase, and therefore this experimental data cannot be taken into consideration.

The PIPE algorithm looks at known protein-protein interactions based on sequence data. The PIPE algorithm has been shown to have an accuracy of 75% allowing for a relatively large margin of error (Pitre et al., 2006).

Therefore, despite algorithmic predictions, there is no evidence for the *in vitro* binding of TRAF 2 to TNAP despite the predicted binding *in silico*. The commercially available TNAP protein, did however contain a HIS tag which may have influenced protein folding and therefore the availability of potential binding sites. In addition when viewing a blue native gel of TNAP and TRAF2 run alongside each other (Figure 6.5) it appeared that TRAF2 formed aggregates as the protein did not leave the well. TRAF 2 is known to form homodimers through its c-terminal TRAF domain (Lee and Lee, 2002). This domain is also known to allow for the formation of heterodimers (Rothe et al., 1995). It is plausible therefore that any interaction between TNAP and TRAF2 may also occur through the TRAF domain. If TRAF 2 preferentially forms homodimers over TNAP heterodimers, any potential binding may have been missed.

Furthermore analysis of TRAF 2 expression and comparing it to TNAP expression shows that it is unlikely that the two proteins are expressed simultaneously within the adipocyte at any significant levels, making an interaction within the adipocyte unlikely (Figure 6.6). It thus seems unlikely that TNAP/TRAF2 binding plays a role in the mechanism through which TNAP mediates intracellular lipid accumulation. However, TRAF 2 mRNA was decreased over the course of intracellular lipid accumulation implicating TRAF 2 as having an anti-adipogenic role, independent of TNAP binding. Furthermore, when TRAF 2 was over expressed during adipogenesis, the level of lipid

accumulation was attenuated when compared to the positive control. This further implicates TRAF 2 as a negative regulator of intracellular lipid accumulation.

The TRAF 2 protein is known to form part of the WNT10B signaling pathway. In this pathway, TNFα, binds to the TNFα receptor activating the TADP/RIP/TRAF2 complex. This complex activates both the JNK and Iκβ kinases which in turn phosphophorylates API and NF- κβ respectively (Katoh and Katoh, 2007). The Iκβ kinase then phosphorylates NF-κβ, which acts as a transcription factor resulting in the transcription of WNT10B, a known negative regulator of adipogenesis (Bennett et al., 2002, Kennell and MacDougald, 2005). It is possible that the decrease in TRAF 2 mRNA which we observe in the 3T3-L1 cells may be to prevent the suppression of adipogenesis through the WNT pathway.

TRAF 2 is known to be phosphorylated at Ser11 (Shen et al., 2012), as well as Ser55 (Thomas et al., 2009). It is therefore possible that TNAP, which is known to dephosphorylate proteins (Kellett and Hooper, 2015), may play a role in dephosphorylating TRAF 2. However as the two proteins are not expressed simultaneously within the adipocyte (Figure 6.6), it seems unlikely that TNAP affects TRAF 2's phosphorylation status.

In conclusion although TRAF 2 and TNAP binding cannot be conclusively ruled out, it appears that due to the two proteins being expressed at different time points during intracellular lipid accumulation, any heterodimers formed are unlikely to be important

in intracellular lipid accumulation. The expression of TRAF 2 is downregulated during preadipocyte differentiation, and when overexpressed it has an inhibitory effect on intracellular lipid accumulation. The TRAF 2 protein is known to function in the WNT 10B pathways which is inhibitory to adipogenesis (Kennell and MacDougald, 2005, Katoh and Katoh, 2007). It is therefore likely that under normal circumstances, TRAF 2 is downregulated during adipogenesis to prevent the inhibitory effects of the WNT 10B pathway, and exogeneous expression of TRAF 2 activates this pathway, thus resulting in reduced adipogenesis and intracellular lipid accumulation.

7 Tissue non-specific alkaline phosphatase activity is required for cholesterol accumulation in the murine adrenocortical cell line Y1

7.1 Background

The adrenal cortex is responsible for the synthesis of steroid hormones, such as cortisol, from cholesterol. The cholesterol is stored in the form of cholesterol esters in lipid droplets in the cytoplasm of the cells of the adrenal cortex. The lipid droplets are similar in both steroidogenic and adipose cells (Servetnick et al., 1995). Cells of the adrenal cortex and adipocytes are derived from mesenchymal stem cells (Yazawa et al., 2014). Cholesterol esters and triglycerides are both neutral lipids and are retained in the cytoplasm in droplets bound by a plasma membrane that contains a number of different peptides including perilipin. Perilipin is expressed exclusively on the membranes of neutral lipid droplets (Brasaemle et al., 1997, Fong et al., 2002).

As cells of the adrenal cortex and adipocytes share a common progenitor, it is likely that they share molecular pathways that control lipid storage. Within adipocytes, tissue non-specific alkaline phosphatase (TNAP) has been shown to be essential for intracellular lipid accumulation (Ali et al., 2006b, Ali et al., 2006a, Ali et al., 2005). Furthermore, previous immunocytochemical studies have identified TNAP in the cells of the adrenal cortex (McComb, 1979, Elftman, 1947). Therefore, we hypothesized that TNAP is essential for lipid droplet formation in the cells of the adrenal cortex and tested this hypothesis using the murine Y1 adrenal cortex cell line. The effect of the TNAP inhibitor, levamisole on intra-cellular lipid accumulation was analysed and

histochemical studies were performed to determine the intra-cellular location of the TNAP in the Y1 cells.

7.2 Methodology

7.2.1 Cell Culture

The Y1 murine adrenocortical cells were obtained from the ECACC and cultured as described in section 2.1.2. Lipid accumulation was stimulated using the methods described in section 2.2.2.

7.2.2 Co-localising of TNAP to the lipid droplets

The Y1 cells were induced to accumulate lipids (section 2.2.2) and analysed at day 8 (section 2.10 and 2.11) and visualised (section 2.12) after staining lipid droplets with Nile Red and detecting TNAP activity with ELF 97 (section 2.22).

7.2.3 Inhibition of TNAP activity

Inhibition of TNAP activity was accomplished by exposing cells to 5 mM levamisole hydrochloride 30 minutes prior to initiation of intracellular lipid accumulation, and throughout the experiment (section 2.3.2).

7.2.4 Oil Red O staining of neutral lipids

The intracellular lipid droplet accumulation was measured using Oil Red O as described in section 2.9

7.2.5 Measurement of alkaline phosphatase activity

Crude protein extracts were obtained at baseline and on days 1, 4 and 8 following the initiation of intracellular lipid accumulation as previously described by Ali and colleagues (Ali et al., 2005) (section 2.4). The TNAP activity was determined using an ADVIA 1800 chemistry analyser (Siemens, Berlin, Germany) according to the manufacturer's instructions (section 2.6). The protein content of the extracts was determined using the Bradford method (Bradford, 1976), and used to correct all TNAP activity results (section 2.5). TNAP activity was calculated as U activity/ mg of protein and expressed as a percentage of the level of baseline activity.

7.2.6 Analysis of ALPL gene expression

Total RNA was extracted (section 2.24.1) and used as the template for cDNA synthesis (section 2.24.2). TNAP expression was determined using real-time PCR and used β-actin as an internal control (section 2.24.3)

7.2.7 Statistical Analysis

Statistical comparisons were carried out as described in section 2.25.

7.3 Results

7.3.1 TNAP activity is up-regulated over the course of intracellular lipid accumulation

The TNAP activity increased significantly for the initial 4 days of incubation with the oleic acid-BSA-cholesterol mixture, reaching 233 ± 37.56% ($p=0.019$ vs. baseline) of baseline levels within the initial 24 hours. Maximal levels of activity were achieved by day 4 (477.78 ± 83.89%; $p=0.016$ vs. baseline), with a slight fall in TNAP activity by day 8 (Figure 7.1). In cells incubated with levamisole, TNAP activity was significantly lower at all time points ($p<0.05$) when compared to cells not incubated with levamisole reaching levels of 41.67 ± 11.67% (compared to 233 ± 37.56% in cells not treated with levamisole; $p=0.013$) within 24 hours of levamisole treatment. Only by day 8 did TNAP activity in levamisole-treated cells increase significantly above baseline levels (207.78 ± 41.67%; $p= 0.046$ vs baseline).

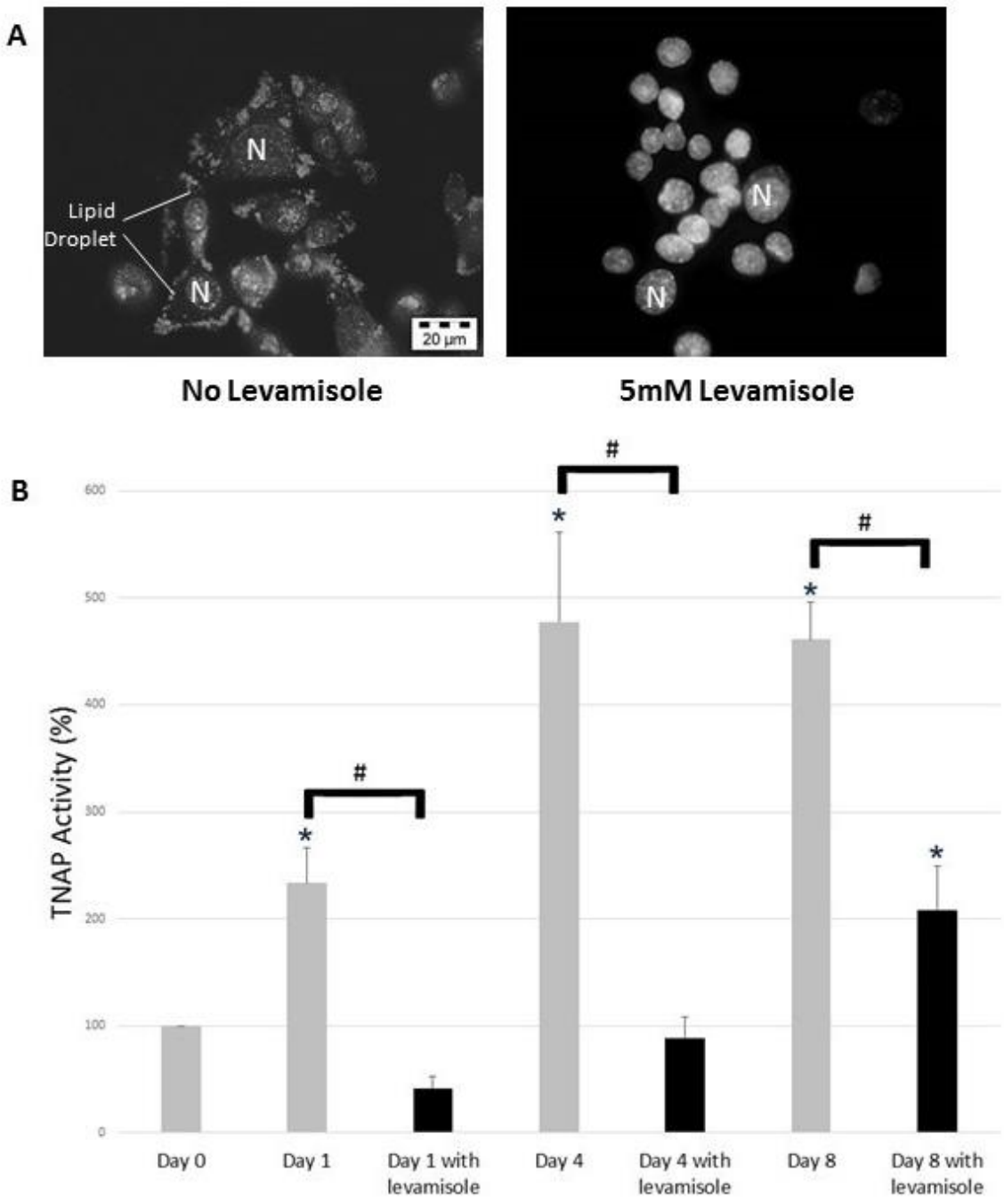

Figure 7.1: Comparison of TNAP activity in the presence and absence of the TNAP inhibitor levamisole. TNAP activity was visualised through the production of a fluorescent by-product of TNAP activity on the lipid droplet (nuclei stained with DAPI) (A) and measured on the ADVIA 1800 (Siemens) (B). TNAP activity was significantly inhibited by levamisole treatment (*indicates values significantly different from untreated cells; # indicates values significantly different between treated and untreated at $p<0.05$). Experiments were conducted in triplicate and error bars represent ± SD.

7.3.2 ALPL mRNA is up-regulated over the course of intracellular lipid accumulation

The Y1 cells were induced to accumulate cholesterol esters for eight days, by which time substantial lipid accumulation was noted (Figure 7.3). The ALPL mRNA levels were determined over the course of the experiment and were significantly raised to 168 ± 38 % of baseline levels (p=0.048) within 24 hours of induction of lipid accumulation. The ALPL mRNA levels remained elevated throughout the duration of the experiment (Figure 7.2).

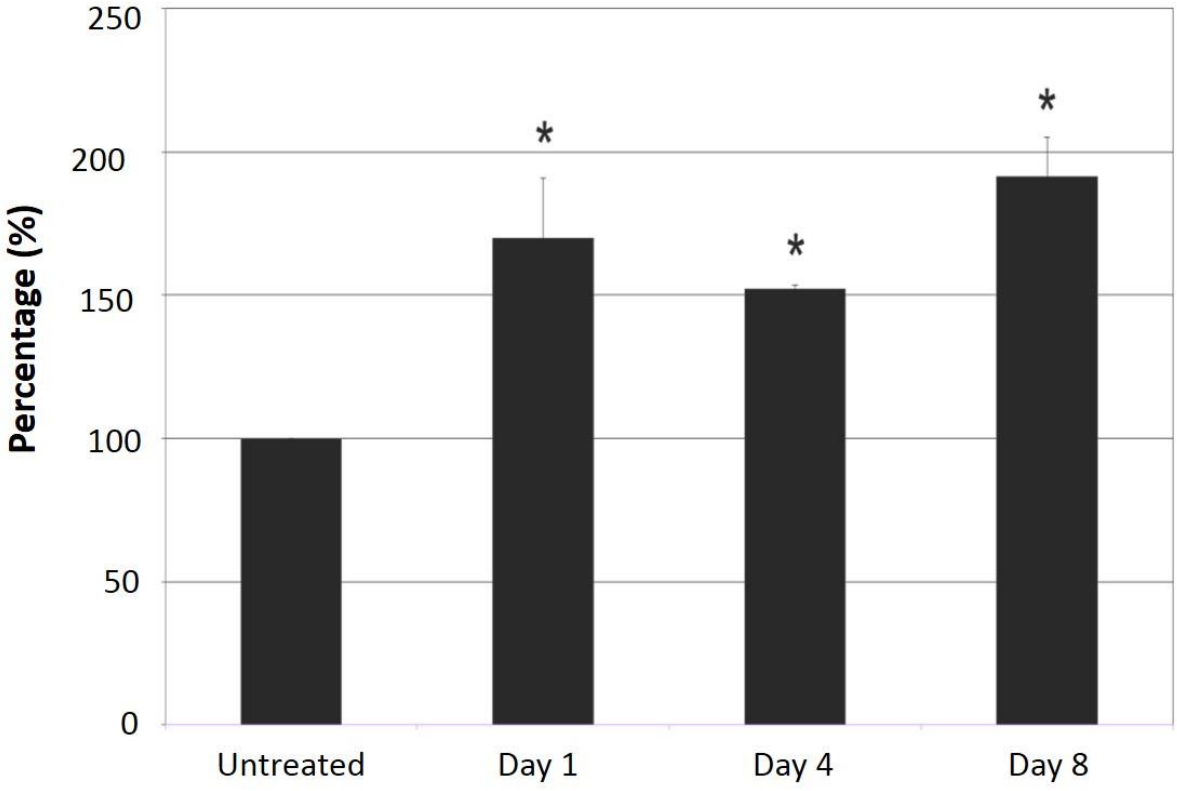

Figure 7.2: ALPL mRNA expression was upregulated within the first 24 hours of intracellular lipid accumulation and remained elevated for the duration of the experiment (*indicates values significantly different from baseline, p<0.05).

7.3.3 Inhibition of TNAP reduces lipid accumulation in Y1 cells

During the course of the incubation with oleic acid-BSA-cholesterol, the lipid content of the Y1 cells increased significantly above baseline levels, reaching a maximum at day 8 (602.68 ± 68.15; p=0.003 vs. baseline) (Figure 7.3). However, in cells incubated with levamisole, intracellular lipid levels never rose above baseline levels, except at day 8 (124.42 ± 17.38%; p=0.23 vs. baseline). At all time points the level of intracellular lipids was significantly lower ($p<0.05$) in the levamisole-treated compared to the untreated cells.

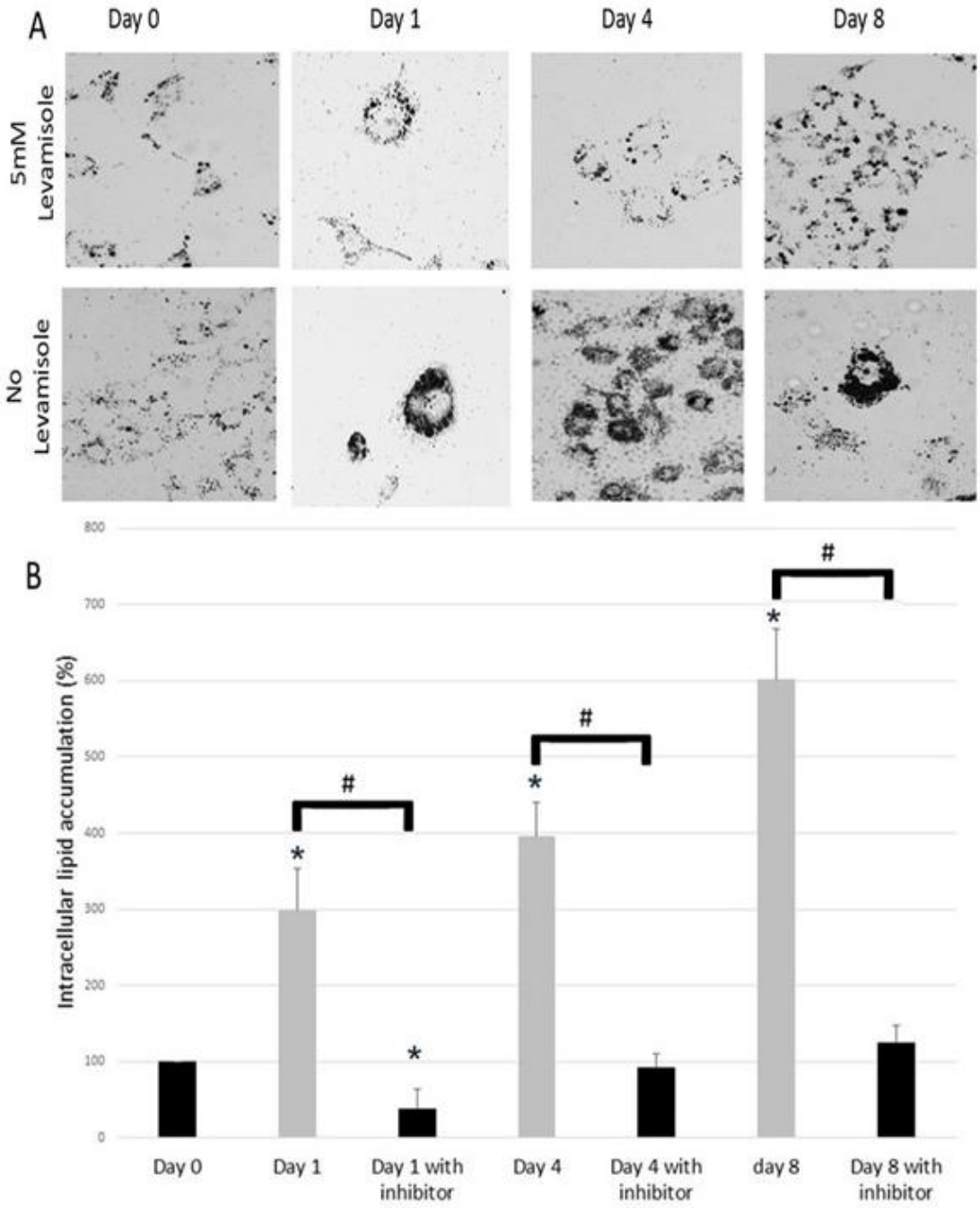

Figure 7.3: Comparison of intracellular lipid accumulation in the presence and absence of the TNAP inhibitor levamisole. Lipid accumulation was determined by visualisation at 100x magnification (A) and measurement (B) of Oil Red O stained lipids. Intracellular lipid accumulation was significantly inhibited by levamisole treatment (*indicates values significantly different from untreated cells; # indicates values significantly different between treated and untreated at $p<0.05$). Experiments were conducted in triplicate and error bars represent ± SD.

7.3.4 TNAP is localized to the lipid droplet in Y1 cells

Tissue non-specific alkaline phosphatase has previously been shown to be expressed in cells of the adrenal cortex (McComb, 1979, Elftman, 1947). To determine the presence and location of TNAP within Y1 cells, the cells were induced to accumulate cholesterol esters within intracellular lipid droplets. Lipids were visualised with Nile red staining. The location of TNAP within the cells was determined through ELF97 staining. The ELF alcohol by-product of TNAP activity was localised to the Nile red-stained lipid droplets (Figure 7.4). Nile red is known to be visualised at two different wavelengths (excitation wavelength, 450-500 nm; emission wavelength, > 528 nm and excitation wavelength, 515-560 nm; emission wavelength > 590 nm), whereas TNAP activity (through ELF-97 hydrolysis) is visualised with an excitation of 345nm and an emission of 530nm (Greenspan et al., 1985, Molecular Probes, 2004). It is therefore possible that the signal seen through the 530nm filter is not ELF-alcohol, but Nile red. However, it is unlikely that this is the case as ELF-alcohol staining is still clearly visible in cells treated with ELF alcohol alone (appendix A.5)

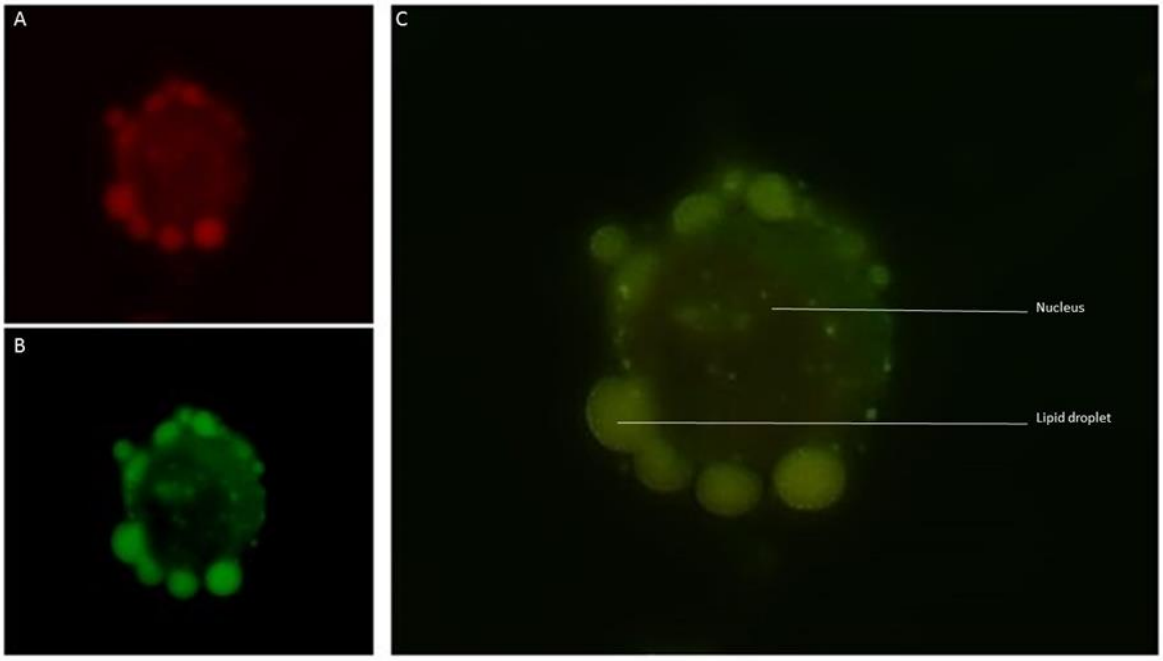

Figure 7.4: TNAP is localised to the lipid droplet. TNAP's intracellular location was determined through hydrolysis of ELF-97 by TNAP to give a green fluorescent end-product (B), and lipid droplets stained with Nile Red (A). TNAP activity localised to the lipid droplet within the Y1 cell (merged image – yellow, C). Images were captured at 100x magnification.

7.4 Discussion

The TNAP enzyme was found to be expressed within the Y1 cell line. This correlates with studies showing that TNAP is present in the murine adrenal cortex (Elftman, 1947). During intracellular cholesterol accumulation within the Y1 cells, ALPL mRNA and activity were upregulated. The use of the TNAP inhibitor, levamisole, inhibited TNAP activity and resulted in a cessation in intracellular lipid accumulation. Within the Y1 cell line, TNAP is localised to the lipid droplet.

Within the murine preadipocyte cell line 3T3-L1, human preadipocytes and the human hepatocellular cell line, HepG2, TNAP has been shown to be important for the accumulation of triglycerides intracellularly, where inhibition of TNAP activity results in the cessation of intracellular lipid accumulation (Ali et al., 2006a, Ali et al., 2005, Chirambo et al., 2017). Additionally, within the murine TNAP-knockout model, the mice showed decreased fat mass (Narisawa et al., 1997). Inhibition of TNAP activity within the murine adrenocortical cell line Y1 shows a similar phenomenon whereby in the absence of TNAP activity there is an inhibition of the accumulation of cholesterol esters within the cells. This data therefore shows an important role for TNAP in the accumulation of both triglycerides and cholesterol esters within cells of the body.

The expression and activity of TNAP was found to increase in the initial stages of intracellular lipid accumulation in the Y1 adrenocortical cells. The rapid increase seen in TNAP activity within the first 24 hours following initiation of intracellular lipid accumulation, strongly suggests that TNAP activity may be important in the initial stages of CE accumulation within the adrenal cortex.

In this study, TNAP was found to be associated with the lipid droplet. This data correlates with previous studies showing TNAP localises to the lipid droplet of preadipocytes (Ali et al., 2005) and liver cells (Chirambo et al., 2017). The enzyme is known to be bound to lipid bilayers through a GPI anchor and most GPI bound proteins are located in lipid rafts (Bolean et al., 2011). Interestingly it does not appear that TNAP is expressed on the plasma membrane of the adrenocortical cells, and is

therefore potentially recruited either to the ER membrane (where the lipid droplet originates (Gross and Silver, 2014)), or alternatively to the lipid droplet membrane.

Adipocytes and cells of the adrenal cortex share a common mesenchymal progenitor (Majka et al., 2011, Walczak and Hammer, 2015). It is therefore not surprising that the lipid droplets of steroidogenic and adipose cells are similar (Servetnick et al., 1995) with both expressing common proteins on the surface of the lipid droplets, including perilipin A, adipose differentiation related protein (ADRP) and p200 (Fong et al., 2002). Whilst there are also differences within the proteins located on the lipid droplets of adrenal and adipogenic cells, the overlap remains substantial. In fact, a recent study showed that there are at least 278 shared proteins between steroidogenic and adipocyte lipid droplets (Khor et al., 2014).

A potential drawback of this study is that levamisole, whilst being a potent inhibitor of TNAP activity, is not specific to TNAP and therefore the effect on cholesterol accumulation may be due to off-site effects. However, pilot data using siRNA suggests that specific TNAP inhibition gives similar results to levamisole in both 3T3-L1 pre-adipocytes and HepG2 liver cells (Chirambo, 2013).

The mechanism through which TNAP mediates the accumulation of neutral lipids is unclear. Within bone, TNAP has a dual function of alleviating an inorganic pyrophosphate induced block on mineral deposition and the generation of phosphate, which acts to stimulate mineralisation (Beck, 2003, Hessle et al., 2002). We therefore

hypothesise that it is through the generation of phosphate that TNAP mediates its effect on the accumulation of cholesterol esters within the adrenal cortex, however further studies will be needed to confirm this. In addition, TNAP has been shown to be capable of dephosphorylating proteins (Lei et al., 2015, Wang et al., 2014) which may be an additional mechanism through which TNAP mediates intracellular lipid accumulation.

In conclusion, this study demonstrates a novel role for TNAP in controlling the accumulation of cholesterol esters within the adrenal cortex and suggests that TNAP acts within a wide variety of lipid-storing cells to regulate lipid droplet formation. The mechanism by which this occurs is not yet fully understood but preliminary data suggests that TNAP may act by generating phosphate from pyrophosphate which then stimulates gene transcription of proteins involved in the lipid storage pathway.

8 Discussion and Conclusions

This thesis aimed to determine the subcellular mechanisms through which TNAP mediates the accumulation of intracellular lipids within 3T3-L1 preadipocytes. The main investigations into the pathways involved in TNAP-mediated lipid accumulation were based on the function of TNAP to catalyse the hydrolysis of pyrophosphate to phosphate, and the possibility that TNAP may bind to other effector peptides. Therefore, the effect of both pyrophosphate and phosphate on ICLA was investigated, and the ability of TNAP to bind to a predicted binder TRAF 2, were determined. The effect of phosphate on the expression of NRF2 (a regulator of adipogenesis) was also investigated. In addition, the function of TRAF2 within the context of adipogenesis was examined. This thesis also aimed to determine whether the function of TNAP- to induce ICLA was conserved in cells of the adrenal cortex.

The addition of extracellular pyrophosphate resulted in increased TNAP activity and an increase in ICLA, thus it was concluded that TNAP did not function within the adipocyte to remove intracellular pyrophosphate. However, in cells deficient in TNAP activity (through treatment with levamisole), which were supplemented with extracellular phosphate, intracellular lipid accumulation was reconstituted to levels similar to that seen in cells not treated with levamisole. Therefore, this work suggests that the function of TNAP, is to generate phosphate.

Phosphate has been shown to induce the expression of NRF2 within osteoblasts, and NRF2 has been implicated in adipogenesis, therefore this thesis investigated whether TNAP-generated phosphate was important in inducing the expression of NRF2. The NRF2 mRNA expression was shown to be rapidly induced in the presence of exogenous phosphate. However expression of NRF2 was not sufficient to completely reconstitute lipid levels in the absence of TNAP activity, suggesting that phosphate may induce the expression of genes in addition to NRF2.

Interestingly, levels of ALPL expression in the presence of levamisole do not increase during ICLA as it does in the absence of levamisole, despite the fact that levamisole functions post-translationally (see Figure 3.4A and Figure 6.6; Figure 7.1 and Figure 7.2). This is most likely due to the observation seen by Orima and Shimada, that TNAP-generated phosphate is able to induce the expression of ALPL through an indirect mechanism (Orimo and Shimada, 2008). Thus by inhibiting TNAP activity and thus eliminating phosphate, mRNA expression in not increase in cells treated with levamisole.

Based on the data accumulated within this thesis Figure 8.1 depicts the subcellular mechanism through which TNAP may induce ICLA within 3T3-L1 murine preadipocytes. This suggested pathway will be discussed below.

Within preadipocytes there is no detectable TNAP activity. Upon the induction of ICLA, TNAP enzymatic activity is rapidly upregulated. The levels of gene and protein

expression continue to rise over the duration of lipid accumulation with the TNAP localized to the lipid droplet membrane. It is likely that TNAP is localised to the membrane due its functioning within the adipocyte to regulate the formation of the lipid droplet.

Tissue non-specific alkaline phosphatase produces phosphate from pyrophosphate, the latter being produced from ATP by ENPP-1 from early in adipogenesis. Ectonucleotide pyrophosphate/phosphodiesterase – 1 is initially upregulated (within the first 16 hours) within the preadipocyte (Liang et al., 2007). Pyrophosphate has been shown to increase TNAP activity within desmal and endochondral organoid culture (Zimmermann, 2008) and the same may be seen within preadipoytes, as shown in this study. This increase in pyrophosphate may be the cause of TNAP activity increase within adipogenesis. Thereafter ENPP-1 is downregulated (Liang et al., 2007) as intracellular lipid accumulation progresses. This may form part of a negative control loop which through the lowering of available TNAP substrate helps prevent excess intracellular lipid accumulation within a single cell caused by high pyrophosphate levels as seen in Chapter 3.

The TNAP-generated phosphate acts as a secondary messenger where it induces the expression of NRF 2 and potentially the expression of additional genes important in the early stage of intracellular lipid accumulation. This is demonstrated by the interruption of phosphate production which then results in near complete cessation of intracellular lipid accumulation. In addition TNAP-generated phosphate is known to induce the expression of TNAP through an indirect mechanism (Orimo and Shimada,

2008) and this may be the reason why, despite the decrease in intracellular pyrophosphate, TNAP expression and activity remains upregulated.

The ANK pyrophosphate transporter is expressed ubiquitously (Kim et al., 2010b). Preliminary data (Brooks et al., unpublished), (Appendix A.3) shows that ANK expression is upregulated within 24 hours of adipogenesis, likely in response to the increase in ENPP-1 described by Liang and colleagues (Liang et al., 2007). It thus appears that high pyrophosphate levels within the cell are not desirable, potentially to limit the resultant hypertrophy observed in the presence of high intra-cellular pyrophosphate levels. It is clear that dysfunction of the pyrophosphate transporter results in augmented intracellular lipid accumulation, and this is emphasized by the finding that polymorphisms within ANKH are associated with increased adiposity within humans (Korostishevsky et al., 2010)

TRAF 2 despite being predicted to bind to TNAP by *in silico* algorithms, was not shown to bind using our experiments. The binding of TNAP to other proteins could not be ruled out. However, TRAF 2 mRNA is downregulated during adipogenesis and overexpression of TRAF 2 resulted in a reduction of intracellular lipid accumulation. This effect may be due to the role TRAF2 plays in inducing the expression of WNT10, a negative regulator of adipogenesis (Kennell and MacDougald, 2005, Bennett et al., 2002, Katoh and Katoh, 2007).

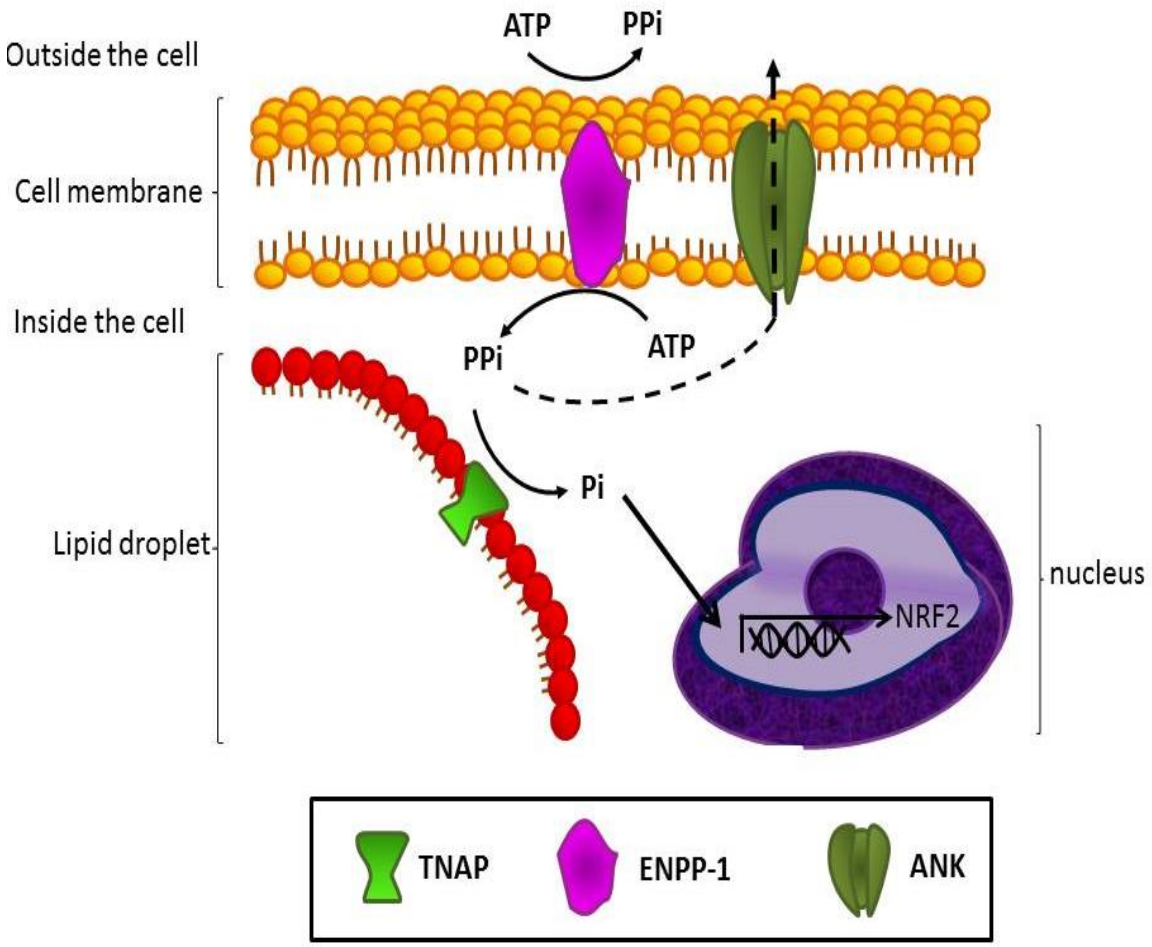

Figure 8.1: Schematic representation of the proposed mechanism through which TNAP functions to mediate intracellular lipid accumulation in the 3T3-L1 preadipocyte. In the initial hours of adipogenesis ENPP-1 expression is increased allowing for an increase in the intracellular pyrophosphate concentration. In response to high pyrophosphate, TNAP is upregulated and is incorporated into the lipid droplet membrane. The TNAP generates phosphate which enters the nucleus and induces the expression of genes essential for adipogenesis, including NRF 2.

Therefore, the function of TNAP within adipocytes and osteoblasts appears to share similarities. Thus, TNAP-generated phosphate is essential within both cell types for maturation, via its ability to induce the expression of NRF 2 within both the adipocyte and the osteoblast (Beck et al., 2003). This finding is not surprising given that both

osteoblasts and adipocytes originate from the same mesenchymal precursors, and 3T3-L1 cells have been shown to be able to transdifferentiate into osteoblasts (Takahashi, 2011, Takada et al., 2007).

Like the adipocyte and the osteoblast, cells of the adrenal cortex are also of mesenchymal origin (Majka et al., 2011), and are also known to accumulate lipids in membrane-bound droplets. In this thesis it was demonstrated that TNAP is expressed in the Y1 adrenocortical cell line where it is localized to the lipid droplet and modulates intracellular deposition of cholesterol. This implicates TNAP as having a role in the accumulation of neutral lipids within many cell types and suggests that one of the primary functions of TNAP, other than stimulating bone mineralization, is to modulate cellular lipid deposition.

9 Limitations and Future Studies

One of the main limitations of this study was the use of a murine preadipocye cell line rather than using primary cells. However, due to the complexities of obtaining and culturing primary human preadipocytes, 3T3-L1 are a recognised model for intracellular lipid accumulation. In addition in previous studies carried out by Ali and colleagues, TNAP was needed for lipid accumulation in both the 3T3-L1 cell line and human preadipocytes (Ali et al., 2005, Ali et al., 2006a). The concern that murine cells may not adequately represent that which occurs within human tissue was addressed in a European Commission workshop held in 2010. The outcome of the workshop was that whilst there is the possibility that the results seen in mice may not always match those in humans, with a genomic similarity of 99% and previous breakthroughs in human medicine originating from mouse experiments (such as the discovery of the genetic mutations responsible for acute promyelocytic leukaemia), the use of mouse models is valid within the context of human disease (European Commission Workshop, 2010).

In addition, the use of non-specific chemical inhibitors of TNAP were employed. It is therefore possible that the effects seen were not a result of the inhibition of TNAP activity, but rather as an off target effect of the inhibitor. Levamisole is able to bind and activate human nicotinic acid receptors (Levandoski et al., 2003) and alter the activity of pyruvate dehydrogenase in rat adipose tissue (Thomaskutty et al., 1993). In addition, levamisole has been shown to interact with muscarinic M-3 receptors (Carmona-Rivera et al., 2017). The M-3 receptor has previously been implicated in

glucose uptake and lipolysis in rat adipose tissue (Yang et al., 2009). However studies within 3T3-L1 adipocytes using both levamisole and employing gene knockout using small interfering RNA molecules specific for TNAP showed similar results (Ali et al., 2006b, Ali et al., 2006a, Ali et al., 2005) and it is therefore unlikely that the results seen are due to off target effects of levamisole.

Probenecid, in addition to its inhibitory effects on ANK, is known to inhibit organic anion transporters in a specific manner (Rosenthal et al., 2013, Silverman et al., 2008). It is therefore a possibility that the effects noted within our experiments were a result of inhibition of these channels rather than the inhibition of ANK.

Determining the ability of TNAP to bind TRAF2 through both band-shift assays and immune co-precipitation is a technical procedure, and various factors including heterodimerisation of native proteins and masking of protein-protein interaction may produce results which indicate that no binding between proteins is occurring. The limitations of this study are described in more detail in Chapter 6.

Future work would entail determining whether the findings laid out in this thesis are comparable to that seen in primary human cells, as well as whether TNAP functions within other lipid accumulating cells of the body such as Leydig cells and macrophage foam cells.

The TNAP-generated phosphate may induce the expression of genes other than NRF2, and therefore to determine which other genes may be altered through phosphate, a microarray gene expression platform should be used.

In addition, the development of an adipocyte specific knock out of TNAP within a mouse model would allow for a more complete investigation of the effect of TNAP within mouse adipose tissue.

These experiments have not ruled out the possibility that TNAP may function to dephosphorylate TRAF2. Therefore the use of phospho-TRAF2 antibodies within a Western blot experiment may be employed to determine the phosphorylation status of TRAF2 in the presence and absence of TNAP activity.

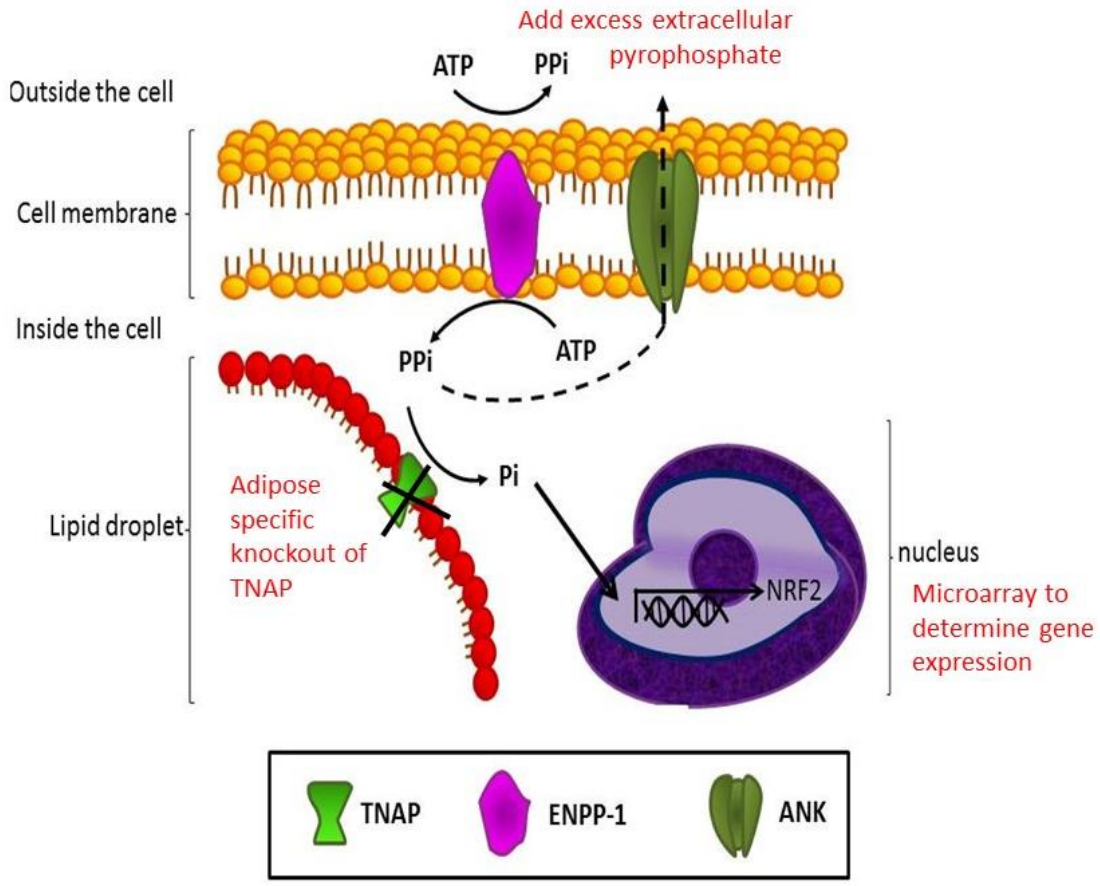

Figure 9.1: Schematic representation of the proposed mechanism through which TNAP functions to mediate intracellular lipid accumulation in the 3T3-L1 preadipocyte. Areas in which future work may be applied to allow for greater understanding of the proposed pathway are shown in red text.

References

ALI, A. T., CHIRAMBO, G., PENNY, C., PAIKER, J. E., IKRAM, F., PSARAS, G. & CROWTHER, N. J. 2015. Ethnic differences in pre-adipocyte intracellular lipid accumulation and alkaline phosphatase activity. *Clin Chim Acta,* 438**,** 382-7.

ALI, A. T., PENNY, C. B., PAIKER, J. E., PSARAS, G., IKRAM, F. & CROWTHER, N. J. 2006a. The effect of alkaline phosphatase inhibitors on intracellular lipid accumulation in preadipocytes isolated from human mammary tissue. *Ann Clin Biochem,* 43**,** 207-13.

ALI, A. T., PENNY, C. B., PAIKER, J. E., PSARAS, G., IKRAM, F. & CROWTHER, N. J. 2006b. The relationship between alkaline phosphatase activity and intracellular lipid accumulation in murine 3T3-L1 cells and human preadipocytes. *Anal Biochem,* 354**,** 247-54.

ALI, A. T., PENNY, C. B., PAIKER, J. E., VAN NIEKERK, C., SMIT, A., FERRIS, W. F. & CROWTHER, N. J. 2005. Alkaline phosphatase is involved in the control of adipogenesis in the murine preadipocyte cell line, 3T3-L1. *Clin Chim Acta,* 354**,** 101-9.

ATHENSTAEDT, K. & DAUM, G. 2006. The life cycle of neutral lipids: synthesis, storage and degradation. *Cell Mol Life Sci,* 63**,** 1355-69.

BALCERZAK, M., HAMADE, E., ZHANG, L., PIKULA, S., AZZAR, G., RADISSON, J., BANDOROWICZ-PIKULA, J. & BUCHET, R. 2003. The roles of annexins and alkaline phosphatase in mineralization process. *Acta Biochim Pol,* 50**,** 1019-38.

BECK, G. R., JR. 2003. Inorganic phosphate as a signaling molecule in osteoblast differentiation. *J Cell Biochem,* 90**,** 234-43.

BECK, G. R., JR., MORAN, E. & KNECHT, N. 2003. Inorganic phosphate regulates multiple genes during osteoblast differentiation, including Nrf2. *Exp Cell Res,* 288**,** 288-300.

BECK, G. R., JR., ZERLER, B. & MORAN, E. 2000. Phosphate is a specific signal for induction of osteopontin gene expression. *Proc Natl Acad Sci U S A,* 97**,** 8352-7.

BELLOWS, C. G., HEERSCHE, J. N. & AUBIN, J. E. 1992. Inorganic phosphate added exogenously or released from beta-glycerophosphate initiates mineralization of osteoid nodules in vitro. *Bone Miner,* 17**,** 15-29.

BENNETT, C. N., ROSS, S. E., LONGO, K. A., BAJNOK, L., HEMATI, N., JOHNSON, K. W., HARRISON, S. D. & MACDOUGALD, O. A. 2002. Regulation of Wnt signaling during adipogenesis. *J Biol Chem,* 277**,** 30998-1004.

BIRSOY, K., CHEN, Z. & FRIEDMAN, J. 2008. Transcriptional regulation of adipogenesis by KLF4. *Cell Metab,* 7**,** 339-47.

BOLEAN, M., SIMAO, A. M., FAVARIN, B. Z., MILLAN, J. L. & CIANCAGLINI, P. 2011. Thermodynamic properties and characterization of proteoliposomes rich in microdomains carrying alkaline phosphatase. *Biophys Chem,* 158**,** 111-8.

BRADFORD, M. M. 1976. A rapid and sensitive method for the quantitation of microgram quantities of protein utilizing the principle of protein-dye binding. *Anal Biochem,* 72**,** 248-54.

BRASAEMLE, D. L., BARBER, T., KIMMEL, A. R. & LONDOS, C. 1997. Post-translational regulation of perilipin expression. Stabilization by stored intracellular neutral lipids. *J Biol Chem,* 272**,** 9378-87.

BROOKS, S., PRIGGE, K. L., CROWTHER, N. J. & CAVE, E. unpublished. ANK mRNA is upregulated for the initial 24 hours of intracellular lipid accumulation within the murine 3T3-L1 cell line

CALDER, P. C., AHLUWALIA, N., BROUNS, F., BUETLER, T., CLEMENT, K., CUNNINGHAM, K., ESPOSITO, K., JONSSON, L. S., KOLB, H., LANSINK, M., MARCOS, A., MARGIORIS, A., MATUSHESKI, N., NORDMANN, H., O'BRIEN, J., PUGLIESE, G., RIZKALLA, S., SCHALKWIJK, C., TUOMILEHTO, J., WARNBERG, J., WATZL, B. & WINKLHOFER-ROOB, B. M. 2011. Dietary factors and low-grade inflammation in relation to overweight and obesity. *Br J Nutr,* 106 Suppl 3**,** S5-78.

CARMONA-RIVERA, C., PURMALEK, M. M., MOORE, E., WALDMAN, M., WALTER, P. J., GARRAFFO, H. M., PHILLIPS, K. A., PRESTON, K. L., GRAF, J., KAPLAN, M. J. & GRAYSON, P. C. 2017. A role for muscarinic receptors in neutrophil extracellular trap formation and levamisole-induced autoimmunity. *JCI Insight,* 2**,** e89780.

CHARTOUMPEKIS, D. V., ZIROS, P. G., PSYROGIANNIS, A. I., PAPAVASSILIOU, A. G., KYRIAZOPOULOU, V. E., SYKIOTIS, G. P. & HABEOS, I. G. 2011a. Nrf2 represses FGF21 during long-term high-fat diet-induced obesity in mice. *Diabetes,* 60**,** 2465-73.

CHARTOUMPEKIS, D. V., ZIROS, P. G., SYKIOTIS, G. P., ZARAVINOS, A., PSYROGIANNIS, A. I., KYRIAZOPOULOU, V. E., SPANDIDOS, D. A. & HABEOS, I. G. 2011b. Nrf2 activation diminishes during adipocyte differentiation of ST2 cells. *Int J Mol Med,* 28**,** 823-8.

CHEN, Y., XUE, P., HOU, Y., ZHANG, H., ZHENG, H., ZHOU, T., QU, W., TENG, W., ZHANG, Q., ANDERSEN, M. E. & PI, J. 2013. Isoniazid suppresses antioxidant response element activities and impairs adipogenesis in mouse and human preadipocytes. *Toxicol Appl Pharmacol,* 273**,** 435-41.

CHIRAMBO, G. 2013. *The role played by alkaline phosphatase in lipid droplet formation in different lipid-storing cell types.* PhD, University of the Witwatersrand.

CHIRAMBO, G. M., VAN NIEKERK, C. & CROWTHER, N. J. 2017. The role of alkaline phosphatase in intracellular lipid accumulation in the human hepatocarcinoma cell line, HepG2. *Exp Mol Pathol,* 102**,** 224-229.

CHIRAMBO, G. V. N., C.; CROWTHER, N. 2010. Post-transcriptional silencing of the tissue non-specific alkaline phosphatase (TNSALP) gene blocks intracellular lipid accumulation in a murine preadipocyte cell line, 3T3-L1 and in a human hepatocarcinoma cell line, HepG2. *J Endocrinol Metab Diabet S Afr,* 15**,** 25-26.

CLIFFORD, G. M., LONDOS, C., KRAEMER, F. B., VERNON, R. G. & YEAMAN, S. J. 2000. Translocation of hormone-sensitive lipase and perilipin upon lipolytic stimulation of rat adipocytes. *J Biol Chem,* 275**,** 5011-5.

CONRADS, K., YI, M., SIMPSON, K., LUCAS, D., CAMALIER, C., YU, L., VEENSTRA, T., STEPHENS, R., CONRADS, T., BECK, JR, G 2005. A Combined Proteome and Microarray Investigation of Inorganic Phosphate-induced Pre-osteoblast Cells. *Molecular & Cellular Proteomics,* 4**,** 1284-1296.

COOK, K. G., YEAMAN, S. J., STRALFORS, P., FREDRIKSON, G. & BELFRAGE, P. 1982. Direct evidence that cholesterol ester hydrolase from adrenal cortex is the same enzyme as hormone-sensitive lipase from adipose tissue. *Eur J Biochem,* 125**,** 245-9.

DELGADO-CALLE, J., SANUDO, C., SANCHEZ-VERDE, L., GARCIA-RENEDO, R. J., AROZAMENA, J. & RIANCHO, J. A. 2011. Epigenetic regulation of alkaline phosphatase in human cells of the osteoblastic lineage. *Bone,* 49**,** 830-8.

DIAZ-HERNANDEZ, M., HERNANDEZ, F., MIRAS-PORTUGAL, M. T. & AVILA, J. 2015. TNAP Plays a Key Role in Neural Differentiation as well as in Neurodegenerative Disorders. *Subcell Biochem,* 76**,** 375-85.

DROLET, R., RICHARD, C., SNIDERMAN, A. D., MAILLOUX, J., FORTIER, M., HUOT, C., RHEAUME, C. & TCHERNOF, A. 2008. Hypertrophy and hyperplasia of abdominal adipose tissues in women. *Int J Obes (Lond),* 32**,** 283-91.

DRUG ENFORCEMENT ADMINISTRATION 2013. Levamisole (Ergamisol®). *In:* OFFICE OF DIVERSION CONTROL, D. C. E. S. (ed.).

ELFTMAN, H. 1947. Response of the alkaline phosphatase of the adrenal cortex of the mouse to androgen. *Endocrinology,* 41**,** 85-91.

ESCARY, J. L., CHOY, H. A., REUE, K. & SCHOTZ, M. C. 1998. Hormone-sensitive lipase overexpression increases cholesteryl ester hydrolysis in macrophage foam cells. *Arterioscler Thromb Vasc Biol,* 18**,** 991-8.

EUROPEAN COMMISSION WORKSHOP. 2010. *Of mice and men - are mice relevant models for human disease* [Online]. London United kingdom: European Commission Available:

http://ec.europa.eu/research/health/pdf/summary-report-25082010_en.pdf [Accessed 17 October 2017].

FONG, T. H., YANG, C. C., GREENBERG, A. S. & WANG, S. M. 2002. Immunocytochemical studies on lipid droplet-surface proteins in adrenal cells. *J Cell Biochem,* 86**,** 432-9.

FUJIMOTO, S., ITSUMURA, N., TSUJI, T., ANAN, Y., TSUJI, N., OGRA, Y., KIMURA, T., MIYAMAE, Y., MASUDA, S., NAGAO, M. & KAMBE, T. 2013. Cooperative functions of ZnT1, metallothionein and ZnT4 in the cytoplasm are required for full activation of TNAP in the early secretory pathway. *PLoS One,* 8**,** e77445.

FUJITA, T., IZUMO, N., FUKUYAMA, R., MEGURO, T., NAKAMUTA, H., KOHNO, T. & KOIDA, M. 2001a. Phosphate provides an extracellular signal that drives nuclear export of Runx2/Cbfa1 in bone cells. *Biochem Biophys Res Commun,* 280**,** 348-52.

FUJITA, T., MEGURO, T., IZUMO, N., YASUTOMI, C., FUKUYAMA, R., NAKAMUTA, H. & KOIDA, M. 2001b. Phosphate stimulates differentiation and mineralization of the chondroprogenitor clone ATDC5. *Jpn J Pharmacol,* 85**,** 278-81.

FUKUNAKA, A., KUROKAWA, Y., TERANISHI, F., SEKLER, I., ODA, K., ACKLAND, M. L., FAUNDEZ, V., HIROMURA, M., MASUDA, S., NAGAO, M., ENOMOTO, S. & KAMBE, T. 2011. Tissue nonspecific alkaline phosphatase is activated via a two-step mechanism by zinc transport complexes in the early secretory pathway. *J Biol Chem,* 286**,** 16363-73.

GAO, J. & SERRERO, G. 1999. Adipose differentiation related protein (ADRP) expressed in transfected COS-7 cells selectively stimulates long chain fatty acid uptake. *J Biol Chem,* 274**,** 16825-30.

GOLDFINE, I. D., MADDUX, B. A., YOUNGREN, J. F., REAVEN, G., ACCILI, D., TRISCHITTA, V., VIGNERI, R. & FRITTITTA, L. 2008. The role of membrane glycoprotein plasma cell antigen 1/ectonucleotide pyrophosphatase phosphodiesterase 1 in the pathogenesis of insulin resistance and related abnormalities. *Endocr Rev,* 29**,** 62-75.

GREENSPAN, P., MAYER, E. P. & FOWLER, S. D. 1985. Nile red: a selective fluorescent stain for intracellular lipid droplets. *J Cell Biol,* 100**,** 965-73.

GROSS, D. A. & SILVER, D. L. 2014. Cytosolic lipid droplets: from mechanisms of fat storage to disease. *Crit Rev Biochem Mol Biol,* 49**,** 304-26.

GUO, Y., XIAO, P., LEI, S., DENG, F., XIAO, G. G., LIU, Y., CHEN, X., LI, L., WU, S., CHEN, Y., JIANG, H., TAN, L., XIE, J., ZHU, X., LIANG, S. & DENG, H. 2008. How is mRNA expression predictive for protein expression? A correlation study on human circulating monocytes. *Acta Biochim Biophys Sin (Shanghai),* 40**,** 426-36.

GURLEY, K. A., REIMER, R. J. & KINGSLEY, D. M. 2006. Biochemical and genetic analysis of ANK in arthritis and bone disease. *Am J Hum Genet,* 79**,** 1017-29.

HAMADE, T., BIANCHI, A., SEBILLAUD, S., NETTER, P., JOUZEAU, J. Y. & CAILOTTO, F. 2010. Inorganic phosphate (Pi) modulates the expression of key regulatory proteins of the inorganic pyrophosphate (PPi) metabolism in TGF-beta1-stimulated chondrocytes. *Biomed Mater Eng,* 20**,** 209-15.

HARMEY, D., HESSLE, L., NARISAWA, S., JOHNSON, K. A., TERKELTAUB, R. & MILLAN, J. L. 2004. Concerted regulation of inorganic pyrophosphate and osteopontin by akp2, enpp1, and ank: an integrated model of the pathogenesis of mineralization disorders. *Am J Pathol,* 164**,** 1199-209.

HARRIS, H. 1990. The human alkaline phosphatases: what we know and what we don't know. *Clin Chim Acta,* 186**,** 133-50.

HERNANDEZ-MOSQUEIRA, C., VELEZ-DELVALLE, C. & KURI-HARCUCH, W. 2015. Tissue alkaline phosphatase is involved in lipid metabolism and gene expression and secretion of adipokines in adipocytes. *Biochim Biophys Acta,* 1850**,** 2485-96.

HESSLE, L., JOHNSON, K. A., ANDERSON, H. C., NARISAWA, S., SALI, A., GODING, J. W., TERKELTAUB, R. & MILLAN, J. L. 2002. Tissue-nonspecific alkaline phosphatase and plasma cell membrane glycoprotein-1 are central antagonistic regulators of bone mineralization. *Proc Natl Acad Sci U S A,* 99**,** 9445-9.

HO, A. M., JOHNSON, M. D. & KINGSLEY, D. M. 2000. Role of the mouse ank gene in control of tissue calcification and arthritis. *Science,* 289**,** 265-70.

HOU, Y., XUE, P., BAI, Y., LIU, D., WOODS, C. G., YARBOROUGH, K., FU, J., ZHANG, Q., SUN, G., COLLINS, S., CHAN, J. Y., YAMAMOTO, M., ANDERSEN, M. E. & PI, J. 2012. Nuclear factor erythroid-derived factor 2-related factor 2 regulates transcription of CCAAT/enhancer-binding protein beta during adipogenesis. *Free Radic Biol Med,* 52**,** 462-72.

HOYLAERTS, M. F., VAN KERCKHOVEN, S., KIFFER-MOREIRA, T., SHEEN, C., NARISAWA, S. & MILLAN, J. L. 2015. Functional significance of calcium binding to tissue-nonspecific alkaline phosphatase. *PLoS One,* 10**,** e0119874.

HU, W. H., MO, X. M., WALTERS, W. M., BRAMBILLA, R. & BETHEA, J. R. 2004. TNAP, a novel repressor of NF-kappaB-inducing kinase, suppresses NF-kappaB activation. *J Biol Chem,* 279**,** 35975-83.

ITOH, K., CHIBA, T., TAKAHASHI, S., ISHII, T., IGARASHI, K., KATOH, Y., OYAKE, T., HAYASHI, N., SATOH, K., HATAYAMA, I., YAMAMOTO, M. & NABESHIMA, Y. 1997. An Nrf2/small Maf heterodimer mediates the induction of phase II detoxifying enzyme genes through antioxidant response elements. *Biochem Biophys Res Commun,* 236**,** 313-22.

ITOH, K., WAKABAYASHI, N., KATOH, Y., ISHII, T., IGARASHI, K., ENGEL, J. D. & YAMAMOTO, M. 1999. Keap1 represses nuclear activation of antioxidant responsive elements by Nrf2 through binding to the amino-terminal Neh2 domain. *Genes Dev,* 13**,** 76-86.

JENSEN, B., FARACH-CARSON, M. C., KENALEY, E. & AKANBI, K. A. 2004. High extracellular calcium attenuates adipogenesis in 3T3-L1 preadipocytes. *Exp Cell Res,* 301**,** 280-92.

JOHNSON, K. A., HESSLE, L., VAINGANKAR, S., WENNBERG, C., MAURO, S., NARISAWA, S., GODING, J. W., SANO, K., MILLAN, J. L. & TERKELTAUB, R. 2000. Osteoblast tissue-nonspecific alkaline phosphatase antagonizes and regulates PC-1. *Am J Physiol Regul Integr Comp Physiol,* 279**,** R1365-77.

KANATANI, M., SUGIMOTO, T., KANO, J., KANZAWA, M. & CHIHARA, K. 2003. Effect of high phosphate concentration on osteoclast differentiation as well as bone-resorbing activity. *J Cell Physiol,* 196**,** 180-9.

KANDA, Y., HINATA, T., KANG, S. W. & WATANABE, Y. 2011. Reactive oxygen species mediate adipocyte differentiation in mesenchymal stem cells. *Life Sci,* 89**,** 250-8.

KARL, I., JOSSBERGER-WERNER, M., SCHMIDT, N., HORN, S., GOEBELER, M., LEVERKUS, M., WAJANT, H. & GINER, T. 2014. TRAF2 inhibits TRAIL- and CD95L-induced apoptosis and necroptosis. *Cell Death Dis,* 5**,** e1444.

KATOH, M. & KATOH, M. 2007. AP1- and NF-kappaB-binding sites conserved among mammalian WNT10B orthologs elucidate the TNFalpha-WNT10B signaling loop implicated in carcinogenesis and adipogenesis. *Int J Mol Med,* 19**,** 699-703.

KELLETT, K. A. & HOOPER, N. M. 2015. The Role of Tissue Non-specific Alkaline Phosphatase (TNAP) in Neurodegenerative Diseases: Alzheimer's Disease in the Focus. *Subcell Biochem,* 76**,** 363-74.

KENNELL, J. A. & MACDOUGALD, O. A. 2005. Wnt signaling inhibits adipogenesis through beta-catenin-dependent and -independent mechanisms. *J Biol Chem,* 280**,** 24004-10.

KHOR, V. K., AHRENDS, R., LIN, Y., SHEN, W. J., ADAMS, C. M., ROSEMAN, A. N., CORTEZ, Y., TERUEL, M. N., AZHAR, S. & KRAEMER, F. B. 2014. The proteome of cholesteryl-ester-enriched versus triacylglycerol-enriched lipid droplets. *PLoS One,* 9**,** e105047.

KHOSHNIAT, S., BOURGINE, A., JULIEN, M., WEISS, P., GUICHEUX, J. & BECK, L. 2011. The emergence of phosphate as a specific signaling molecule in bone and other cell types in mammals. *Cell Mol Life Sci,* 68**,** 205-18.

KILEDJIAN, M. & KADESCH, T. 1990. Analysis of the human liver/bone/kidney alkaline phosphatase promoter in vivo and in vitro. *Nucleic Acids Res,* 18**,** 957-61.

KIM, H. J., DELANEY, J. D. & KIRSCH, T. 2010a. The role of pyrophosphate/phosphate homeostasis in terminal differentiation and apoptosis of growth plate chondrocytes. *Bone,* 47**,** 657-65.

KIM, H. J., MINASHIMA, T., MCCARTHY, E. F., WINKLES, J. A. & KIRSCH, T. 2010b. Progressive ankylosis protein (ANK) in osteoblasts and osteoclasts controls bone formation and bone remodeling. *J Bone Miner Res,* 25**,** 1771-83.

KOBAYASHI, A., KANG, M. I., OKAWA, H., OHTSUJI, M., ZENKE, Y., CHIBA, T., IGARASHI, K. & YAMAMOTO, M. 2004. Oxidative stress sensor Keap1 functions as an adaptor for Cul3-based E3 ligase to regulate proteasomal degradation of Nrf2. *Mol Cell Biol,* 24**,** 7130-9.

KOMARU, K., SATOU, Y., AL-SHAWAFI, H. A., NUMA-KINJOH, N., SOHDA, M. & ODA, K. 2016. Glycosylation-deficient mutations in tissue-nonspecific alkaline phosphatase impair its structure and function and are linked to infantile hypophosphatasia. *FEBS J,* 283**,** 1168-79.

KOROSTISHEVSKY, M., COHEN, Z., MALKIN, I., ERMAKOV, S., YARENCHUK, O. & LIVSHITS, G. 2010. Morphological and biochemical features of obesity are associated with mineralization genes' polymorphisms. *Int J Obes (Lond),* 34**,** 1308-18.

KOZLENKOV, A., LE DU, M. H., CUNIASSE, P., NY, T., HOYLAERTS, M. F. & MILLAN, J. L. 2004. Residues determining the binding specificity of uncompetitive inhibitors to tissue-nonspecific alkaline phosphatase. *J Bone Miner Res,* 19**,** 1862-72.

KRAEMER, F. B., KHOR, V. K., SHEN, W. J. & AZHAR, S. 2013. Cholesterol ester droplets and steroidogenesis. *Mol Cell Endocrinol,* 371**,** 15-9.

KRAEMER, F. B., SHEN, W. J., NATU, V., PATEL, S., OSUGA, J. I., ISHIBASHI, S. & AZHAR, S. 2002. Adrenal Neutral Cholesteryl Ester Hydrolase: Identification, Subcellular Distribution, and Sex Differences. *Endocrinology,* 143**,** 801-806.

KRAUSS, R. M., HERBERT, P. N., LEVY, R. I. & FREDRICKSON, D. S. 1973. Further observations on the activation and inhibition of lipoprotein lipase by apolipoproteins. *Circ Res,* 33**,** 403-11.

LAEMMLI, U. K. 1970. Cleavage of structural proteins during the assembly of the head of bacteriophage T4. *Nature,* 227**,** 680-5.

LE DU, M. H. & MILLAN, J. L. 2002. Structural evidence of functional divergence in human alkaline phosphatases. *J Biol Chem,* 277**,** 49808-14.

LEE, H., LEE, Y. J., CHOI, H., KO, E. H. & KIM, J. W. 2009. Reactive oxygen species facilitate adipocyte differentiation by accelerating mitotic clonal expansion. *J Biol Chem,* 284**,** 10601-9.

LEE, N. K. & LEE, S. Y. 2002. Modulation of life and death by the tumor necrosis factor receptor-associated factors (TRAFs). *J Biochem Mol Biol,* 35**,** 61-6.

LEI, W., NI, H., HERINGTON, J., REESE, J. & PARIA, B. C. 2015. Alkaline phosphatase protects lipopolysaccharide-induced early pregnancy defects in mice. *PLoS One,* 10**,** e0123243.

LEUNG, C. T., MALEEFF, B. E. & FARRELL, H. M., JR. 1989. Subcellular and ultrastructural localization of alkaline phosphatase in lactating rat mammary glands. *J Dairy Sci,* 72**,** 2495-509.

LEVANDOSKI, M. M., PIKET, B. & CHANG, J. 2003. The anthelmintic levamisole is an allosteric modulator of human neuronal nicotinic acetylcholine receptors. *Eur J Pharmacol,* 471**,** 9-20.

LIANG, J., FU, M., CIOCIOLA, E., CHANDALIA, M. & ABATE, N. 2007. Role of ENPP1 on adipocyte maturation. *PLoS One,* 2**,** e882.

LISTENBERGER, L. L. & BROWN, D. A. 2008. Lipid droplets. *Curr Biol,* 18**,** R237-8.

LIU, J., DEYOUNG, S. M., ZHANG, M., ZHANG, M., CHENG, A. & SALTIEL, A. R. 2005. Changes in integrin expression during adipocyte differentiation. *Cell Metab,* 2**,** 165-77.

LIVAK, K. J., FLOOD, S. J., MARMARO, J., GIUSTI, W. & DEETZ, K. 1995. Oligonucleotides with fluorescent dyes at opposite ends provide a quenched probe system useful for detecting PCR product and nucleic acid hybridization. *PCR Methods Appl,* 4**,** 357-62.

LIVAK, K. J. & SCHMITTGEN, T. D. 2001. Analysis of relative gene expression data using real-time quantitative PCR and the 2(-Delta Delta C(T)) Method. *Methods,* 25**,** 402-8.

LOWE, C. E., O'RAHILLY, S. & ROCHFORD, J. J. 2011. Adipogenesis at a glance. *J Cell Sci,* 124**,** 2681-6.

LUU-THE, V. 2013. Assessment of steroidogenesis and steroidogenic enzyme functions. *J Steroid Biochem Mol Biol,* 137**,** 176-82.

MACGREGOR, G. R., ZAMBROWICZ, B. P. & SORIANO, P. 1995. Tissue non-specific alkaline phosphatase is expressed in both embryonic and extraembryonic lineages during mouse embryogenesis but is not required for migration of primordial germ cells. *Development,* 121**,** 1487-96.

MADDUX, B. A., SBRACCIA, P., KUMAKURA, S., SASSON, S., YOUNGREN, J., FISHER, A., SPENCER, S., GRUPE, A., HENZEL, W., STEWART, T. A. & ET AL. 1995. Membrane glycoprotein PC-1 and insulin resistance in non-insulin-dependent diabetes mellitus. *Nature,* 373**,** 448-51.

MAJKA, S. M., BARAK, Y. & KLEMM, D. J. 2011. Concise review: adipocyte origins: weighing the possibilities. *Stem Cells,* 29**,** 1034-40.

MALKIN, I., ERMAKOV, S., KOBYLIANSKY, E. & LIVSHITS, G. 2006. Strong association between polymorphisms in ANKH locus and skeletal size traits. *Hum Genet,* 120**,** 42-51.

MANSUROVA, S. E. 1989. Inorganic pyrophosphate in mitochondrial metabolism. *Biochim Biophys Acta,* 977**,** 237-47.

MCCOMB, R. B., G.; POSEN, S. 1979. *Alkaline Phosphatase,* New York and London, Plenum Press.

MEYRE, D., BOUATIA-NAJI, N., TOUNIAN, A., SAMSON, C., LECOEUR, C., VATIN, V., GHOUSSAINI, M., WACHTER, C., HERCBERG, S., CHARPENTIER, G., PATSCH, W., PATTOU, F., CHARLES, M. A., TOUNIAN, P., CLEMENT, K., JOURET, B., WEILL, J., MADDUX, B. A., GOLDFINE, I. D., WALLEY, A., BOUTIN, P., DINA, C. & FROGUEL, P. 2005. Variants of ENPP1 are associated with childhood and adult obesity and increase the risk of glucose intolerance and type 2 diabetes. *Nat Genet,* 37**,** 863-7.

MILLAN, J. L. & WHYTE, M. P. 2016. Alkaline Phosphatase and Hypophosphatasia. *Calcif Tissue Int,* 98**,** 398-416.

MILLER, W. L. & AUCHUS, R. J. 2011. The molecular biology, biochemistry, and physiology of human steroidogenesis and its disorders. *Endocr Rev,* 32**,** 81-151.

MOLECULAR PROBES. 2004. *ELF® 97 Endogenous Phosphatase Detection Kit (E6601)* [Online]. Invitrogen. Available: https://tools.thermofisher.com/content/sfs/manuals/mp06601.pdf [Accessed 12 January 2017].

MOLECULAR PROBES. 2006. *PiPer™ Pyrophosphate Assay Kit* [Online]. Invitrogen. Available: https://tools.thermofisher.com/content/sfs/manuals/mp22062.pdf [Accessed 12 January 2017].

MURALIDHARAN-CHARI, V., CLANCY, J. W., SEDGWICK, A. & D'SOUZA-SCHOREY, C. 2010. Microvesicles: mediators of extracellular communication during cancer progression. *J Cell Sci,* 123**,** 1603-11.

MURPHY, J. & RILEY, J. 1962. A modified single solution method for the determination of phosphate in natural waters. *Analytica Chimica Acta,* 27**,** 31-36.

NAGASHIMA, H., OKUYAMA, Y., HAYASHI, T., ISHII, N. & SO, T. 2016. TNFR-Associated Factors 2 and 5 Differentially Regulate the Instructive IL-6 Receptor Signaling Required for Th17 Development. *J Immunol*.

NARISAWA, S., FROHLANDER, N. & MILLAN, J. L. 1997. Inactivation of two mouse alkaline phosphatase genes and establishment of a model of infantile hypophosphatasia. *Dev Dyn,* 208**,** 432-46.

NARULA, N. & STOW, J. L. 1995. Distinct coated vesicles labeled for p200 bud from trans-Golgi network membranes. *Proc Natl Acad Sci U S A,* 92**,** 2874-8.

NAVIGLIO, S., SPINA, A., CHIOSI, E., FUSCO, A., ILLIANO, F., PAGANO, M., ROMANO, M., SENATORE, G., SORRENTINO, A., SORVILLO, L. & ILLIANO, G. 2006. Inorganic phosphate inhibits growth of human osteosarcoma U2OS cells via adenylate cyclase/cAMP pathway. *J Cell Biochem,* 98**,** 1584-96.

NEAL, J. W. & CLIPSTONE, N. A. 2002. Calcineurin mediates the calcium-dependent inhibition of adipocyte differentiation in 3T3-L1 cells. *J Biol Chem,* 277**,** 49776-81.

NGUYEN, T., NIOI, P. & PICKETT, C. B. 2009. The Nrf2-antioxidant response element signaling pathway and its activation by oxidative stress. *J Biol Chem,* 284**,** 13291-5.

NOSJEAN, O., KOYAMA, I., GOSEKI, M., ROUX, B. & KOMODA, T. 1997. Human tissue non-specific alkaline phosphatases: sugar-moiety-induced enzymic and antigenic modulations and genetic aspects. *Biochem J,* 321 (Pt 2)**,** 297-303.

ORIMO, H. & SHIMADA, T. 2008. The role of tissue-nonspecific alkaline phosphatase in the phosphate-induced activation of alkaline phosphatase and mineralization in SaOS-2 human osteoblast-like cells. *Mol Cell Biochem,* 315**,** 51-60.

PAKKANEN, K. I., DUELUND, L., QVORTRUP, K., PEDERSEN, J. S. & IPSEN, J. H. 2011. Mechanics and dynamics of triglyceride-phospholipid model membranes: Implications for cellular properties and function. *Biochim Biophys Acta,* 1808**,** 1947-56.

PATEL, Y. M. & LANE, M. D. 2000. Mitotic clonal expansion during preadipocyte differentiation: calpain-mediated turnover of p27. *J Biol Chem,* 275**,** 17653-60.

PETERSEN, S. L., KRISHNAN, S., AGGISON, L. K., INTLEKOFER, K. A. & MOURA, P. J. 2012. Sexual differentiation of the gonadotropin surge release mechanism: a new role for the canonical NfkappaB signaling pathway. *Front Neuroendocrinol,* 33**,** 36-44.

PI, J., LEUNG, L., XUE, P., WANG, W., HOU, Y., LIU, D., YEHUDA-SHNAIDMAN, E., LEE, C., LAU, J., KURTZ, T. W. & CHAN, J. Y. 2010. Deficiency in the nuclear factor E2-related factor-2 transcription factor results in impaired adipogenesis and protects against diet-induced obesity. *J Biol Chem,* 285**,** 9292-300.

PIKE, A. F., KRAMER, N. I., BLAAUBOER, B. J., SEINEN, W. & BRANDS, R. 2013. A novel hypothesis for an alkaline phosphatase 'rescue' mechanism in the hepatic acute phase immune response. *Biochim Biophys Acta,* 1832**,** 2044-56.

PITRE, S., DEHNE, F., CHAN, A., CHEETHAM, J., DUONG, A., EMILI, A., GEBBIA, M., GREENBLATT, J., JESSULAT, M., KROGAN, N., LUO, X. & GOLSHANI, A. 2006. PIPE: a protein-protein interaction prediction engine based on the re-occurring short polypeptide sequences between known interacting protein pairs. *BMC Bioinformatics,* 7**,** 365.

POULOS, S. P., DODSON, M. V. & HAUSMAN, G. J. 2010. Cell line models for differentiation: preadipocytes and adipocytes. *Exp Biol Med (Maywood),* 235**,** 1185-93.

PROSDOCIMO, D. A., DOUGLAS, D. C., ROMANI, A. M., O'NEILL, W. C. & DUBYAK, G. R. 2009. Autocrine ATP release coupled to extracellular pyrophosphate accumulation in vascular smooth muscle cells. *Am J Physiol Cell Physiol,* 296**,** C828-39.

RAINEY, W. E., SANER, K. & SCHIMMER, B. P. 2004. Adrenocortical cell lines. *Mol Cell Endocrinol,* 228**,** 23-38.

ROBERTS, S., MCCUNE, R. W., CREANGE, J. E. & YOUNG, P. L. 1967. Adenosine 3',5'-cyclic phosphate: stimulation of steroidogenesis in sonically disrupted adrenal mitochondria. *Science,* 158**,** 372-4.

RONCHETTI, I., BORALDI, F., ANNOVI, G., CIANCIULLI, P. & QUAGLINO, D. 2013. Fibroblast involvement in soft connective tissue calcification. *Front Genet,* 4**,** 22.

ROSENTHAL, A. K., GOHR, C. M., MITTON-FITZGERALD, E., LUTZ, M. K., DUBYAK, G. R. & RYAN, L. M. 2013. The progressive ankylosis gene product ANK regulates extracellular ATP levels in primary articular chondrocytes. *Arthritis Res Ther,* 15**,** R154.

ROTHE, M., SARMA, V., DIXIT, V. M. & GOEDDEL, D. V. 1995. TRAF2-mediated activation of NF-kappa B by TNF receptor 2 and CD40. *Science,* 269**,** 1424-7.

SANTORO, N., CIRILLO, G., LEPORE, M. G., PALMA, A., AMATO, A., SAVARESE, P., MARZUILLO, P., GRANDONE, A., PERRONE, L. & DEL GIUDICE, E. M. 2009. Effect of the rs997509 polymorphism on the association between ectonucleotide pyrophosphatase phosphodiesterase 1 and metabolic syndrome and impaired glucose tolerance in childhood obesity. *J Clin Endocrinol Metab,* 94**,** 300-5.

SCHNEIDER, M. R. 2016. Beyond the adipocyte paradigm: Heterogeneity of lipid droplets and associated proteins. *Exp Cell Res,* 340**,** 171.

SERVETNICK, D. A., BRASAEMLE, D. L., GRUIA-GRAY, J., KIMMEL, A. R., WOLFF, J. & LONDOS, C. 1995. Perilipins are associated with cholesteryl ester droplets in steroidogenic adrenal cortical and Leydig cells. *J Biol Chem,* 270**,** 16970-3.

SHEN, R. R., ZHOU, A. Y., KIM, E., LIM, E., HABELHAH, H. & HAHN, W. C. 2012. IkappaB kinase epsilon phosphorylates TRAF2 to promote mammary epithelial cell transformation. *Mol Cell Biol,* 32**,** 4756-68.

SHEN, W. J., AZHAR, S. & KRAEMER, F. B. 2016. Lipid droplets and steroidogenic cells. *Exp Cell Res,* 340**,** 209-14.

SHI, H., HALVORSEN, Y. D., ELLIS, P. N., WILKISON, W. O. & ZEMEL, M. B. 2000. Role of intracellular calcium in human adipocyte differentiation. *Physiol Genomics,* 3**,** 75-82.

SHIN, S., WAKABAYASHI, N., MISRA, V., BISWAL, S., LEE, G. H., AGOSTON, E. S., YAMAMOTO, M. & KENSLER, T. W. 2007. NRF2 modulates aryl hydrocarbon receptor signaling: influence on adipogenesis. *Mol Cell Biol,* 27**,** 7188-97.

SHOHAM, N. & GEFEN, A. 2012. Mechanotransduction in adipocytes. *J Biomech,* 45**,** 1-8.

SILVENT, J., GASSE, B., MORNET, E. & SIRE, J. Y. 2014. Molecular evolution of the tissue-nonspecific alkaline phosphatase allows prediction and validation of missense mutations responsible for hypophosphatasia. *J Biol Chem,* 289**,** 24168-79.

SILVERMAN, W., LOCOVEI, S. & DAHL, G. 2008. Probenecid, a gout remedy, inhibits pannexin 1 channels. *Am J Physiol Cell Physiol,* 295**,** C761-7.

SON, Y. H., KA, S., KIM, A. Y. & KIM, J. B. 2014. Regulation of Adipocyte Differentiation via MicroRNAs. *Endocrinol Metab (Seoul),* 29**,** 122-35.

STOCKINGER, B. & VELDHOEN, M. 2007. Differentiation and function of Th17 T cells. *Curr Opin Immunol,* 19**,** 281-6.

SZKLARCZYK, D., FRANCESCHINI, A., WYDER, S., FORSLUND, K., HELLER, D., HUERTA-CEPAS, J., SIMONOVIC, M., ROTH, A., SANTOS, A., TSAFOU, K. P., KUHN, M., BORK, P., JENSEN, L. J. & VON MERING, C. 2015. STRING v10: protein-protein interaction networks, integrated over the tree of life. *Nucleic Acids Res,* 43**,** D447-52.

TAKADA, I., SUZAWA, M., MATSUMOTO, K. & KATO, S. 2007. Suppression of PPAR transactivation switches cell fate of bone marrow stem cells from adipocytes into osteoblasts. *Ann N Y Acad Sci,* 1116**,** 182-95.

TAKAHASHI, T. 2011. Overexpression of Runx2 and MKP-1 stimulates transdifferentiation of 3T3-L1 preadipocytes into bone-forming osteoblasts in vitro. *Calcif Tissue Int,* 88**,** 336-47.

TANG, Q. Q., OTTO, T. C. & LANE, M. D. 2003. Mitotic clonal expansion: a synchronous process required for adipogenesis. *Proc Natl Acad Sci U S A,* 100**,** 44-9.

TANG, X., GUILHERME, A., CHAKLADAR, A., POWELKA, A. M., KONDA, S., VIRBASIUS, J. V., NICOLORO, S. M., STRAUBHAAR, J. & CZECH, M. P. 2006. An RNA interference-based screen identifies MAP4K4/NIK as a negative regulator of PPARgamma, adipogenesis, and insulin-responsive hexose transport. *Proc Natl Acad Sci U S A,* 103**,** 2087-92.

THOMAS, G. S., ZHANG, L., BLACKWELL, K. & HABELHAH, H. 2009. Phosphorylation of TRAF2 within its RING domain inhibits stress-induced cell death by promoting IKK and suppressing JNK activation. *Cancer Res,* 69**,** 3665-72.

THOMASKUTTY, K. G., BASI, N. S., MCKENZIE, M. L. & POINTER, R. H. 1993. Regulation of pyruvate dehydrogenase activity in rat fat pads and isolated hepatocytes by levamisole. *Pharmacol Res,* 27**,** 263-71.

TOWBIN, H., STAEHELIN, T. & GORDON, J. 1979. Electrophoretic transfer of proteins from polyacrylamide gels to nitrocellulose sheets: procedure and some applications. *Proc Natl Acad Sci U S A,* 76**,** 4350-4.

TURCU, A. F. & AUCHUS, R. J. 2015. Adrenal steroidogenesis and congenital adrenal hyperplasia. *Endocrinol Metab Clin North Am,* 44**,** 275-96.

UHLEN, M., FAGERBERG, L., HALLSTROM, B. M., LINDSKOG, C., OKSVOLD, P., MARDINOGLU, A., SIVERTSSON, A., KAMPF, C., SJOSTEDT, E., ASPLUND, A., OLSSON, I., EDLUND, K., LUNDBERG,

E., NAVANI, S., SZIGYARTO, C. A., ODEBERG, J., DJUREINOVIC, D., TAKANEN, J. O., HOBER, S., ALM, T., EDQVIST, P. H., BERLING, H., TEGEL, H., MULDER, J., ROCKBERG, J., NILSSON, P., SCHWENK, J. M., HAMSTEN, M., VON FEILITZEN, K., FORSBERG, M., PERSSON, L., JOHANSSON, F., ZWAHLEN, M., VON HEIJNE, G., NIELSEN, J. & PONTEN, F. 2015. Proteomics. Tissue-based map of the human proteome. *Science,* 347**,** 1260419.

VRIEND, J. & REITER, R. J. 2015. The Keap1-Nrf2-antioxidant response element pathway: a review of its regulation by melatonin and the proteasome. *Mol Cell Endocrinol,* 401**,** 213-20.

WALCZAK, E. M. & HAMMER, G. D. 2015. Regulation of the adrenocortical stem cell niche: implications for disease. *Nat Rev Endocrinol,* 11**,** 14-28.

WANG, J., TSUI, H. W., BEIER, F., PRITZKER, K. P., INMAN, R. D. & TSUI, F. W. 2008. The ANKH DeltaE490Mutation in Calcium Pyrophosphate Dihydrate Crystal Deposition Disease (CPPDD) affects tissue non-specific Alkaline Phosphatase (TNAP) activities. *Open Rheumatol J,* 2**,** 23-30.

WANG, T. & RAINEY, W. E. 2012. Human adrenocortical carcinoma cell lines. *Mol Cell Endocrinol,* 351**,** 58-65.

WANG, Y., BISHOP, N. M., TAATJES, D. J., NARISAWA, S., MILLAN, J. L. & PALMER, B. M. 2014. Sex-dependent, zinc-induced dephosphorylation of phospholamban by tissue-nonspecific alkaline phosphatase in the cardiac sarcomere. *Am J Physiol Heart Circ Physiol,* 307**,** H933-8.

WEISS, M. J., RAY, K., HENTHORN, P. S., LAMB, B., KADESCH, T. & HARRIS, H. 1988. Structure of the human liver/bone/kidney alkaline phosphatase gene. *J Biol Chem,* 263**,** 12002-10.

XU, J., KULKARNI, S. R., DONEPUDI, A. C., MORE, V. R. & SLITT, A. L. 2012. Enhanced Nrf2 activity worsens insulin resistance, impairs lipid accumulation in adipose tissue, and increases hepatic steatosis in leptin-deficient mice. *Diabetes,* 61**,** 3208-18.

XUE, P., HOU, Y., CHEN, Y., YANG, B., FU, J., ZHENG, H., YARBOROUGH, K., WOODS, C. G., LIU, D., YAMAMOTO, M., ZHANG, Q., ANDERSEN, M. E. & PI, J. 2013. Adipose deficiency of Nrf2 in ob/ob mice results in severe metabolic syndrome. *Diabetes,* 62**,** 845-54.

YAMAGUCHI, T., FUJIKAWA, N., NIMURA, S., TOKUOKA, Y., TSUDA, S., AIUCHI, T., KATO, R., OBAMA, T. & ITABE, H. 2015. Characterization of lipid droplets in steroidogenic MLTC-1 Leydig cells: Protein profiles and the morphological change induced by hormone stimulation. *Biochim Biophys Acta,* 1851**,** 1285-95.

YANG, H., GALEA, A., SYTNYK, V. & CROSSLEY, M. 2012. Controlling the size of lipid droplets: lipid and protein factors. *Curr Opin Cell Biol,* 24**,** 509-16.

YANG, T. T., CHANG, C. K., TSAO, C. W., HSU, Y. M., HSU, C. T. & CHENG, J. T. 2009. Activation of muscarinic M-3 receptor may decrease glucose uptake and lipolysis in adipose tissue of rats. *Neurosci Lett,* 451**,** 57-9.

YAZAWA, T., IMAMICHI, Y., MIYAMOTO, K., UMEZAWA, A. & TANIGUCHI, T. 2014. Differentiation of mesenchymal stem cells into gonad and adrenal steroidogenic cells. *World J Stem Cells,* 6**,** 203-12.

ZHANG, J., TANG, H., ZHANG, Y., DENG, R., SHAO, L., LIU, Y., LI, F., WANG, X. & ZHOU, L. 2014. Identification of suitable reference genes for quantitative RT-PCR during 3T3-L1 adipocyte differentiation. *Int J Mol Med,* 33**,** 1209-18.

ZHAO, G., XU, M. J., ZHAO, M. M., DAI, X. Y., KONG, W., WILSON, G. M., GUAN, Y., WANG, C. Y. & WANG, X. 2012. Activation of nuclear factor-kappa B accelerates vascular calcification by inhibiting ankylosis protein homolog expression. *Kidney Int,* 82**,** 34-44.

ZIMMERMANN, B. 2008. Effects of pyrophosphate on desmal and endochondral mineralization and TNAP activity in organoid culture. *Ann Anat,* 190**,** 167-77.

Appendices

A1. Ethics Waiver

University
of the Witwatersrand,
Johannesburg

Human Research Ethics Committee (Medical)
(formerly Committee for Research on Human Subjects (Medical)

Secretariat: Research Office, Room 9H10005, 10th floor, Senate House • Telephone: +27 11 717-1234 • Fax: +27 11 339-5708
Private Bag 3, Wits 2050, South Africa

Ref: W-CJ-120213-1

13/02/2012

TO WHOM IT MAY CONCERN:

Waiver: This certifies that the following research does not require clearance from the Human Research Ethics Committee (Medical).

Investigator: **Prof N Crowther, Miss E Cave**

Project title: **Assessing the role of tissue non-specific alkaline phosphatase in lipid accumulation in adipose and adrenal cortex tissues.**

Reason: This is a wholly laboratory study using commercial cell lines. No human participants are involved.

UNIVERSITY OF THE WITWATERSRAND
PROF PE CLEATON-JONES
HREC (MEDICAL)
2012 -02- 1
JOHANNESBURG

Professor Peter Cleaton-Jones
Chair: Human Research Ethics Committee (Medical)

copy: Anisa Keshav, Research Office, Senate House, Wits

A2. Toxic dose experiment to determine maximal usable concentration of sodium phosphate

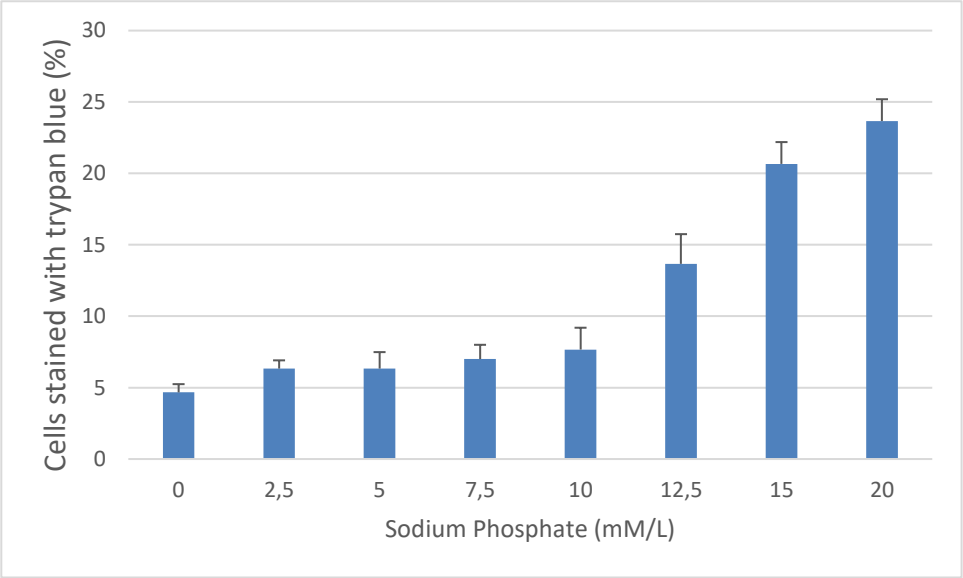

Appendix 2: Toxic dose experiment to determine cell viability after the addition of differing concentrations of sodium phosphate. Viability was determined through trypan blue staining and determining the percentage of dead cells.

A3. Real-time expression of ANK mRNA during intracellular lipid accumulation

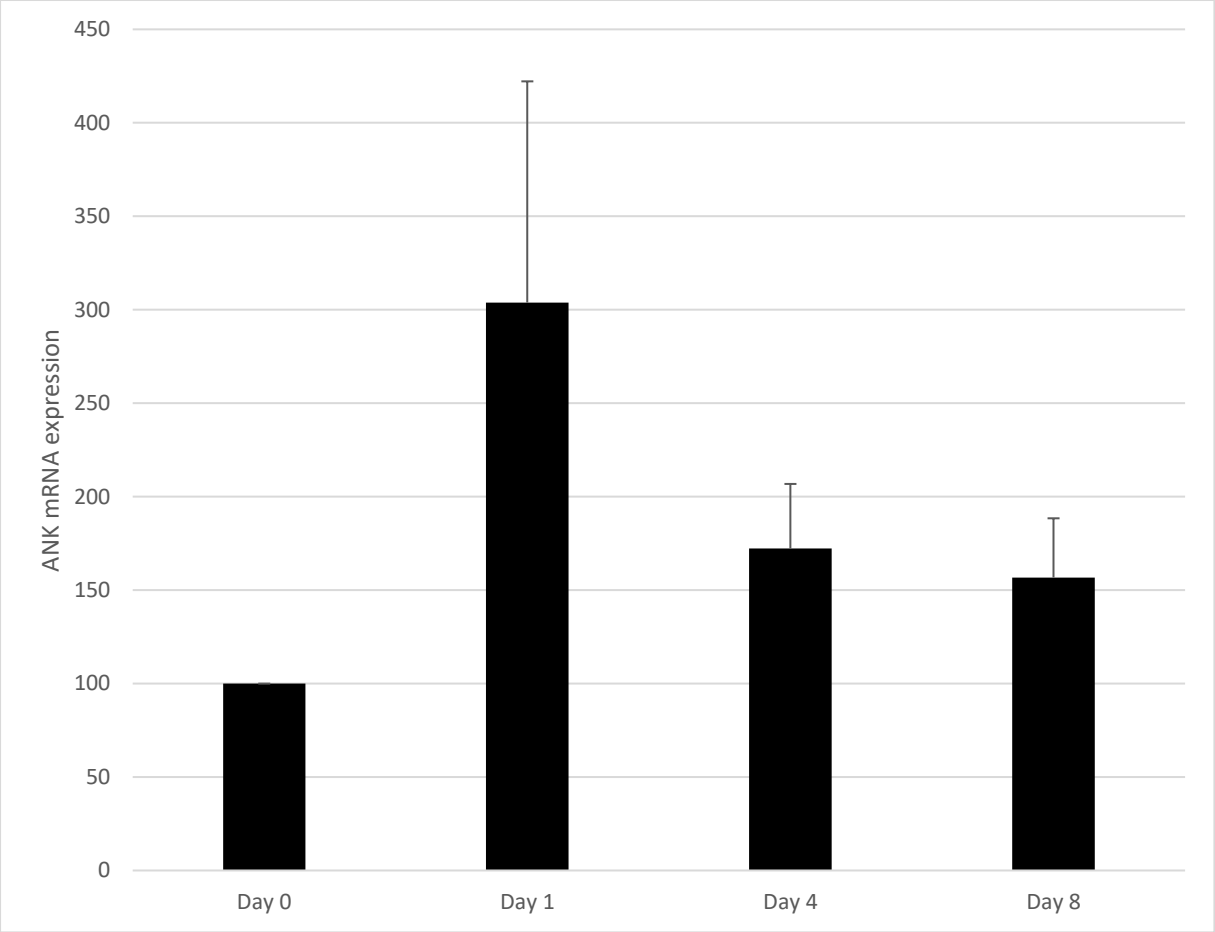

Appendix 3: Expression of ANK in the 3T3-L1 cell line over the initial 8 days of intracellular lipid accumulation. ANK expression was determined through real time PCR and normalized to β-actin expression levels.

A4. Expression data of NRF2 and TRAF2 mRNA confirming gene expression from pReceiver-MO2 plasmids

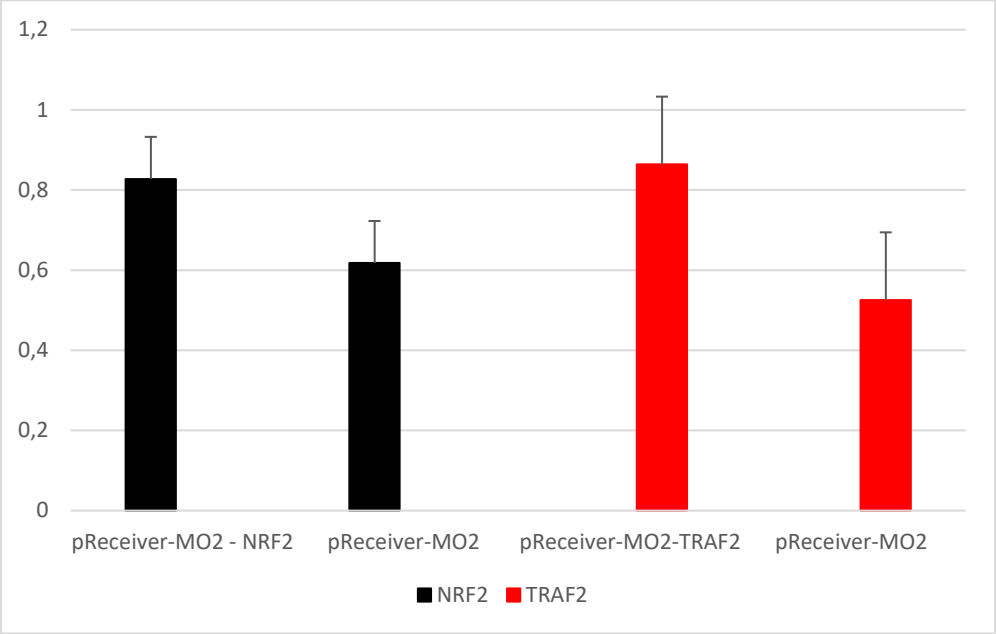

Appendix 4: Expression of NRF2 and TRAF2 from pReceiver-MO2-NRF2 and pReceiver-MO2-TRAF2 plasmids in the 3T3-L1 cell line 24 hours post transfection. Expression was compared to cells transfected with the empty vector pReceiver-MO2. Gene expression was determined through real time PCR and normalized to β-actin expression levels (Error bars represent standard error).

A5. ELF-97 staining is localized to lipid droplets in the absence of Nile red

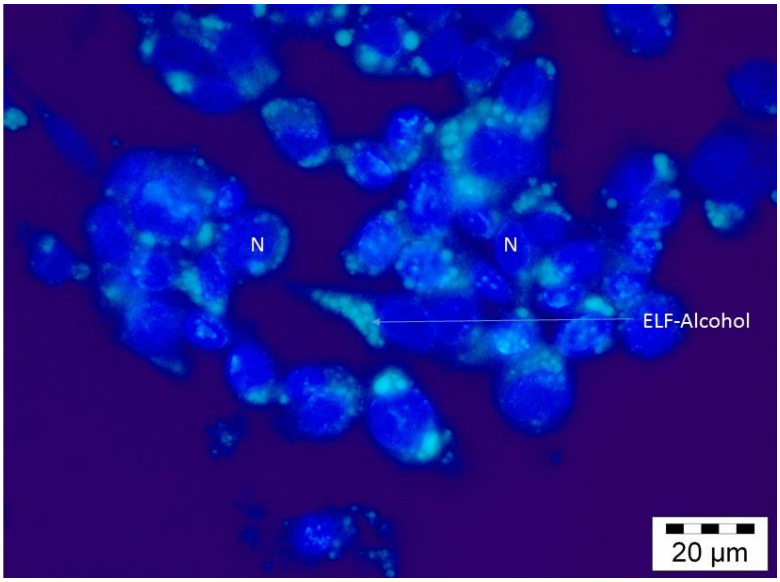

Appendix 5: Y1 cells were treated with ELF-97 and the resultant fluorescent byproduct of TNAP activity, ELF-Alcohol was visualised in the absence of Nile Red staining to confirm that ELF staining localised to the lipid droplet seen in figure 7.4 was true staining and not Nile red staining being visualised in the 530nm channel. Cells were visualised under 100x magnification.